LBL-31792
UC-404

Lawrence Berkeley Laboratory
UNIVERSITY OF CALIFORNIA

Materials Sciences Division

NMR Studies of the Conformation and Motion of Tetrahydrofuran in Graphite Intercalation Compounds

D.F. Caplan
(M.S. Thesis)

November 1991

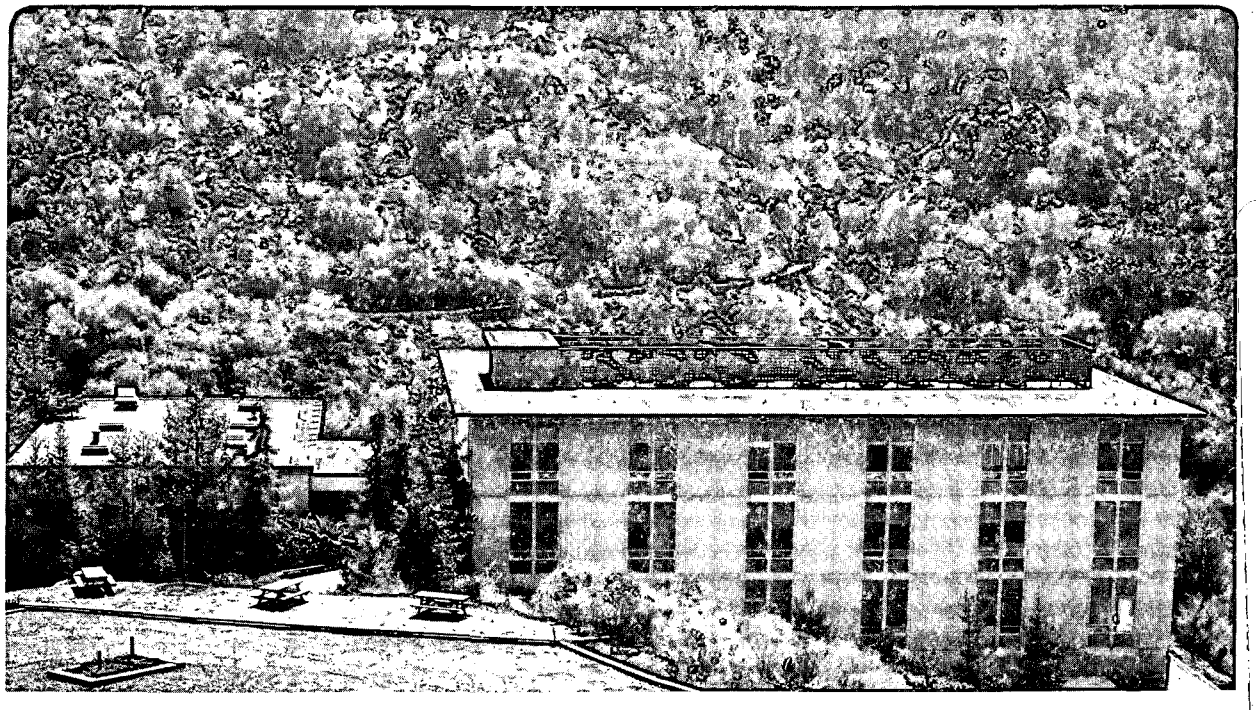

REFERENCE COPY
Does Not
Circulate
Bldg. 50 Library.
LBL-31792
Copy 1

Prepared for the U.S. Department of Energy under Contract Number DE-AC03-76SF00098

DISCLAIMER

This document was prepared as an account of work sponsored by the United States Government. Neither the United States Government nor any agency thereof, nor The Regents of the University of California, nor any of their employees, makes any warranty, express or implied, or assumes any legal liability or responsibility for the accuracy, completeness, or usefulness of any information, apparatus, product, or process disclosed, or represents that its use would not infringe privately owned rights. Reference herein to any specific commercial product, process, or service by its trade name, trademark, manufacturer, or otherwise, does not necessarily constitute or imply its endorsement, recommendation, or favoring by the United States Government or any agency thereof, or The Regents of the University of California. The views and opinions of authors expressed herein do not necessarily state or reflect those of the United States Government or any agency thereof or The Regents of the University of California and shall not be used for advertising or product endorsement purposes.

Lawrence Berkeley Laboratory is an equal opportunity employer.

This publication has been reproduced from the best available copy

DISCLAIMER

This document was prepared as an account of work sponsored by the United States Government. While this document is believed to contain correct information, neither the United States Government nor any agency thereof, nor the Regents of the University of California, nor any of their employees, makes any warranty, express or implied, or assumes any legal responsibility for the accuracy, completeness, or usefulness of any information, apparatus, product, or process disclosed, or represents that its use would not infringe privately owned rights. Reference herein to any specific commercial product, process, or service by its trade name, trademark, manufacturer, or otherwise, does not necessarily constitute or imply its endorsement, recommendation, or favoring by the United States Government or any agency thereof, or the Regents of the University of California. The views and opinions of authors expressed herein do not necessarily state or reflect those of the United States Government or any agency thereof or the Regents of the University of California.

LBL 31792

NMR Studies of the Conformation and Motion of Tetrahydrofuran in Graphite Intercalation Compounds

by

Daniel Franz Caplan

Department of Chemistry
University of California

and

Materials Sciences Division
Lawrence Berkeley Laboratory
University of California
Berkeley, California 94720

November 1991

This work was supported by the Director, Office of Energy Research, Office of Basic Energy Sciences, Materials Sciences Division of the U.S. Department of Energy, under Contract No. DE-AC03-76SF00098.

Abstract

The behavior of tetrahydrofuran (THF) molecules intercalated in graphite layers in the compounds $Cs(THF)_{1.3}C_{24}$ and $K(THF)_{2.5}C_{24}$ was studied by proton NMR. The graphite layers in these compounds impose a uniform ordering on the THF molecules, giving rise to sharp NMR spectra. Experimental and simulated proton NMR spectra were used to investigate the geometry, orientation and conformation of the intercalated THF, and to determine whether pseudorotation, a large amplitude low frequency vibration observed in gaseous THF, can also occur in the constrained environment provided by the graphite intercalation compounds. Deuterium and multiple quantum proton NMR spectra were also simulated in order to determine if these techniques could further refine the proton NMR results.

Contents

1 Introduction: THF, Pseudorotation, and GIC's **1**

2 The GIC Samples **6**
- 2.1 The Samples 6
- 2.2 Other Alkali Metal GIC's 10

3 Theoretical **11**
- 3.1 Spin Mechanics 11
  - 3.1.1 Spin 1/2 11
  - 3.1.2 The Molecular Spin Hamiltonian 15
  - 3.1.3 The Effects of Molecular Motion 17
- 3.2 Calculating the Single Quantum Spectrum 18
- 3.3 Modeling the THF Molecule 21

4 Simulation and Experiments **26**
- 4.1 Technical 26
- 4.2 Theoretical and Experimental Results 27
  - 4.2.1 Results for $Cs(THF)_{1.3}C_{24}$ 27
  - 4.2.2 Results for $K(THF)_{2.5}C_{24}$ 39

5 Deuterium and Multiple Quantum Simulations **52**
- 5.1 Multiple Quantum Simulations 52
- 5.2 Deuterium Spectra 56

6 Conclusions **64**

Appendix I **67**

Appendix II **80**

References **87**

List of Figures

1.1 Pseudorotation of the THF molecule 3

2.1 Daumas-Herold pleated layer model 8
2.2 Mosaic spread of the samples 9

3.1 Angles determining the rotational scaling 18
3.2 Plot of $(3\cos^2\Theta - 1)/2$ 19
3.3 Parameters used to model the THF molecule 23
3.4 The symmetric conformations of the THF molecule 24
3.5 Calculation of the hydrogen atom coordinates 25

4.1 Spectra of $Cs(THF)_{1.3}C_{24}$ as a function of Θ 28
4.2 $Cs(THF)_{1.3}C_{24}$ simulations for q = 0.38 Å 30
4.3 $Cs(THF)_{1.3}C_{24}$ simulations for q = 0.38 Å 31
4.4 $Cs(THF)_{1.3}C_{24}$ simulations for q =0.32 Å 33
4.5 The best fits for $Cs(THF)_{1.3}C_{24}$ 34
4.6 $Cs(THF)_{1.3}C_{24}$ simulations for different chemical shifts 36
4.7 Pseudorotation potentials for THF 37
4.8 Spectra of $Cs(THF)_{1.3}C_{24}$ at 213 K 40
4.9 Powder spectrum simulation for $Cs(THF)_{1.3}C_{24}$ 41
4.10 THF molecule in $Cs(THF)_{1.3}C_{24}$ 42
4.11 Spectra of $K(THF)_{2.5}C_{24}$ as a function of Θ 43
4.12 Orientation of the THF molecule in the $K(THF)_{2.5}C_{24}$ 45
4.13 $K(THF)_{2.5}C_{24}$ simulations with $\beta = 90°$ 46
4.14 $K(THF)_{2.5}C_{24}$ simulations for several THF orientations 48
4.15 $K(THF)_{2.5}C_{24}$ simulations for $\beta = 56°$ 49
4.16 The best fits for $K(THF)_{2.5}C_{24}$ 50
4.17 THF molecule in $K(THF)_{2.5}C_{24}$ 51
4.18 THF molecule in $K(THF)_{2.5}C_{24}$ 51

5.1 Six quantum simulations for $Cs(THF)_{1.3}C_{24}$ 54
5.2 Seven quantum simulations for $Cs(THF)_{1.3}C_{24}$ 55
5.3 Six quantum simulations for $K(THF)_{2.5}C_{24}$. 57
5.4 Seven quantum simulations for $K(THF)_{2.5}C_{24}$ 58
5.5 Simulated deuterium spectra for $Cs(THF)_{1.3}C_{24}$ 62
5.6 Simulated deuterium spectra for $K(THF)_{2.5}C_{24}$ 63

Acknowledgements

Thanks, of course, to Professor Alex Pines for the opportunity to work under his guidance. Without his encouragement and support this work would not have been possible. Special thanks to Professor Claudia Schmidt, who collaborated on this project, for being a knowledegeable, insightful and patient mentor, as well as a cheerful coworker. Thanks to Dr. M. F. Quinton, at the ESPCI in Paris, for sharing her experimental data and knowledge of GIC's , and for her long-distance collaboration and advice, and to Mark Rosen, who is continuing this project, for many helpfull discussions and for meticulously proofreading this thesis. Finally, thanks also to the Pinenuts, including Dan Raftery, Tom Jarvie, and many others, for making my stay in Berkeley fun.

Chapter 1

Introduction: THF, Pseudorotation, and GIC's

This thesis describes work carried out to investigate the properties and behavior of molecules of thetrahydrofuran, THF, intercalated in graphite layers. Graphite intercalation compounds, or GIC's, are interesting for several reasons. First, the conductivity of GIC's depends on the nature and behavior of the intercalated species, so they may be of practical use in batteries and conductors [1]. Second, GIC's are models for quasi-two-dimensional systems [2, 3]. Finally, the graphite layers can impose spatial ordering on the intercalated species, as do liquid crystals when they are solvents for other molecules. This ordering makes GIC's a useful means of examining the behavior of oriented molecules.

The two GIC's studied here are ternary, consisting of THF and an alkali metal intercalated in the graphite layers. Both compounds are nonstoichiometric, and have approximate compositions $Cs(THF)_{1.3}C_{24}$, and $K(THF)_{2.5}C_{24}$. They are first stage, meaning that there is each graphene sheet is sandwiched between two layers of the intercalated species. The compounds are formed from single platelets of HOPG (highly oriented pyrolytic graphite), so the orientation of the graphite layers is to a large

extent uniform throughout the samples. THF is a particularly good intercalant to study both because of its interesting intramolecular motions and because its behavior in gaseous and liquid crystal phases have been extensively researched.

The THF molecule is not planar, but puckered, as has been shown by experiment and calculations [4–9]. It is the first molecule for which spectroscopic evidence was found for pseudorotation [4, 5], a large amplitude vibration mode in which the phase of the puckering moves about the ring [10–16]. (See Fig. 1.1) Pseudorotation was first postulated in 1947 by Kilpatrick, Pitzer and Spitzer [10, 11] to account for the Raman spectrum and anomalously high entropy of cyclopentane. In their model of pseudorotation, the carbon distance of the carbon atoms from the mean molecular plane is given by

$$z_i = (2/5)^{1/2} q \cos[(4\pi/5)i + \phi]; \tag{1.1}$$

where $i = 0, 1 \ldots 4$ labels the ring atoms, q is the amplitude of the puckering, and ϕ is the phase of the pseudorotation. The motion is called pseudorotation because it can cause a molecule to appear to be rotating. For example, for cyclopentane, at $\phi = 0°$, C_0 is the atom with the largest displacement from the mean molecular plane. If the puckering phase changes to $\phi = 72°$, C_3 is now the atom with maximum displacement from the mean molecular plane. This change in puckering phase makes it appear that the molecule has rotated about its z axis without changing its value of ϕ.

The structure of THF has been studied extensively in the gas phase by theoretical calculations and experiment [4–9, 17, 18]. The results of these studies indicate that the molecule has a high barrier to planarity, between 1200 cm^{-1} and 1400 cm^{-1}

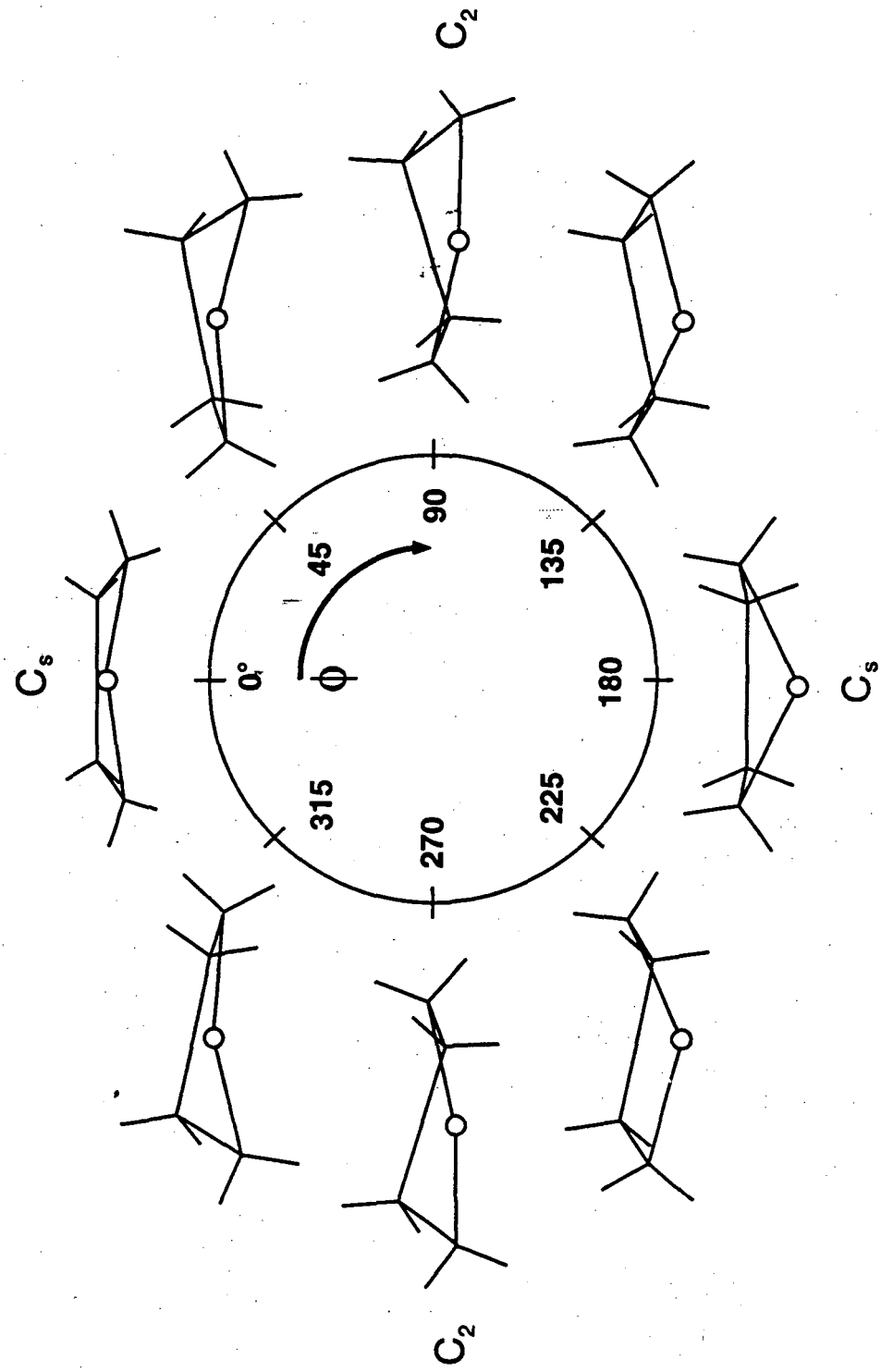

Figure 1.1: Pseudorotation of the THF molecule.

(14.3 to 16.7 kJ/mol) [4, 18], a much lower barrier to pseudorotation, between 40 cm^{-1} and 50 cm^{-1} (0.48 to 0.60 kJ/mol) [4, 7, 18], and a puckering amplitude between q = 0.38 Å and q = 0.44 Å [4, 6, 8, 9, 18]. The pseudorotation potential has been analyzed in terms of the function

$$V(\phi) = V_2 \cos(2\phi) + V_4 \cos(4\phi) \tag{1.2}$$

using data from the far IR and microwave spectra [5, 7, 17], with the coefficients determined to be $V_2 = 13.5$ cm^{-1} (0.161 kJ/mol) and $V_4 = 20$ cm^{-1} (0.239 kJ/mol). This function has maxima at $\phi = 0°$ and 180° and minima at $\phi = 50°$, 130°, 230° and 310°.

More recently, the conformation of THF has been studied for THF dissolved in a liquid crystal by Esteban et. al. [19, 20, 21], giving results that are consistent with the gas phase data. The puckering amplitude was found to be q = 0.39 Å. Although analysis of the molecular conformation in terms of Eq. (1.2) was attempted, the lack of well defined minima in the rms deviation between the observed and calculated dipole couplings prevented the authors from determining unique values for V_2 and V_4. It was concluded, however, that the data is consistent with free pseudorotation.

Proton NMR spectroscopy is a particularly informative way of studying THF/alkali metal GIC's for three reasons. First, previous work shows that the THF molecules in these compounds move rapidly at room temperature, which effectively averages out the intermolecular proton-proton couplings. This leaves only the intramolecular couplings, and their dependence on the orientation and length of the proton–proton internuclear vectors provides valuable information about the molecular conformation, orientation and mobility. Second, the uniform alignment of the graphene layers in

the HOPG results in a single orientational environment for the THF, producing well resolved single-crystal-like spectra. Third, the THF molecule is an eight proton system, generating NMR spectra that, while complicated, are nonetheless amenable to analysis and simulation.

In addition to single quantum proton spectra, simulations were also carried out for six and seven quantum proton spectra, and for single quantum spectra of fully deuterated THF molecules in order to determine if they could refine the results from the single quantum proton spectra. Both of these techniques can greatly reduce the complexity of an NMR spectrum.

The emphasis of this project was to determine the effect of the GIC environment on the THF molecule. Our specific goals were to determine the applicability geometrical model of Kilpatrick, Pitzer and Spitzer [10, 11] to THF in a constrained environment, to investigate the molecular orientation, conformation and the possibility of pseudorotation, and to determine the mobility of the THF molecules and their degree of orientational order. The approach used was to compare experimental spectra with simulations based on different models of molecular conformation, motion and orientation. The next chapter gives more details about the samples and their preparation, and the following one explains the method used to simulate their spectra.

Chapter 2

The GIC Samples

2.1 The Samples

Alkali Metal/THF GIC's were first synthesized in 1969 by Nomine and Bonnetain [22], and can be prepared with several different alkali metals and different stoichiometries, as will be discussed in the following section. The samples studied here are ternary, nonstoichiometric first stage GIC's having compositions $Cs(THF)_{1.3}C_{24}$ and $K(THF)_{2.5}C_{24}$. The stoichiometry of the second sample is typical of K/THF GIC's [23–25], but the Cs/THF ratio of the first differs from the usual value of 1.6 or 1.7 [23, 26]. However, this THF deficiency has no effect on the proton NMR spectra [27]. The differences between $Cs(THF)_{1.3}C_{24}$ and $Cs(THF)_{1.6}C_{24}$ are currently under investigation by M. F. Quinton [27].

Most work on these compounds has been done on powdered samples since they are easier to prepare; however the samples studied here were synthesized from single platelets of Highly Oriented Pyrolytic Graphite, HOPG, which has graphite planes that are parallel throughout the sample. This imposes a uniform alignment on the intercalant, resulting in single crystal-like spectra.

HOPG is actually not a single crystal of graphite, but consists of microcrystallites

of graphite, about 1 μm in size, compacted so that their crystallographic $\vec{c}$ axes, which are perpendicular to the graphene sheets, are aligned to better than 1° [27].

The samples are prepared from second stage MC_{24} HOPG platelets, where M is either Cs or K, by connecting them to a reservoir of liquid THF and allowing gaseous THF to reach the MC_{24}. This must be done in the absence of air and water vapor, and the THF must be highly purified [28, 29]. In order to prevent the THF from condensing on the surface of the MC_{24}, the graphite compound's temperature is kept higher than that of the THF reservoir; usually about 20°C for the GIC and 0 to 10°C for the reservoir [26, 30]. The composition of the sample is determined by monitoring the level of the THF reservoir with a calibrated capillary tube to measure the amount of THF consumed during the synthesis [29, 30].

The results of the synthesis are the first stage compounds studied here. The change from second stage MC_{24} to first stage ternary GIC can be explained using the pleated layer model of Daumas and Herold [3, 31], Fig. 2.1. According to this model the intercalant in an n-stage compound covers a fraction of 1/n of the area of each graphene sheet, rather than the intercalant being present only in one of every n sheets.

The samples were examined by x-ray diffraction to verify that they were uniformly first stage and measure their identity period I_c, which is the distance between the layers of intercalant. For $K(THF)_{2.5}C_{24}$, $I_c = 8.86$ Å and for $Cs(THF)_{1.3}C_{24}$, $I_c = 7.07$ Å. These values are in good agreement with other reported results [23–26]. It should be noted that the interlayer spacing is determined by the size and orientation of the THF molecules, since they are larger than the alkali metals [28].

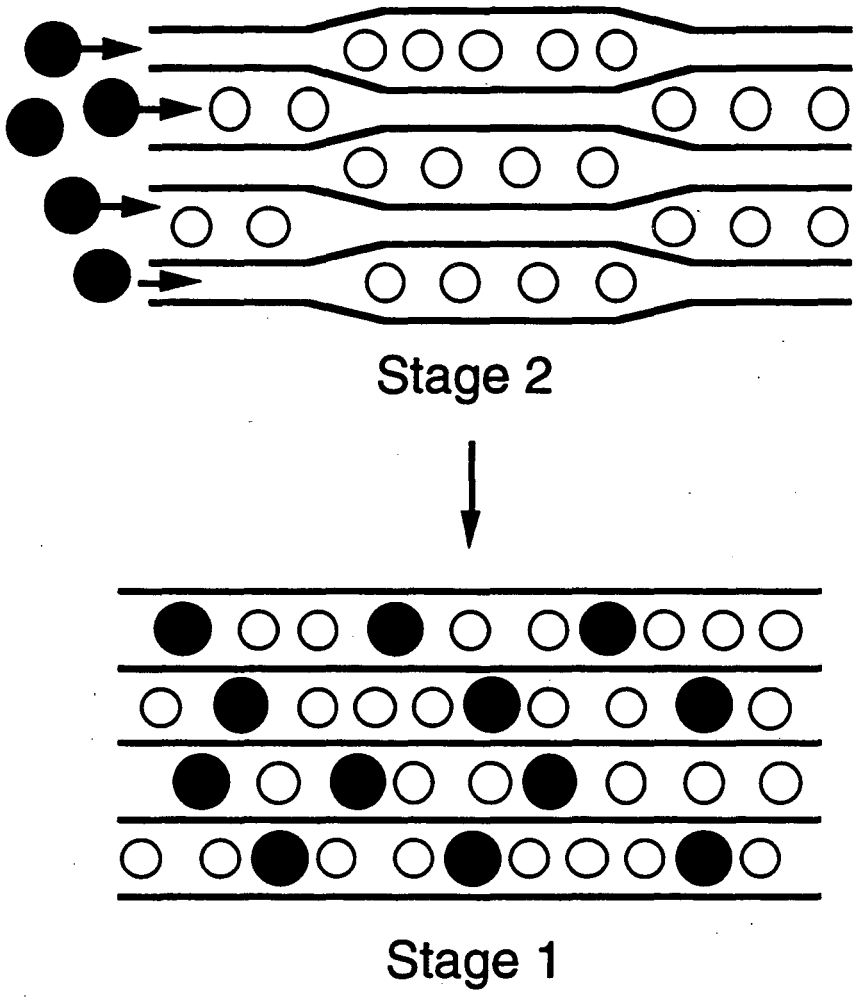

Figure 2.1: Pleated Layer model of Daumas and Herold.

X-ray diffraction was also used to study the mosaic spread of the samples, which corresponds to the misalignment of the $\vec{c}$ axis of the microcrystallites. The results, shown in Fig. 2.2, indicate that there is greater disorder in the $Cs(THF)_{1.3}C_{24}$ compound. The experimental points for the $K(THF)_{2.5}C_{24}$ compound were fit adequately by using one Gaussian, while the $Cs(THF)_{1.3}C_{24}$ sample required three Gaussians, possibly indicating the presence of three separate domains within the sample. The greater disorder in $Cs(THF)_{1.3}C_{24}$ may be due to its faster rate of THF intercalation, which can disturb the alignment of the microcrystallites that constitute the HOPG. The intercalation takes about one day for the Cs compounds and about eight days

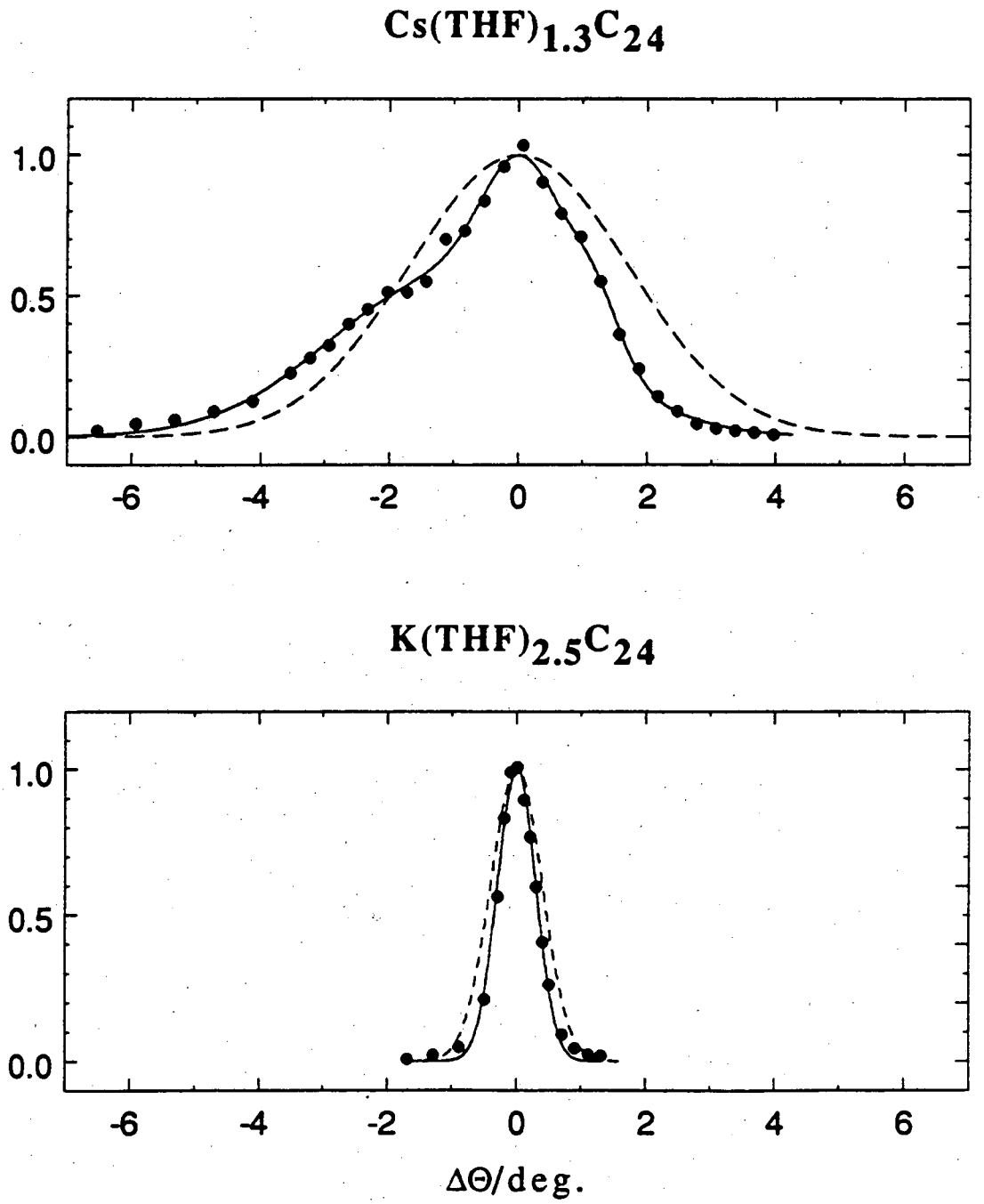

Figure 2.2: Mosaic spread of the $Cs(THF)_{1.3}C_{24}$ and $K(THF)_{2.5}C_{24}$. The dots represent experimental points, the solid lines are Gaussian fits to the points, and the dashed lines represent the distributions used to in the simulated spectra in Figs. 4.1 and 4.11.

for the K compound [27].

2.2 Other Alkali Metal GIC's

Before proceeding to the experimental results, it should be noted that the two compounds studied here represent only a fraction of the known alkali metal GIC's. Both $K(THF)_{2.5}C_{24}$ and $Cs(THF)_{1.6}C_{24}$ are known as saturated compounds, since THF can be deintercalated from either by cryopumping (keeping the GIC at about 20°C and the THF reservoir at -196°C). The resulting compounds, called residual, are first stage $K(THF)_{1.7}C_{24}$, with $I_c = 7.1$ Å, and second stage $Cs(THF)_{0.9}C_{24}$, with $I_c = 10.2$ Å [23, 26, 30, 32, 33]. RbC_{24} can be used to prepare saturated and residual THF-GIC's with the same stoichiometries and I_c's found for the K compounds [23, 28, 30, 32, 34].

All the THF-GIC's mentioned so far have their intercalants arranged in monomolecular layers, but the first stage compound $Li(THF)_{2.1}C_{12}$, with $I_c = 12.45$ Å appears to have the THF molecules arranged in bimolecular layers [22, 24, 35, 36]. Finally, it is also possible to synthesize alkali metal GIC's with other organic molecules such as n-hexane [37] and benzene [38].

Chapter 3

Theoretical

3.1 Spin Mechanics

The purpose of this section is to establish the definitions of the Hermitian spin operators which will be used in the following sections of this thesis. Readers wanting a more detailed explanation should refer to a quantum mechanics or NMR text [39–42].

3.1.1 Spin 1/2

The square of the total spin angular momentum is given by $\hbar^2\mathbf{I}^2$ where

$$\mathbf{I}^2 = \mathbf{I}_x^2 + \mathbf{I}_y^2 + \mathbf{I}_z^2 \tag{3.1}$$

and,

$$[\mathbf{I}^2, \mathbf{I}_x] = [\mathbf{I}^2, \mathbf{I}_y] = [\mathbf{I}^2, \mathbf{I}_z] = 0. \tag{3.2}$$

From this point on, the equations will be presented in units in which $\hbar = 1$ in order to simplify the notation, and operators will be presented in bold type.

The commutation relations between the three orthogonal operators $\mathbf{I}_x$, $\mathbf{I}_y$, and $\mathbf{I}_z$ are:

$$[\mathbf{I}_x, \mathbf{I}_y] = i\mathbf{I}_z; \tag{3.3}$$

$$[\mathbf{I}_y, \mathbf{I}_z] = i\mathbf{I}_x; \tag{3.4}$$

$$[\mathbf{I}_z, \mathbf{I}_x] = i\mathbf{I}_y. \tag{3.5}$$

The very useful raising and lowering operators, $\mathbf{I}_+$ and $\mathbf{I}_-$, can be defined in terms of $\mathbf{I}_x$ and $\mathbf{I}_y$ as follows:

$$\mathbf{I}_+ = \mathbf{I}_x + i\mathbf{I}_y; \tag{3.6}$$

$$\mathbf{I}_- = \mathbf{I}_x - i\mathbf{I}_y. \tag{3.7}$$

The states on which the above operators act are defined as eigenstates of $\mathbf{I}^2$ and $\mathbf{I}_z$, and written as $|I, m>$, where I is the total spin angular momentum and m its $\vec{z}$ component, which can have values of $(-I, -I+1, \ldots I)$. Thus for a spin $\mathbf{I} = 1/2$ particle, the two states are: $|\alpha> = |\frac{1}{2}, \frac{1}{2}>$ and $|\beta> = |\frac{1}{2}, -\frac{1}{2}>$. The eigenvalues of the spin operators, when acting on $|\alpha>$ and $|\beta>$ are:

$$\mathbf{I}_+|\alpha> = 0; \tag{3.8}$$

$$\mathbf{I}_-|\alpha> = |\beta>; \tag{3.9}$$

$$\mathbf{I}_+|\beta> = |\alpha>; \tag{3.10}$$

$$\mathbf{I}_-|\beta> = 0; \tag{3.11}$$

$$\mathbf{I}_z|\alpha> = \frac{1}{2}|\alpha>; \tag{3.12}$$

$$\mathbf{I}_z|\beta> = -\frac{1}{2}|\beta>; \tag{3.13}$$

The expectation value of an operator $\mathbf{A}$ in terms of the wavefunction $|b>$ is:

$$<\mathbf{A}> = <b|\mathbf{A}|b>. \tag{3.14}$$

If $|b>$ is a normalized eigenfunction of $\mathbf{A}$ with an eigenvalue of a then:

$$< \mathbf{A} > \; = < b|\mathbf{A}|b > \; = < b|a|b > \; = \; a < b|b > \; = \; a. \tag{3.15}$$

Otherwise $|b>$ can be a linear combination of eigenfunctions of $\mathbf{A}$:

$$|b> \; = \; c_1|r> + c_2|s>, \tag{3.16}$$

with

$$\mathbf{A}|r> \; = \; r|r> \tag{3.17}$$

and

$$\mathbf{A}|s> = \; s|s> . \tag{3.18}$$

In this case the expectation value of $\mathbf{A}$ is:

$$< \mathbf{A} > = < b|\mathbf{A}|b > = (< r|c_1^* + < s|c_2^*)\mathbf{A}(c_1|r> + c_2|s>) = c_1^* c_1 r + c_2^* c_2 s \tag{3.19}$$

This result indicates that for a single measurement of $\mathbf{A}$ made on a single particle in a superposition of states defined in Eq. (3.16) there is a probability equal to $c_1^* c_1$ of obtaining r as a result and $c_2^* c_2$ of obtaining s.

NMR experiments, however, are carried out on large numbers of particles whose individual wavefunctions are not known, so it would be more useful to be able to predict the result of a measurement made on a large number of particles. The following definitions, combined with use of the density matrix, will allow us to make such predictions. For a system of n particles, the operators for the system are the sum of the operators for the individual particles, while the wavefunctions for the system are the products of the wavefunctions of the individual particles (This is known as the

uncoupled representation and is not the only possible meaningful representation. See Ref. 39). For example, for a system consisting of two spin 1/2's:

$$\mathbf{I}_z = \mathbf{I}_{z1} + \mathbf{I}_{z2} \tag{3.20}$$

$$|\phi_1> = |\alpha_1> |\alpha_2> = |\alpha_1\alpha_2>, \tag{3.21}$$

$$|\phi_2> = |\beta_1\alpha_2>, \tag{3.22}$$

$$|\phi_3> = |\alpha_1\beta_2>, \tag{3.23}$$

$$|\phi_4> = |\beta_1\beta_2> . \tag{3.24}$$

The density operator ρ allows calculation of the results of a measurement made on an ensemble without knowing the details of the wavefunction of each of its members. Some useful definitions and properties of ρ are:

$$\rho = \frac{1}{Z} e^{-\mathbf{H}/kT} \tag{3.25}$$

where $Z = \sum_{m=1}^{n} e^{-E_m/kT}$ and $\mathbf{H}$ is the system's time independent Hamiltonian;

$$Tr(\rho) = \sum_{m=1}^{n} <\phi_m|\rho|\phi_m> = 1 \tag{3.26}$$

$$Tr(\rho\mathbf{A}) = Tr(\mathbf{A}\rho) \tag{3.27}$$

$$<A> = Tr(\rho\mathbf{A}) = \sum_{m=1}^{n} <\phi_m|\rho\mathbf{A}|\phi_m> \tag{3.28}$$

$$\rho(t) = e^{i\mathbf{H}t}\rho(0)e^{-i\mathbf{H}t}. \tag{3.29}$$

The property defined in Eq. (3.27) does not only apply to density matrices but is a general property of the trace of two operators.

The density operator, defined in Eq. (3.25) above, can be expanded in a power series as:

$$\rho = \frac{1}{Z}(1 - \mathbf{H}/kT + \ldots) \tag{3.30}$$

Only the first two terms were retained because at room temperature $E << kT$ for the range of energies typically encountered in an NMR experiment. The expression can be further simplified by noting that, in our experiments, we are only measuring the oscillating part of a signal; while the factors $1/Z$, the unity matrix (1 in Eq. (3.30) above), and $1/kT$ will not vary in time. Eliminating these constants results in

$$\rho = \mathbf{H} \tag{3.31}$$

which greatly simplifies our calculations.

3.1.2 The Molecular Spin Hamiltonian

In its simplest form a pulsed NMR experiment is carried out by irradiating the sample with a radio frequency pulse of sufficient duration to rotate the sample's magnetization from its initial alignment along the z axis to one along the x axis. After this, the magnetization evolves under the influence of the sample's Hamiltonian, and the precessing magnetization is monitored by coils which define the laboratory x and y axes. The Hamiltonian is given by:

$$\mathbf{H} = \mathbf{H}_0 + \mathbf{H}_{CS} + \mathbf{H}_D + \mathbf{H}_J \tag{3.32}$$

where $\mathbf{H}_0$ describes the Zeeman interaction, $\mathbf{H}_{CS}$ the chemical shift, $\mathbf{H}_D$ the dipole interaction, and $\mathbf{H}_J$ the J coupling, which is a term commonly encountered in NMR of liquids. Here $\mathbf{H}_J$ can be ignored since its effects are negligible compared to the

linewidths of our samples. The three remaining terms will now be explained in more detail.

The Zeeman Hamiltonian $\mathbf{H}_0$, in units of Hz, is given by

$$\mathbf{H}_0 = -\sum_j \nu_j \mathbf{I}_{z,j} \tag{3.33}$$

where ν_j is the Larmour frequency. This term exists because of the interaction between the magnetic moments of the spins and the static magnetic field $\vec{B}_0$. The chemical shift Hamiltonian, for a molecule undergoing random motion, is given by:

$$\mathbf{H}_{CS} = \sum_j \Delta\nu_j \mathbf{I}_{z,j} \tag{3.34}$$

where $\Delta\nu_j$ is the shift in frequency corresponding to nucleus j. The Zeeman interaction will be ignored here because the frequency of the rotating frame (the RF frequency) is assumed to be at the resonance frequency of one of the nuclei (i. e. the Larmour frequency of the nucleus plus its chemical shift). The chemical shift in Eq. (3.34) then represents the difference in chemical shift between that nucleus and the remaining nuclei, which is also known as resonance offset.

The dipole Hamiltonian is the term of greatest interest to us, since its effects dominate the spectra presented in this thesis. The full dipole Hamiltonian is given by

$$\mathbf{H}_D = \sum_i \sum_{j>i} \mathbf{H}_D^{ij}, \tag{3.35}$$

where i and j label the spins and where

$$\mathbf{H}_D^{ij} = -\frac{\gamma^2\hbar}{2\pi r_{ij}^3}\frac{1}{2}(3\cos^2\theta_{ij} - 1)(\mathbf{I}_j\mathbf{I}_k - \frac{3(\mathbf{I}_j\cdot\vec{r})(\mathbf{I}_j\cdot\vec{r})}{r_{ij}^2}). \tag{3.36}$$

where $\vec{r}$ is the vector joining the two spins i and j, r_{ij} is the distance between the spins, θ_{ij} is the angle between $\vec{r}$ and $\vec{B}_0$, and the units are given in Hz. By converting

$\vec{r}$ to spherical coordinates and truncating the terms that do not commute with the much larger Zeeman Hamiltonian, the dipole Hamiltonian becomes:

$$\mathbf{H}_D^{ij} = -\frac{\gamma^2\hbar}{2\pi r_{ij}^3}\frac{1}{2}(3\cos^2\theta_{ij} - 1)[2\mathbf{I}_{z,i}\mathbf{I}_{z,j} - \frac{1}{2}(\mathbf{I}_{+,i}\mathbf{I}_{-,j} + \mathbf{I}_{-,i}\mathbf{I}_{+,j})] \tag{3.37}$$

In summary, the Hamiltonian relevant to the simulations presented here is:

$$\mathbf{H} = \sum_j \Delta\nu_j \mathbf{I}_{z,j} - \sum_i \sum_{j>i} \mathbf{H}_D^{ij} \tag{3.38}$$

which is the sum of the chemical shift and dipole Hamiltonians, as written in Eqs. (3.34) and (3.37).

3.1.3 The Effects of Molecular Motion

There are two kinds of motion that are of interest to this study: rapid conformational changes, and rapid rotation, where rapid means that the changes occur quickly compared to the timescale of the NMR experiment. For rapid motion the spectrum can be calculated using a Hamiltonian which has been averaged over the motion. For example, for a THF molecule rapidly interconverting between the $\phi = 0°$ and $\phi = 90°$ conformations, the spectrum is calculated using dipole couplings that are averaged over the two conformations, and any intermediate conformations that occur during the conversion.

Another type of molecular motion relevant to the simulations presented here is rapid rotation. If a molecule rotates about an axis $\vec{c}$, the factor $(3\cos^2\theta_{ij} - 1)$ in Eq. (3.37) becomes:

$$\frac{1}{2}(3\cos^2\Theta - 1)(3\cos^2\beta_{ij} - 1) \tag{3.39}$$

where Θ is the angle between the applied field $\vec{B}_0$ and the axis of rotation $\vec{c}$, and β_{ij} is the angle between the internuclear vector $\vec{r}_{ij}$ and $\vec{c}$ [43, 44] as shown in Fig. 3.1.

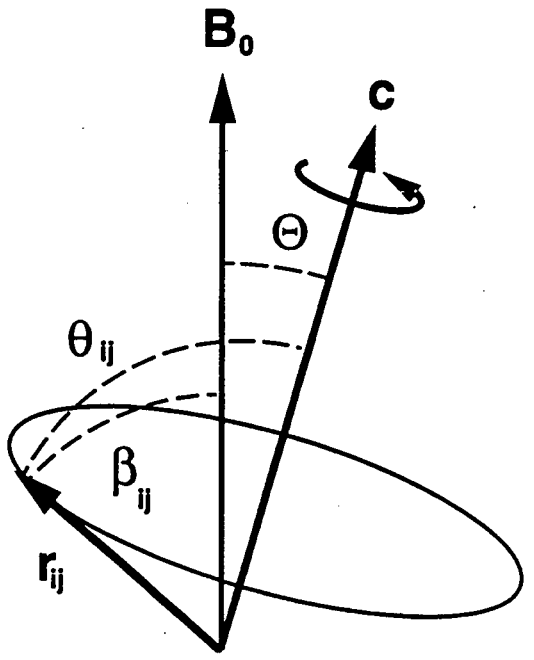

Figure 3.1: Angles used in Eq. (3.39).

This means that the spectrum of a rapidly spinning molecule will scale by a factor of $(3\cos^2\Theta - 1)$ as the axis of rotation is changed. This function is plotted in Fig. 3.2. If $\vec{c}$ and $\vec{B}_0$ coincide, the rotation will have no effect since the scaling factor becomes 1; if the $\vec{c}$ is perpendicular to $\vec{B}_0$ the spectrum scales by a factor of -1/2, and at the Magic Angle, $\Theta_M = 54.7°$, the dipole coupling disappears altogether.

3.2 Calculating the Single Quantum Spectrum

The signal from a single quantum experiment can be calculated using the density operator as follows:

$$Signal \;=\; Tr[\rho(t)\mathbf{A}] \tag{3.40}$$

where $\mathbf{A}$ is the observable to be measured. The experimental observables are the magnetization along the x axis, proportional to $\mathbf{I}_x$, which is digitized and stored in

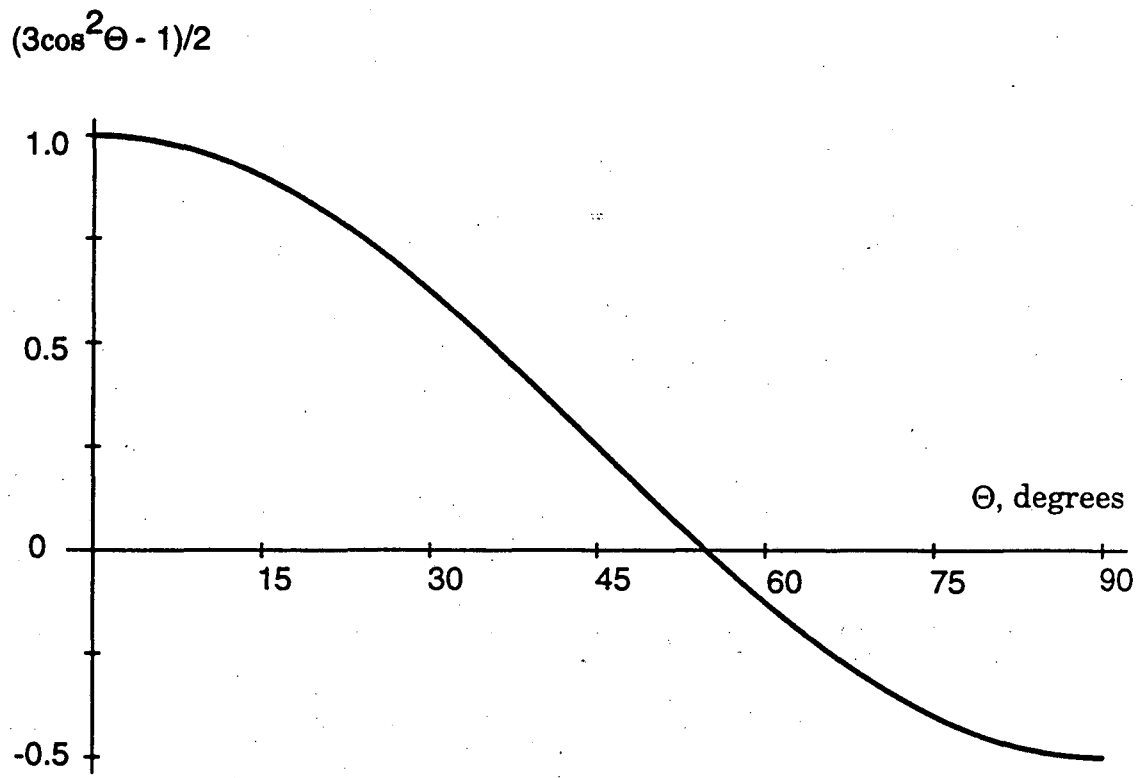

Figure 3.2: Plot of $(3cos^2\Theta - 1)/2$.

computer memory as real numbers, and the magnetization along the y axis, $\mathbf{I}_y$, which is digitized and stored as imaginary numbers. The observable is therefore

$$\mathbf{A} = \mathbf{I}_x + i\mathbf{I}_y = \mathbf{I}_+. \tag{3.41}$$

The initial density operator can be approximated by the system's initial Hamiltonian, Eq. (3.31), which is $\mathbf{I}_x$ after the application of the 90° pulse that begins the experiment. The time evolution of the density matrix is given by Eq. (3.29), so the time dependent signal is given by:

$$S(t) = Tr(e^{-i\mathbf{H}t}\mathbf{I}_x e^{i\mathbf{H}t}\mathbf{I}_+) \tag{3.42}$$

or,

$$S(t) = \sum_i < i|e^{-i\mathbf{H}t}\mathbf{I}_x e^{i\mathbf{H}t}\mathbf{I}_+|i > \tag{3.43}$$

where $\mathbf{H}$ is the Hamiltonian given in Eq. (3.38) and $\sum_i < i|\ldots|i >$ is shorthand notation for $\sum_{n=1}^{256} < i_n|\ldots|i_n >$, a sum over the 256 eigenstates of the eight spin operator $\mathbf{I}_z$. This equation contains everything needed to calculate the simulations presented here, but it must now be converted to a form which can be numerically evaluated on a computer. The remainder of this section is dedicated to this task.

The internal Hamiltonian, $\mathbf{H}$, can be rewritten as

$$\mathbf{H} = BDB^\dagger \tag{3.44}$$

where D is a diagonal matrix whose elements are the eigenvalues of $\mathbf{H}$, and the unitary matrix B and its adjoint $B^\dagger$ diagonalize $\mathbf{H}$. Now the time development operator can be rewritten as

$$e^{i\mathbf{H}t} = e^{iBDB^\dagger t} = Be^{iDt}B^\dagger \tag{3.45}$$

which can be verified by a series expansion of both sides of the equation. The signal can now be written as:

$$S(t) = \sum_i < i|Be^{-iDt}B^\dagger \mathbf{I}_x Be^{iDt}B^\dagger \mathbf{I}_+|i > \tag{3.46}$$

$$= \sum_i < i|e^{-iDt}B^\dagger \mathbf{I}_x Be^{iDt}B^\dagger \mathbf{I}_+ B|i > \tag{3.47}$$

where Eq. (3.27) was used. This will be further modified by using the identity operator:

$$\sum_a |a >< a| = 1 \tag{3.48}$$

(see Ref. 40), to break this sum into four independent summations:

$$S(t) = \sum_{i,j,k,m} < i|e^{-iDt}|j >< j|B^\dagger \mathbf{I}_x B|k >< k|e^{iDt}|m >< m|B^\dagger \mathbf{I}_+ B|i > \tag{3.49}$$

where $\sum_{i,j,k,m}$ is shorthand for $\sum_i \sum_j \sum_k \sum_m$. Since D is diagonal, $< n|e^{iDt}|m >= e^{iD_{nm}t}\delta_{nm}$, so the signal can be rewritten as:

$$S(t) = \sum_{i,j} e^{-i\omega_i t} < i|B^\dagger \mathbf{I}_x B|k > e^{i\omega_k t} < k|B^\dagger \mathbf{I}_+ B|i > \tag{3.50}$$

where $\omega_i = D_{ii}$ and $\omega_k = D_{kk}$; leaving:

$$S(t) = \sum_{i,k} e^{-i(\omega_i - \omega_k)t} < i|B^\dagger \mathbf{I}_x B|k >< k|B^\dagger \mathbf{I}_+ B|i > \tag{3.51}$$

At this point the signal's time dependence could be calculated by carrying out the sums over i and j in Eq. (3.51) above for increasing values of t until an FID of the desired length and resolution is accumulated, which could be Fourier transformed to provide a spectrum. On the other hand, much calculation can be avoided by noting the similarity between Eq. (3.51) and the formula for the Fourier transform of a spectrum, and realizing that the term $e^{-i(\omega_i - \omega_k)t}$ corresponds to the frequency in a spectrum, and the term $\sum_{i,k} < i|B^\dagger \mathbf{I}_x B|k >< k|B^\dagger \mathbf{I}_+ B|i >$ to the intensity at that frequency. This means that Eq. (3.51) can be used to obtain a spectrum directly. In order to match the experimental resolution, the lines falling within a bandwidth of frequencies equal to the experimental resolution can be added together. The experimental linewidth can be matched by inverse Fourier transforming the spectrum, multiplying the resulting FID by a decaying exponential, and Fourier transforming again. For details about the calculations, see Appendix I, which contains the programs used to simulate the spectra.

3.3 Modeling the THF Molecule

The preceding section described a method to predict the spectrum of a system of dipole coupled spins. In order to apply this method to a molecule such as THF, it

is necessary to know the geometry of the spins which generate the spectrum. This section describes the relatively simple and accurate geometrical model used here, originally used by Geise et. al. [6] to calculate the electron diffraction spectrum of gaseous THF.

Geise's model only applies to the "heavy" atoms, i. e. carbon and oxygen, since the hydrogen atoms do not affect the electron diffraction spectrum. The heavy atoms are labeled C_0, $C_1 \ldots C_4$, where C_0 corresponds to the oxygen, and C_1 through C_4 are the carbons. First the z coordinates are calculate using:

$$z_i = (2/5)^{1/2} q \cos[(4\pi/5)i + \phi]; \; j = 0, 1 \ldots 4 \tag{3.52}$$

where q is a measure of the amount of "puckering" in the molecule and ϕ is the pseudorotation angle. At this point the x, y coordinates are calculated using Geise's improved version of the model of Pitzer et. al. [6, 10–12].

Each atom is connected to the origin by an imaginary spoke of length S_0, shown in Fig. 3.3. To account for the different lengths of the C–O and C–C bonds, two different angles, ϵ and δ, are used to separate the spokes; δ is used for the C–O bonds, and ϵ for the C–C bonds. In order to leave the bond lengths approximately unchanged as the atom's z coordinate varies, the spoke length S_0 is replaced by S_j, defined as follows:

$$S_j = S_0(1 - kz_j^2); \tag{3.53}$$

with $k = 0.65$ Å^{-2}. The C atom coordinates are given by

$$x_j = S_j \cos[\delta + (j-1)\epsilon]; \tag{3.54}$$

$$y_j = S_j \sin[\delta + (j-1)\epsilon]; \tag{3.55}$$

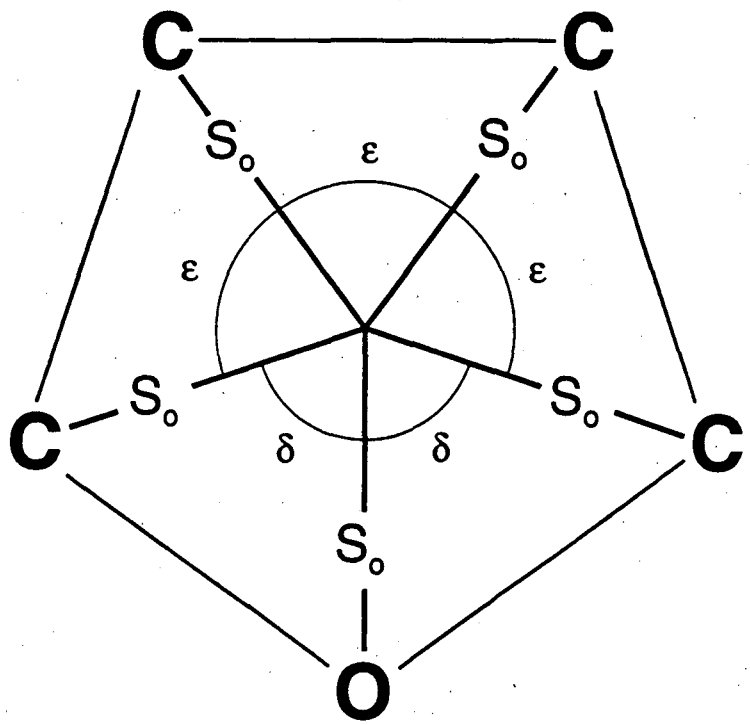

Figure 3.3: Definitions of the parameters used to determine the molecular geometry. The oxygen atom's x, y coordinates are defined as $x_0 = S$ and $y_0 = 0$.

According to the definitions above there are four values of ϕ which will produce a molecule of defined symmetry: $\phi = 0°$ and $\phi = 180°$ produce C_s symmetry; $\phi = 90°$ and $\phi = 270°$ produce C_2 symmetry. Two of the symmetric conformations are shown in Fig. 3.4.

The hydrogen atoms are attached to the carbon atoms so that the plane formed by the carbon and its two hydrogens is perpendicular to the plane formed by that same carbon and its two nearest heavy atom neighbors (see Fig. 3.5). The bisector of the H–C–H angle lies along the intersection of these two planes. This geometry was achieved by defining a local x, y and z axis determined for each carbon atom C_j using the vectors $\vec{V}_n$, which goes from C_{j+1} to C_j; and $\vec{V}_p$, which goes from C_{j-1} to

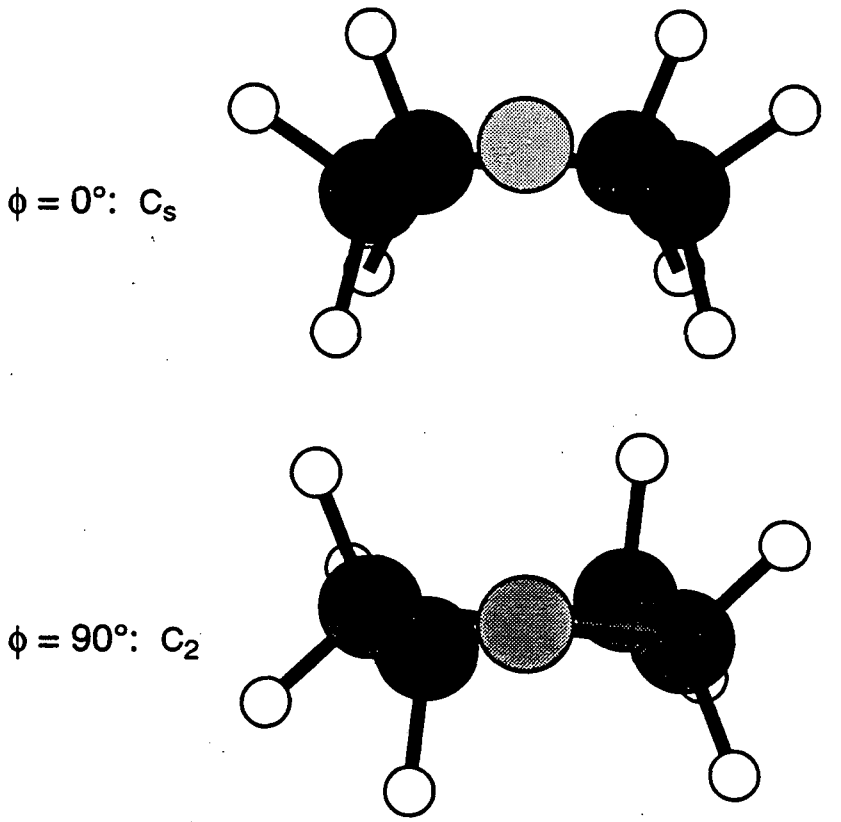

Figure 3.4: The C_s and C_2 conformations of the THF molecule.

C_j as follows:

$$\vec{x}_{loc} = \vec{V}_n + \vec{V}_p \tag{3.56}$$

$$\vec{y}_{loc} = \vec{V}_n - \vec{V}_p \tag{3.57}$$

$$\vec{z}_{loc} = \vec{x}_{loc} \times \vec{y}_{loc}. \tag{3.58}$$

The hydrogen atoms are now positioned in this local reference frame according to:

$$x_{loc} = 0; \tag{3.59}$$

$$y_{loc} = (b_{CH})\cos(a_{HCH}/2); \tag{3.60}$$

$$z_{loc} = \pm(b_{CH})\sin(a_{HCH}/2); \tag{3.61}$$

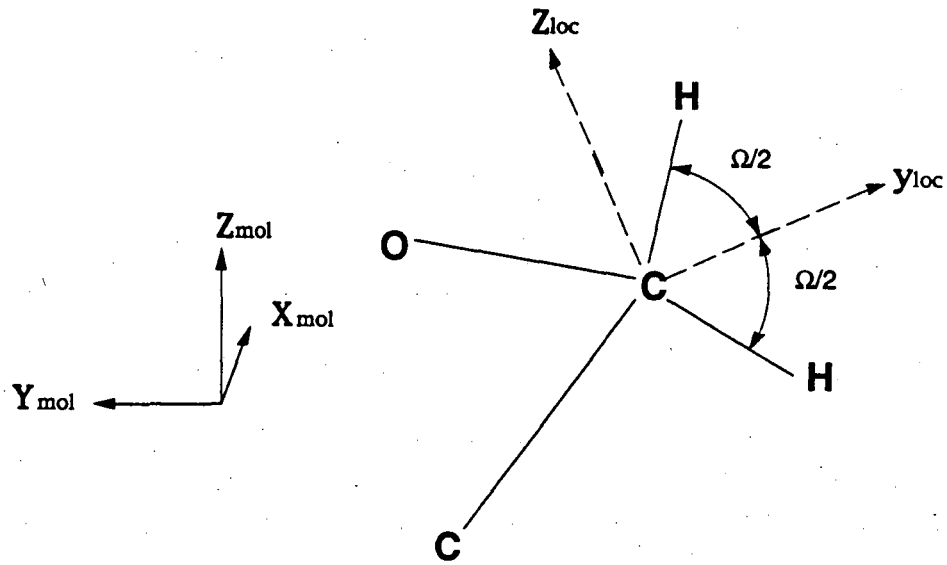

Figure 3.5: The local and molecular axis systems used to calculate the hydrogen atom positions.

where b_{CH} is the length of the C-H bond and a_{HCH} is the H–C–H angle.

The hydrogen atom positions determined in terms of these local vectors are then added to the vector from the molecular origin to C_j to obtain the H atom positions in terms of the overall molecular coordinates. (For a more detailed description, see Appendix II, which contains a copy of the program used to generate the molecular coordinates.) The parameters used to generate the THF molecule are listed in Table 3.1.

Parameter	Value
δ	74.52°
ϵ	68.22°
k	0.65 $Å^{-2}$
S_0	1.277 Å
C-H Bond	1.115 Å
H-C-H Angle	109.5°

Table 3.1: Geometrical Parameters for THF

Chapter 4

Simulation and Experiments

4.1 Technical

The simulations presented here were carried out with programs written in Modula 2, Pascal and Fortran by Dr. Claudia Schmidt and the author. The program used to calculate the single quantum proton spectra followed the method outlined in the preceding chapter, and took approximately 45 minutes to run on a Micro Vax II computer, and is given in Appendix I.

The experimental spectra presented here were taken by Dr. M. F. Quinton and the samples were prepared by F. Beguin, both at the Laboratoire de Physique Quantique at the Ecole Superieure de Physique et de Chimie Industrielles in Paris. The experiments were performed on a Bruker CXP 100 spectrometer, at a proton frequency of 100 MHz. Typical experimental parameters are listed and explained in Table 4.1. The experimental spectra were truncated to 512 points and zero-filled back to 2048 points. Baseline correction and constant phase correction were required, but linear phase correction was not. Exponential multiplication was not performed. The angle Θ between the sample's $\vec{c}$ axis and $\vec{B}_0$ was determined by eye; according to M. F. Quinton the alignment uncertainty is $\pm 2.5°$ for $\Theta = 0°$ and $90°$, and $\pm 10°$ for in-

Sample	Cs, 293 K	Cs, 213 K	K, 293 K
RF Frequency	100.13 MHz	100.13 MHz	100.09 MHz
RF Field	39.15 G	29.35 G	63.05 G
Pulse Length (90°)	1.5 μsec	2 μ sec	0.92 μ sec
Dead Time	1 μsec	1 μ sec	2 μ sec
T_1	0.3 $\sim$ 0.6 sec	$\approx$ 4 sec	0.3 $\sim$ 0.6 sec
Scans	250	256	360
Resolution	61.76 Hz/pt	123.52 Hz/pt	122.07 Hz/pt

Table 4.1: Experimental parameters.

termediate angles, although our simulations suggest that the error for intermediate angles was in some cases slightly larger.

4.2 Theoretical and Experimental Results

4.2.1 Results for $Cs(THF)_{1.3}C_{24}$

Figure 4.1 shows experimental spectra for $Cs(THF)_{1.3}C_{24}$ with the mean plane of the graphite layers at several orientations. The spectra all have the same general features, but are scaled by a factor of $(3\cos^2\Theta - 1)$, where Θ is the angle between $\vec{c}$ and the applied field $\vec{B}_0$. This indicates that the THF molecules are rotating rapidly. Furthermore, since the difference in scaling between the 90° and 0° spectra is a factor of two (allowing for error in the sample alignment), the rotation axis is perpendicular to the graphite layers (i. e. parallel to the $\vec{c}$ axis). While the lines are relatively sharp at $\Theta = 0°$ and 90°, they broaden at intermediate orientations because of orientational disorder among the graphite layers. The broadening can be explained by the $(3\cos^2\Theta - 1)$ scaling factor. This function is plotted in Fig. 3.2. While flat near $\Theta = 0°$ and 90°, it changes rapidly for intermediate angles. This means that small differences in the orientation of the rotation axis will have a larger effect on the scaling factor at intermediate angles, resulting in spectra that are less defined at

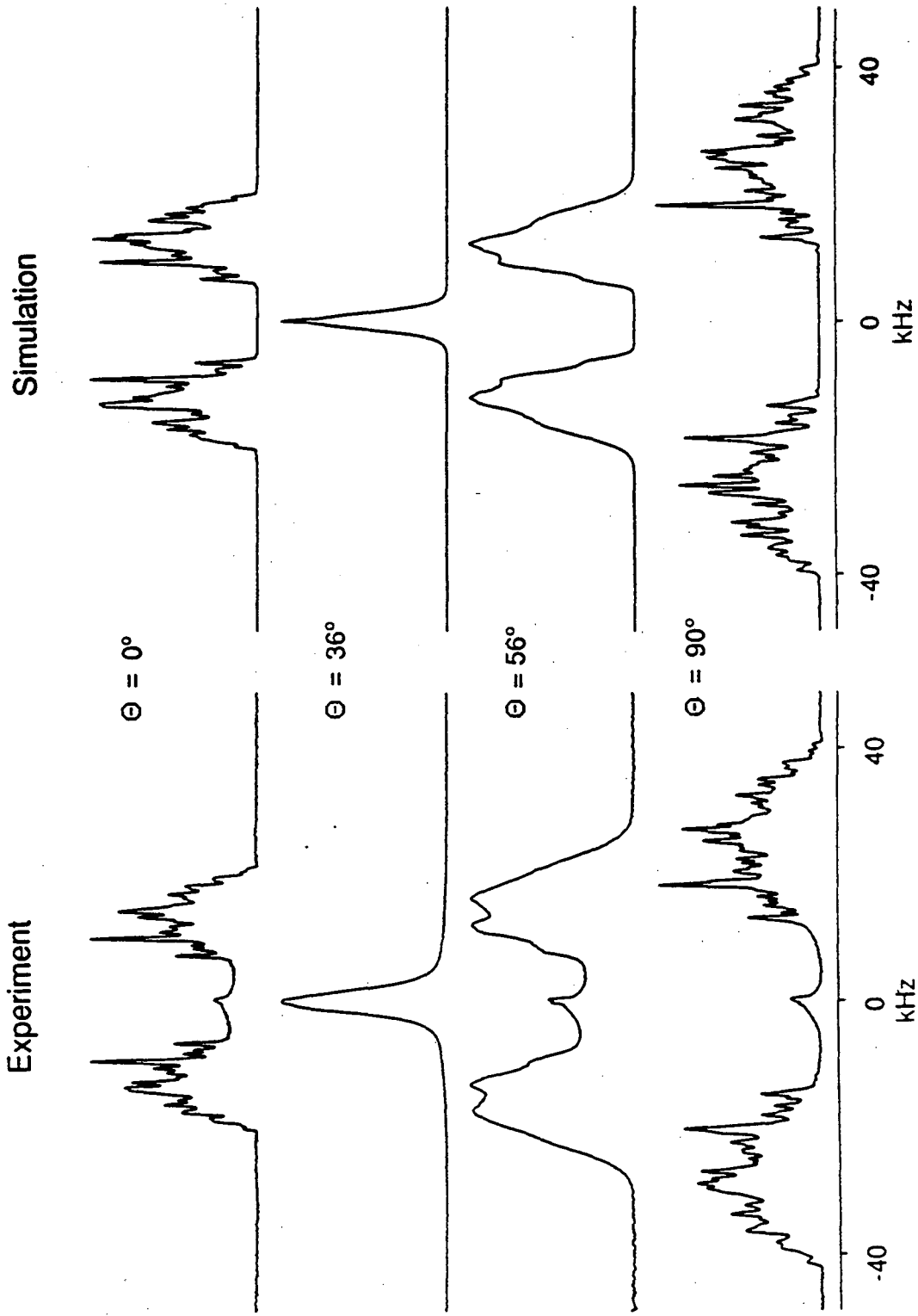

Figure 4.1: Experimental and simulated spectra of $Cs(THF)_{1.3}C_{24}$ as a function of Θ The spectra were calculated for a THF molecule in the C_s conformation with q = 0.32 Å.

these sample orientations.

Although broadening is usually considered to be undesirable, in this case it can be used to advantage, since it gives an idea of the amount of orientational disorder present in the samples. Figure 4.1 shows simulated and experimental spectra for $Cs(THF)_{1.3}C_{24}$ with its $\vec{c}$ axis at several orientations relative to $\vec{B_0}$ The samples were positioned at approximately $\Theta = 0°$, $30°$, Θ_M (54.7°), and 90°, and the values of Θ used in the simulations are indicated in the figure. The simulated spectra were obtained by adding appropriately weighted spectra for THF molecules with a Gaussian orientational distribution of angles θ centered about Θ, with each spectrum scaled by a factor of $(3\cos^2\theta - 1)$. This procedure matches both the sharper lines at $\Theta = 0°$ and 90°, as well as the broader lines at intermediate orientations. For the $Cs(THF)_{1.3}C_{24}$ sample a Gaussian of width of $\sigma = 1.7°$ resulted in good agreement with the experimental spectra. In Fig. 2.2, this Gaussian distribution, given by a dashed line, is compared to the mosaic spread of the samples.

Calculations based on the thickness of a graphene sheet, the size of a THF molecule, and the distance I_c between neighboring graphene layers indicate that in $Cs(THF)_{1.3}C_{24}$, the THF molecules are lying flat against the graphene sheets [28, 45]. Figures 4.2 and 4.3 show an experimental spectrum and several simulations, all for a THF molecule oriented with its mean molcular plane parallel to the graphite planes. The simulations were carried out using the generally accepted parameters for the THF molecular geometry [6, 9] which are listed in Table 3.1. Several different conformations were simulated, including free pseudorotation (Fig. 4.2a, 4.2b), hindered pseudorotation, which averages over the four symmetric conformations: $\phi = 0°$,

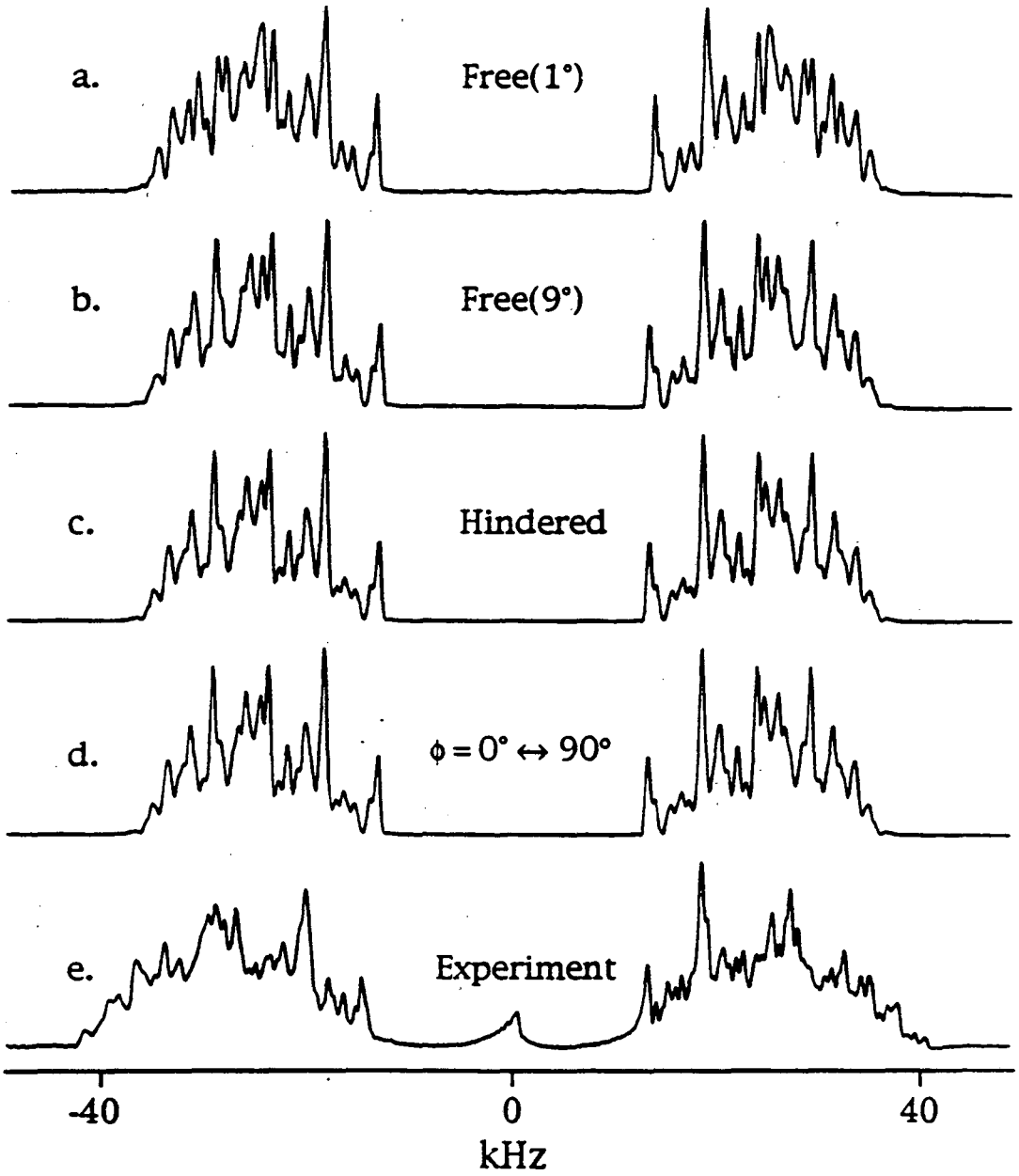

Figure 4.2: Simulated and experimental spectra of the Cs compound. The first two spectra simulate pseudorotation by averaging over dipole couplings for conformations that range from $\phi = 0°$ to $\phi = 360°$ incremented by 1° and 9°, respectively. Hindered pseudorotation averages over $\phi = 0$, 90, 180 and 270°. The last simulation represents interconversion between $\phi = 0°$ and 90° by averaging the dipole couplings over these two conformations.

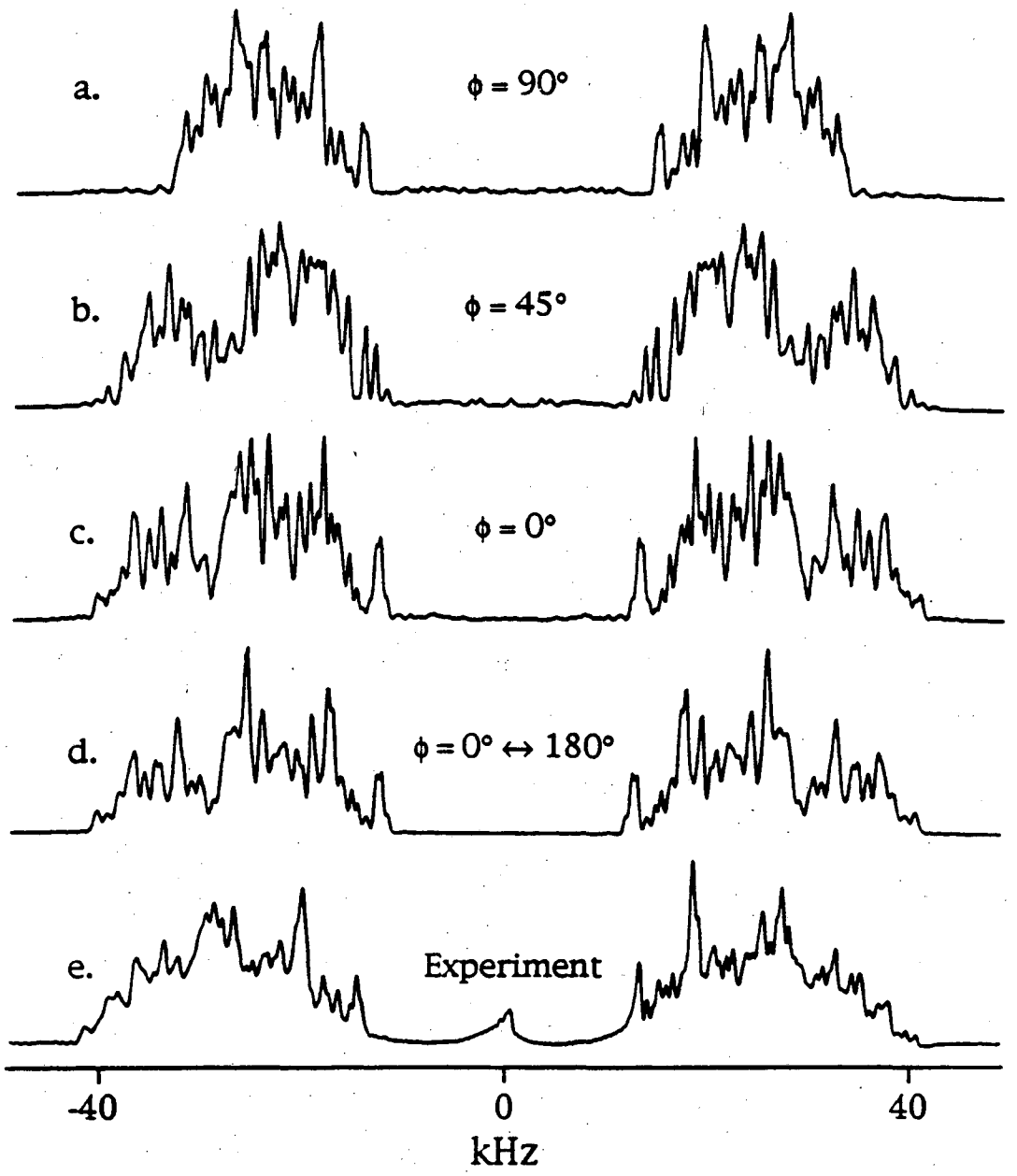

Figure 4.3: Simulated and experimental spectra of $Cs(THF)_{1.3}C_{24}$. The simulat... include several fixed conformations and interconversion between $\phi = 0°$ and 1...

$\phi = 90°$, $\phi = 180°$, and $\phi = 270°$ (Fig. 4.2c), interconversion between a C_s and a C_2 conformation (Fig. 4.2d), interconversion between the two C_s conformations (Fig. 4.3d), and three fixed conformations (Fig. 4.3a, 4.3b and 4.3c). All of these were noticeably narrower than the experimental spectrum (Fig. 4.2e, 4.3e). However, it is interesting to note the similarity between the spectra for interconversion between $\phi = 0°$ and 90°, hindered pseudorotation, and pseudorotation averaged every 9° (i. e. averaged over 0°, 9°, 18°... 360°). This means that single quantum high field NMR would be unable to distinguish between an interconversion that sampled all four symmetric conformations (hindered pseudorotation) and an interconversion that sampled only one C_S and one C_2 conformation. It also indicates that increments of smaller than 9° are necessary to simulate free pseudorotation.

Because none of the above simulations adequately fit the experimental data, simulations were carried out using variations of the standard parameters of THF's molecular geometry. Varying the H–C–H bond angle and the C–H bond length did not produce satisfactory fits. Varying the puckering amplitude from q = 0.38 Å to q = 0.32 ± 0.01 Å resulted in much better fits for some conformations. As shown in Fig. 4.4 the C_2 conformations, and interconversions that sample the C_2 conformations, such as pseudorotation, do not fit the experimental spectrum. Good fits are, however, obtained for q = 0.32 Å with the C_s conformation or with interconversion between the two C_s conformations, as shown in Fig. 4.5. It should be pointed out here that, while both C_s conformations produce identical spectra, interconversion between these two conformations results in a slightly different spectrum since interconversion averages the dipole couplings. Although both fixed and interconverting conformations

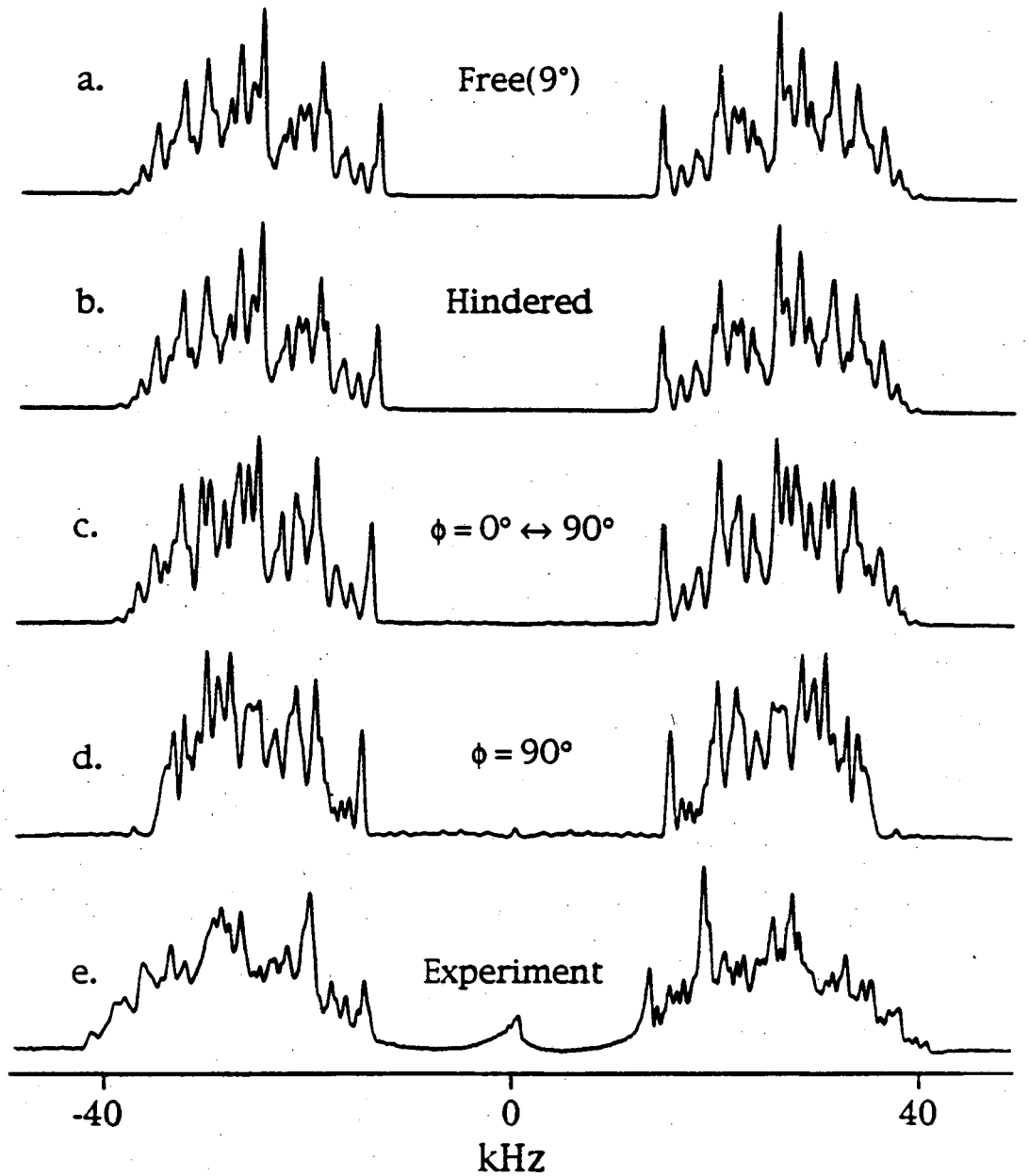

Figure 4.4: Simulated and experimental spectra of $Cs(THF)_{1.3}C_{24}$ using q = 0.32

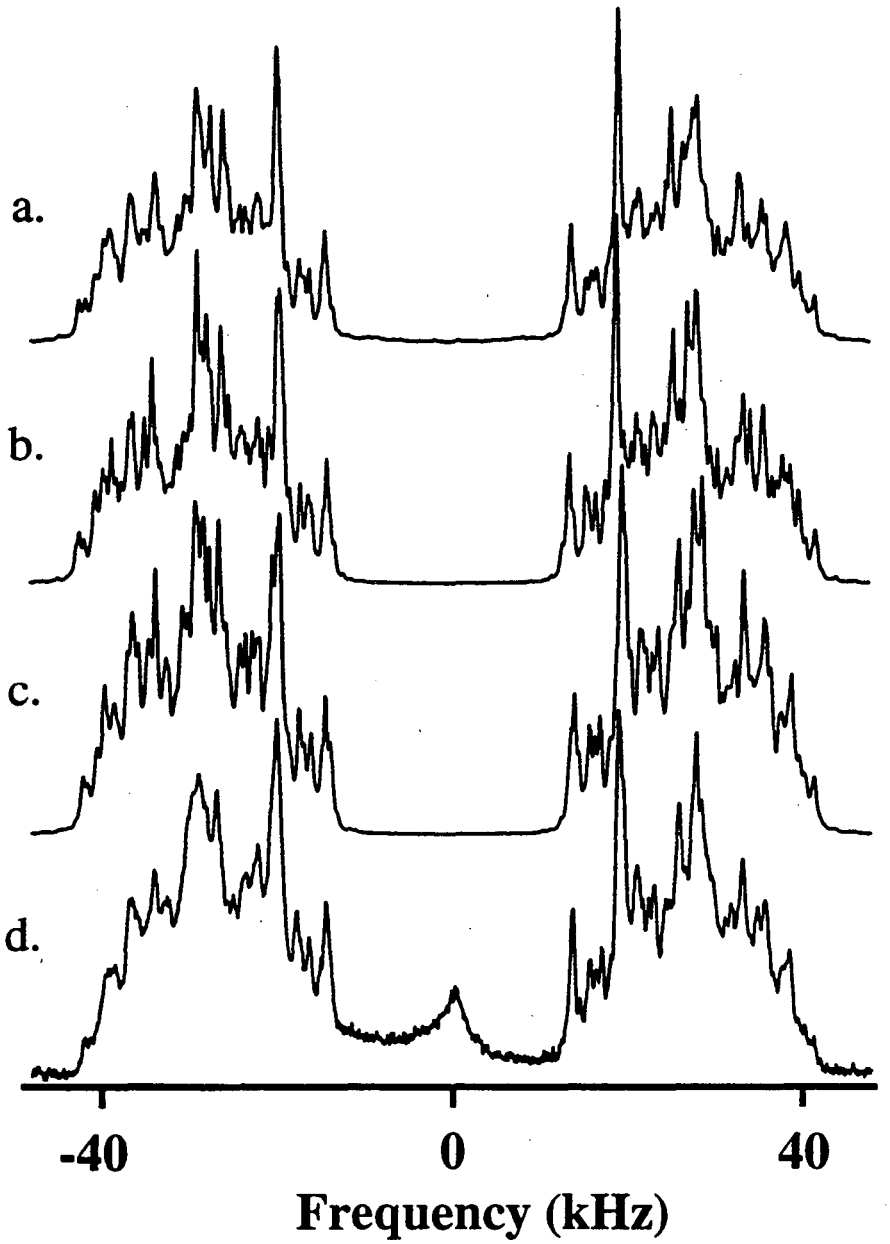

Figure 4.5: The best fits for $Cs(THF)_{1.3}C_{24}$:
a. Fixed C_S conformation.
b. Direct interconversion between C_S conformations.
c. Molecular potential.
d. Experimental.

result in good fits, neither agrees perfectly with the experimental spectrum and it is impossible to determine which agrees best with experiment.

The spectra shown in Fig. 4.5, unlike those shown before, were calculated taking chemical shift into account. The slight asymmetry of the experimental spectra indicates the presence of a chemical shift difference that is small compared to the dipole couplings. Since the spectra of the THF molecule for $\Theta = 0°$ and $\Theta = 90°$ were nearly identical, except for a small overall shift in frequencies and the 1/2 scaling factor, it was decided to simulate the spectra with isotropic chemical shift. It was found that a chemical shift difference of 200 ± 50 kHz for the α protons fits the experimental spectra well, and is in good agreement with the isotropic chemical shift values [19, 46]. The simulations in Fig. 4.5 use a chemical shift difference of 200 Hz, and Fig. 4.6 shows how varying the chemical shift from 0 to 200 to 400 Hz affects the spectrum.

More recently, Mark Rosen in the Pines laboratory continued this investigation analyzing the conformational motion in terms of the potential function

$$V(\phi) = V_2\cos(2\phi) + V_4\cos(4\phi) \tag{4.1}$$

where ϕ is the pseudorotation angle. The best fit to experimental data was found for V_2 = -15 ± 5 kJ/mol, and V_4 = 3 ± 2 kJ/mol, with q = 0.30 ± 0.01 Å. This function is plotted in Fig. 4.7, along with the potential found for gaseous THF [5, 7, 17]. The large difference between the potential found for intercalated and gas phase THF may be due to the constraining effects of the graphite layers. The potential for intercalated THF corresponds to interconversion between the two C_s conformations through a pseudorotation pathway that samples the intervening conformations, with a barrier of 30 kJ/mol between the two C_s conformations. The simulation for this potential fits

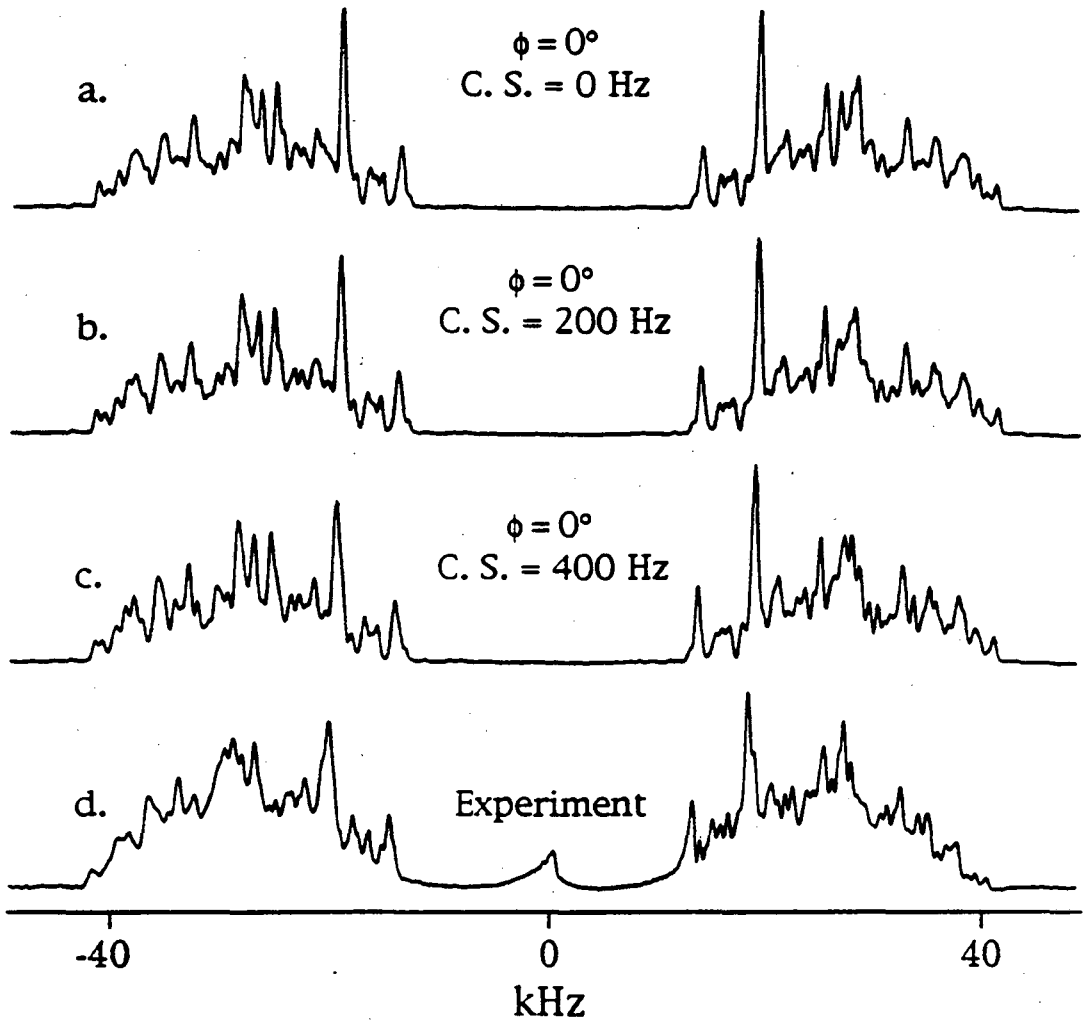

Figure 4.6: Simulated and experimental spectra of $Cs(THF)_{1.3}C_{24}$ using q = 0.32 Å, $\phi = 0°$, chemical shift differences of 0, 200 and 400 Hz.

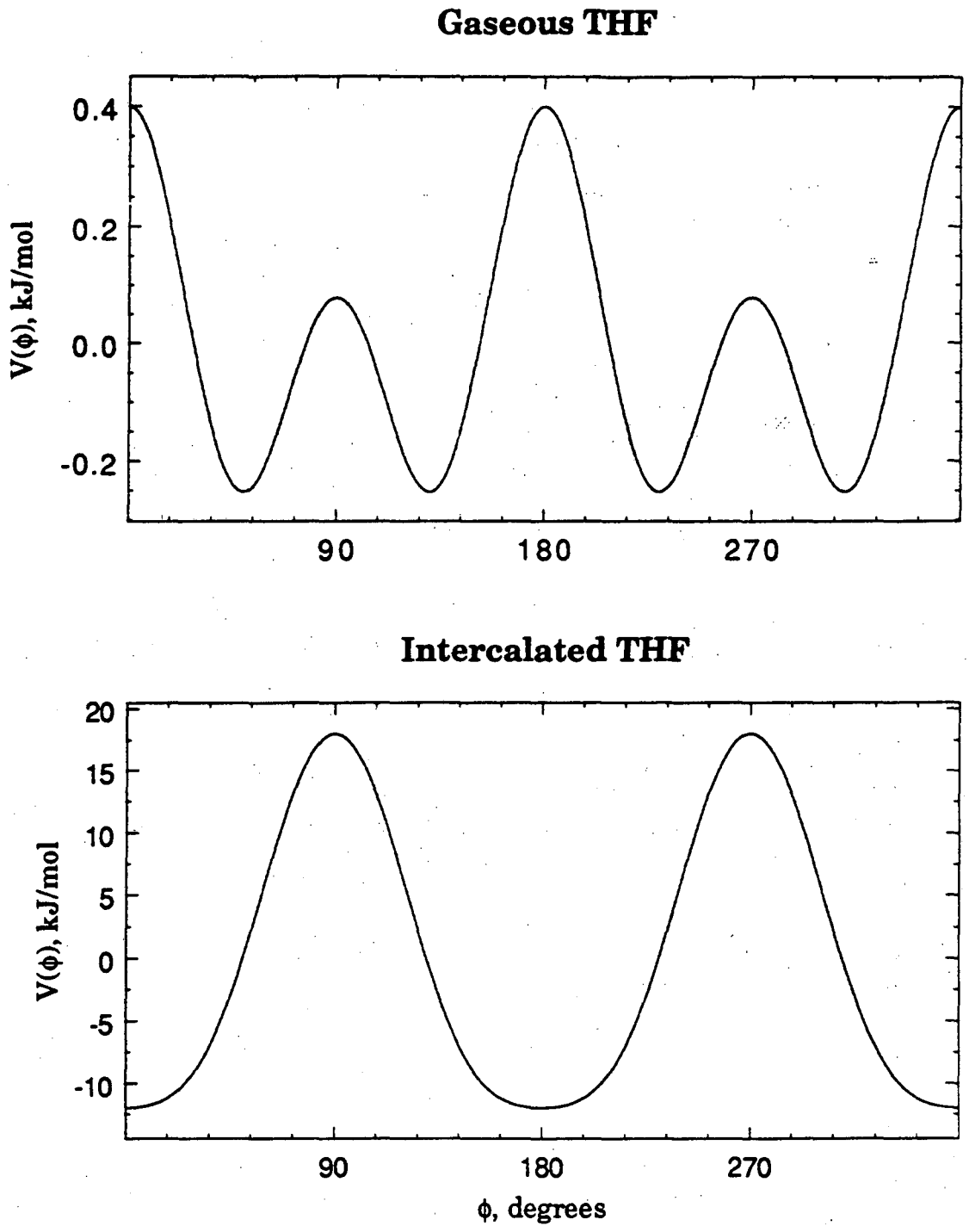

Figure 4.7: Pseudorotation potentials for THF.
Top: Potential found for gaseous THF.
Bottom: Potential for intercalated THF.

the experimental spectrum as well as the simulations for fixed and interconverting C_s conformations mentioned above do. These three simulations, which represent the best fits to the experimental data found so far, are compared to the experimental spectrum in Fig. 4.5. It should be noted, however, that if the THF molecule is interconverting between the two C_s conformations, it is more likely go through a planar conformation than to do so by sampling intermediate conformations, since the barrier to planarity, found to be about 16 kJ/mol in the gas phase [4, 18], is roughly half the height of the barrier found for the pseudorotation potential given above.

It would be interesting to determine if a better fit to the experimental spectra can be found by using the molecular potential for puckering instead of pseudorotation. The puckering potential is described by the function

$$V(q) = aq^4 - bq^2 \tag{4.2}$$

where q is the puckering amplitude and a and b are variable parameters [4, 48].

Variable temperature studies of the THF-GIC's provide more information about the intra- and inter- molecular motion of THF [26, 47, 49]. Neutron and x-ray diffraction, and previous NMR results indicate that below about 250 K, the THF molecules freeze into place, and the NMR lines broaden considerably because the intermolecular dipole couplings are no longer averaged out by molecular motions. In this solid phase, the spectrum is no longer scaled by a factor of $(3\cos^2\Theta - 1)$ when the sample's orientation changes, because the molecules are no longer rotating. The spectrum for $\phi = 90°$ was simulated by adding many spectra, in each of which the THF's mean plane is perpendicular to $\vec{B}_0$, but where the orientation of the vector connecting the center of the THF molecule to the oxygen atom ranges from 0° to 360°, and is shown

in Fig. 4.8. Both simulations used long values for T_2 to simulate the effect of intermolecular dipole-dipole couplings. The x-ray and neutron diffraction results [26, 36] indicate that as the THF solidifies two distinct phases appear, one corresponding to $Cs(THF)_1C_{24}$ and the other to $Cs(THF)_2C_{24}$. The reader is cautioned that in Ref. [30], the inference of two different phases of THF at room temperature, one mobile and the other not, is not supported by the NMR powder spectrum. The central peak in Fig. 1a of Ref. [30], does not represent a second phase, as claimed in the paper, but is a feature of the room temperature powder spectrum of $Cs(THF)_{1.3}C_{24}$, simulated here in Fig. 4.9.

As the temperature is lowered further a second phase change occurs at about 120 K, as indicated by line broadening of the ^1H NMR spectrum [49]. It is possible that this transition is due to interconversion of the THF molecule between the two C_s conformations stopping below 120 K.

In summary, the data presented so far indicate that the THF molecules in $Cs(THF)_{1.3}C_{24}$ are oriented with their mean molecular planes parallel to the graphite layers, and the C_s conformations are very strongly favored. They are probably arranged with the oxygen atom near the Cs^+ ion and two or three THF molecules either rotating about the ion or hopping from one ion to another [36]. Figure 4.10 shows THF molecules intercalated in graphite layers, with the molecules and layers drawn to scale.

4.2.2 Results for $K(THF)_{2.5}C_{24}$

In $K(THF)_{2.5}C_{24}$, as in $Cs(THF)_{1.3}C_{24}$, the THF molecules also rotate about the graphite's $\vec{c}$ axis, as indicated by the scaling of the spectra in Fig. 4.11. The sample

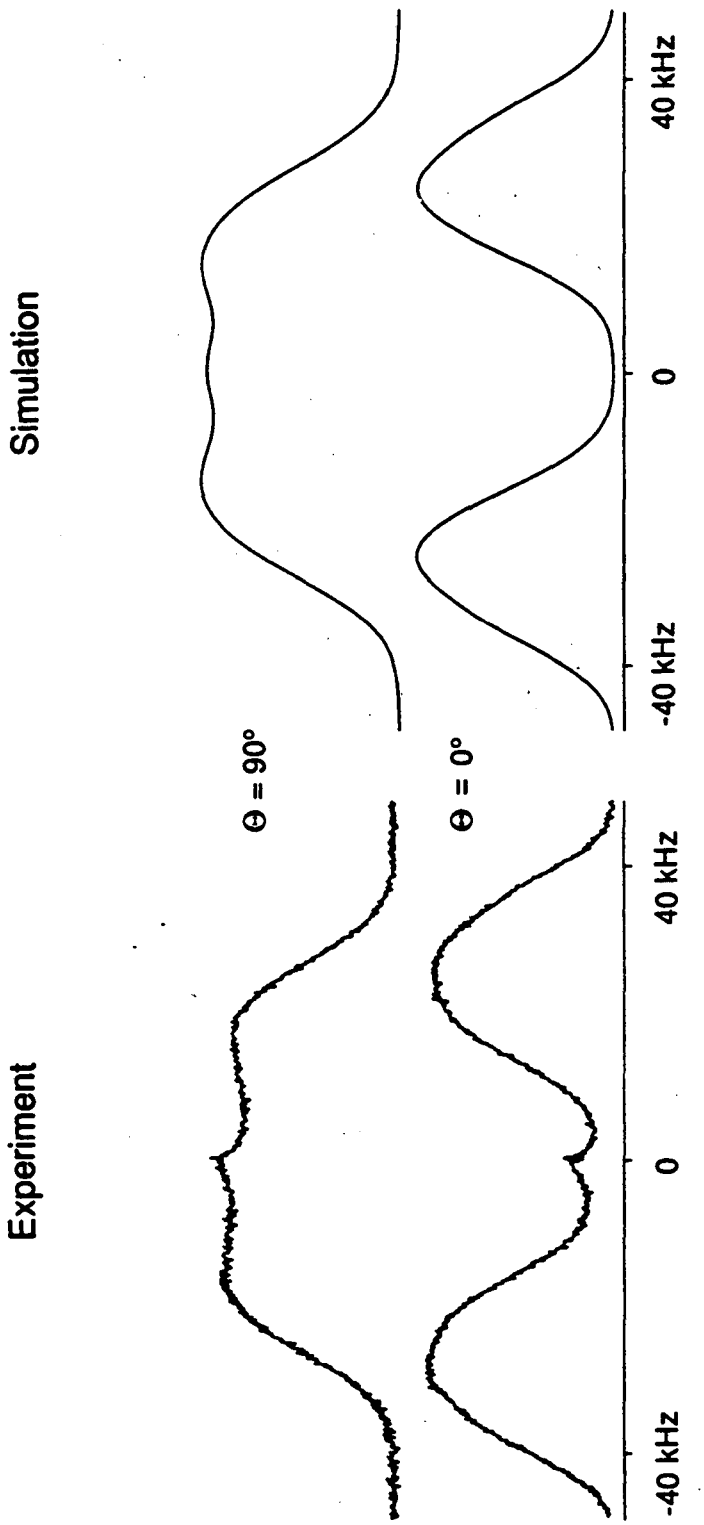

Figure 4.8: Simulated and experimental spectra of $Cs(THF)_{1.3}C_{24}$ as function of Θ at T = 213 K.

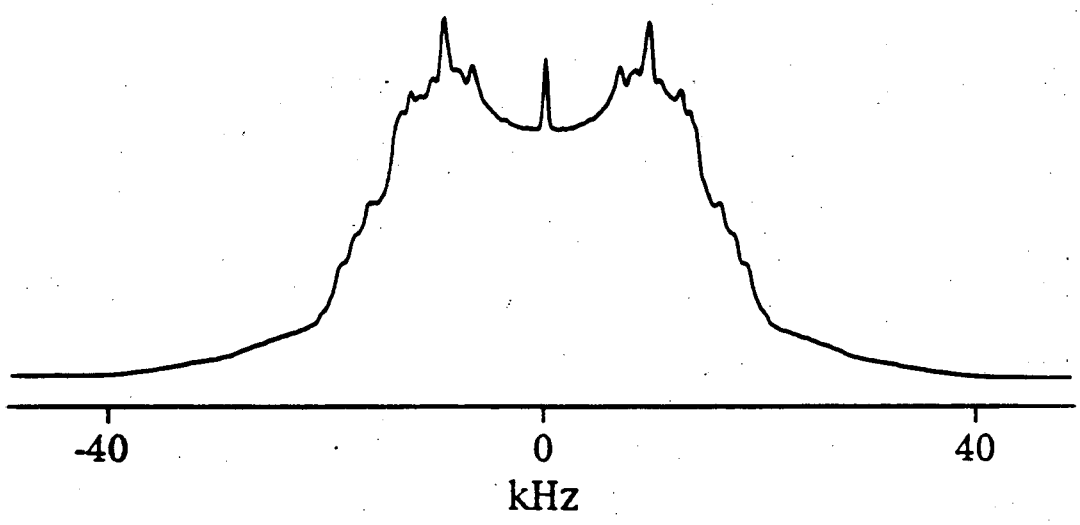

Figure 4.9: Powder spectrum simulation for $Cs(THF)_{1.3}C_{24}$ at room temperature

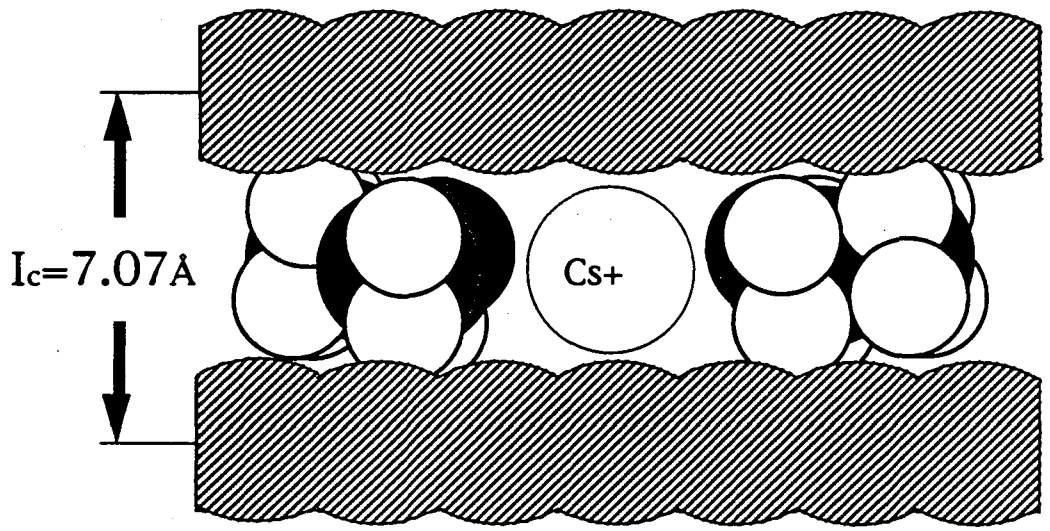

Figure 4.10: THF molecules in C_s conformations in graphite layers. The hydrogen and oxygen atom were drawn using the Van der Waals radii, the Cs^+ was drawn with its ionic radius, and the graphite layers were drawn with a thickness of 3.35 Å, and an interlayer spacing of 5.48 Å.

orientations were once again approximately 0°, 30°, Θ_M, and 90°. The relatively large width of the spectrum near the magic angle is due not so much to orientational disorder, since the mosaic spread of this sample is relatively small (Fig. 2.2), as to the uncertainty in positioning the sample. An error in sample orientation would have especially large effects since the function $(3cos^2\Theta - 1)$ changes rapidly near Θ_M. As indicated by the values of Θ used in the simulations (Fig. 4.11), the error in the sample's orientation appears larger than ±10°. A Gaussian distribution of width $\sigma = 0.9$ was used to fit the simulations in Fig. 4.11 and is shown in Fig. 2.2. The relatively narrow mosaic spread of the graphite layers in the $K(THF)_{2.5}C_{24}$ explains why the lines in the spectra of the $K(THF)_{2.5}C_{24}$ are sharper than those of the $Cs(THF)_{1.3}C_{24}$ at $\Theta = 0°$ and 90°.

It is generally accepted that the orientation of the THF molecules is not par-

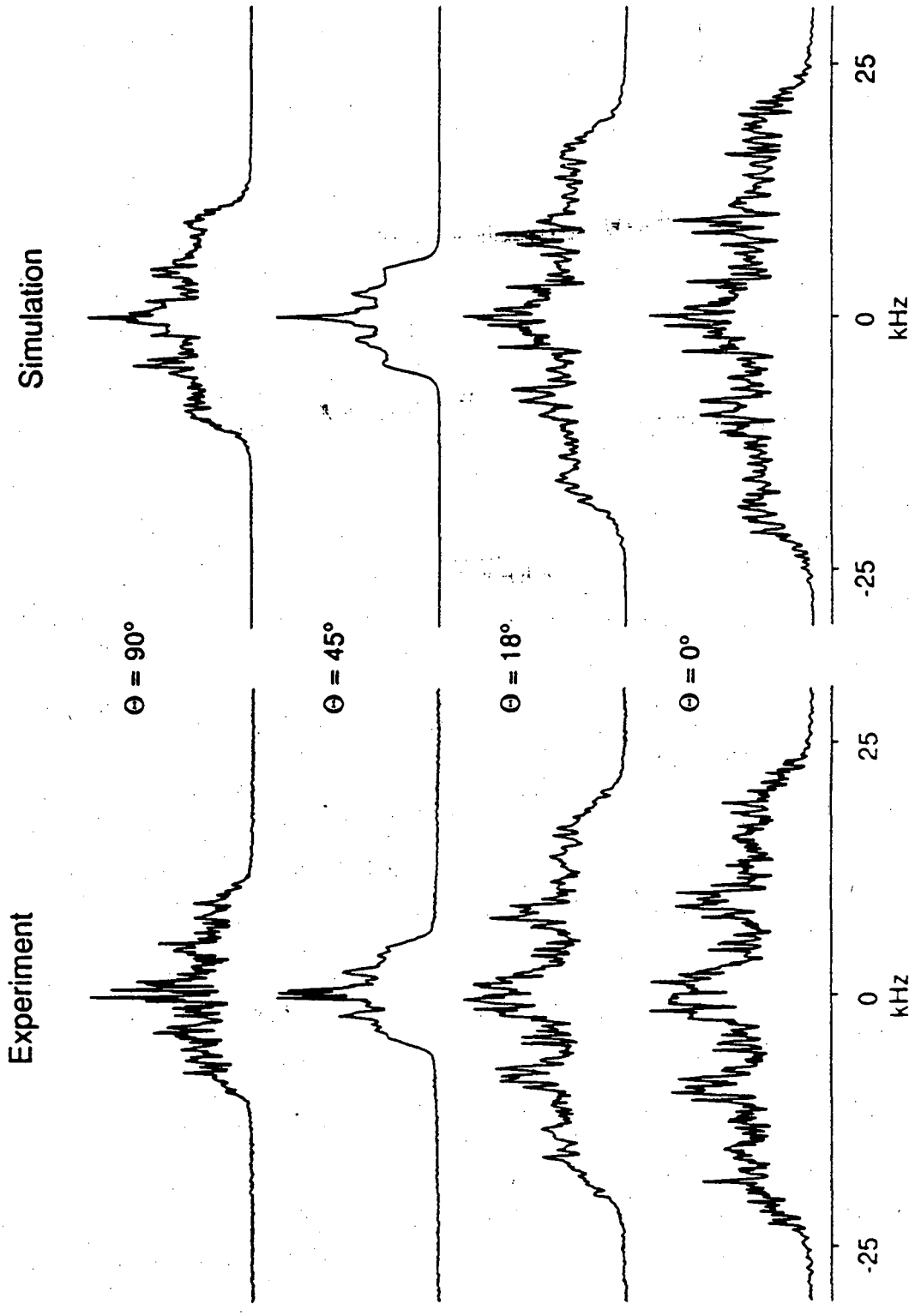

Figure 4.11: Experimental and simulated spectra of $K(THF)_{2.5}C_{24}$ as a function of Θ

allel to the graphite layers in $K(THF)_{2.5}C_{24}$. Because the difference between the I_c = 8.83 Å and the thickness of the graphene sheets, 3.35 Å, leaves 5.48 Å free, which is larger than the thickness of a THF molecule, it has been assumed until now that the THF molecules were oriented with their mean molecular planes perpendicular to the graphite layers [25, 28]. An alignment that is not parallel to the layers introduces two new degrees of freedom: the angle between the mean molecular plane and the graphite layers, called β, and the orientation of the molecular x axis within the molecule's mean plane, α (in $Cs(THF)_{1.3}C_{24}$, $\beta = 0$ and α does not have a unique value since the molecules are rotating about the graphite's $\vec{c}$ axis). For these simulations, the molecule's orientation is defined by rotating it relative to a fixed axis system that coincides with the molecular axis system before the initial rotation. The molecule is first rotated by an angle α about the fixed z axis, and then by an angle β about the fixed y axis, as is shown in Fig. 4.12. Because of the introduction of these two new degrees of freedom, simplifying assumptions were made when simulating the spectrum of the THF molecule in $K(THF)_{2.5}C_{24}$. Except as indicated below, all the simulations were carried out with the molecular parameters that were found to give the best fits in $Cs(THF)_{1.3}C_{24}$: q = 0.32 Å, $\phi = 0°$, and a chemical shift difference of 200 Hz.

Figure 4.13 shows several simulations for a THF molecule with its mean molecular plane perpendicular to the graphite layers ($\beta = 90°$). None of these simulations agrees with the experimental spectrum. Several other possibilities with $\beta = 90°$ were tried, including different conformations, interconversion between several conformations, and rotation about an axis perpendicular to the molecular plane, but none of

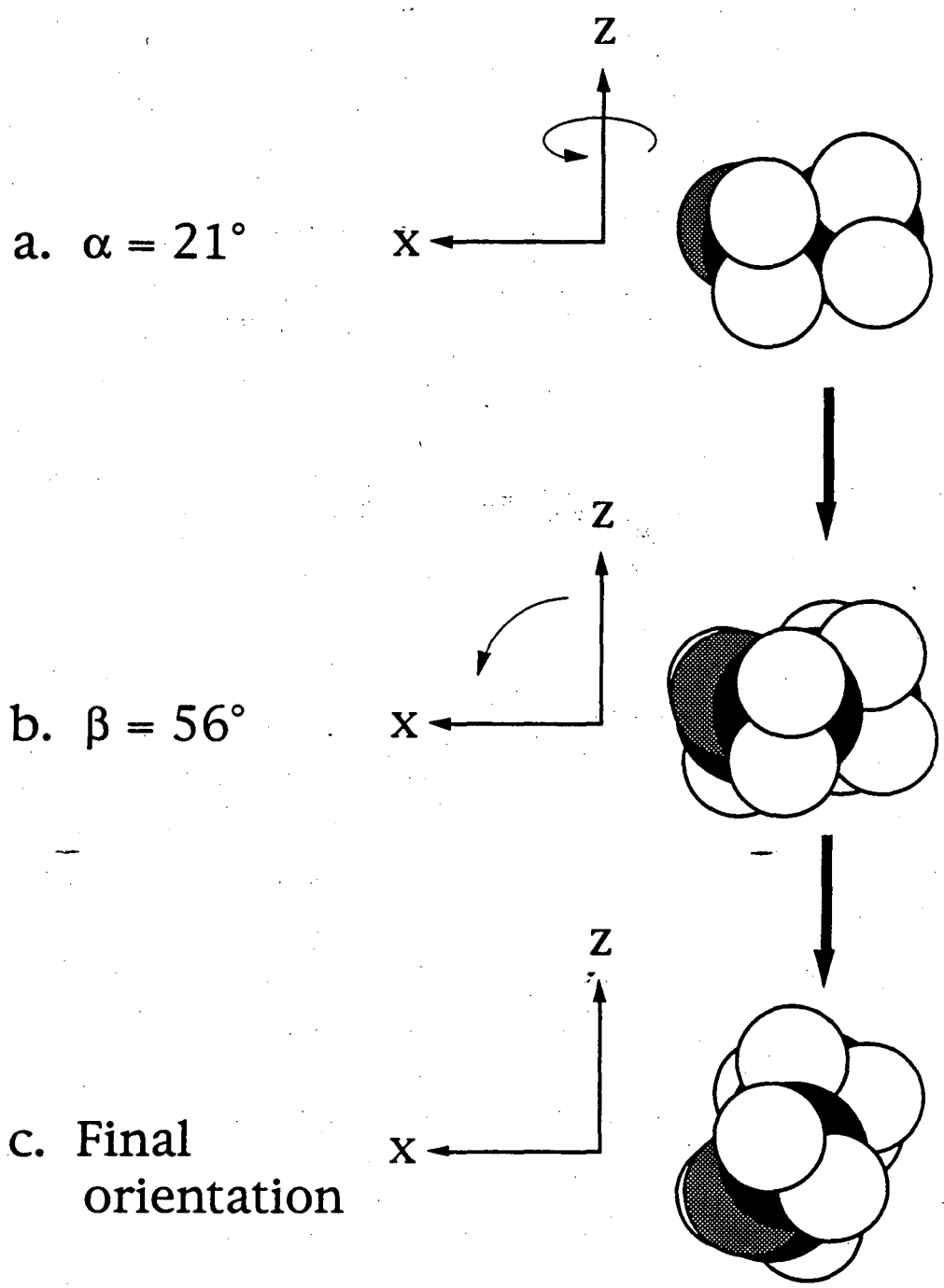

Figure 4.12: Definition of the angles describing the orientation of the THF molecule in the $K(THF)_{2.5}C_{24}$. In this illustration the graphite layers, if shown, would be perpendicular to the z axis.

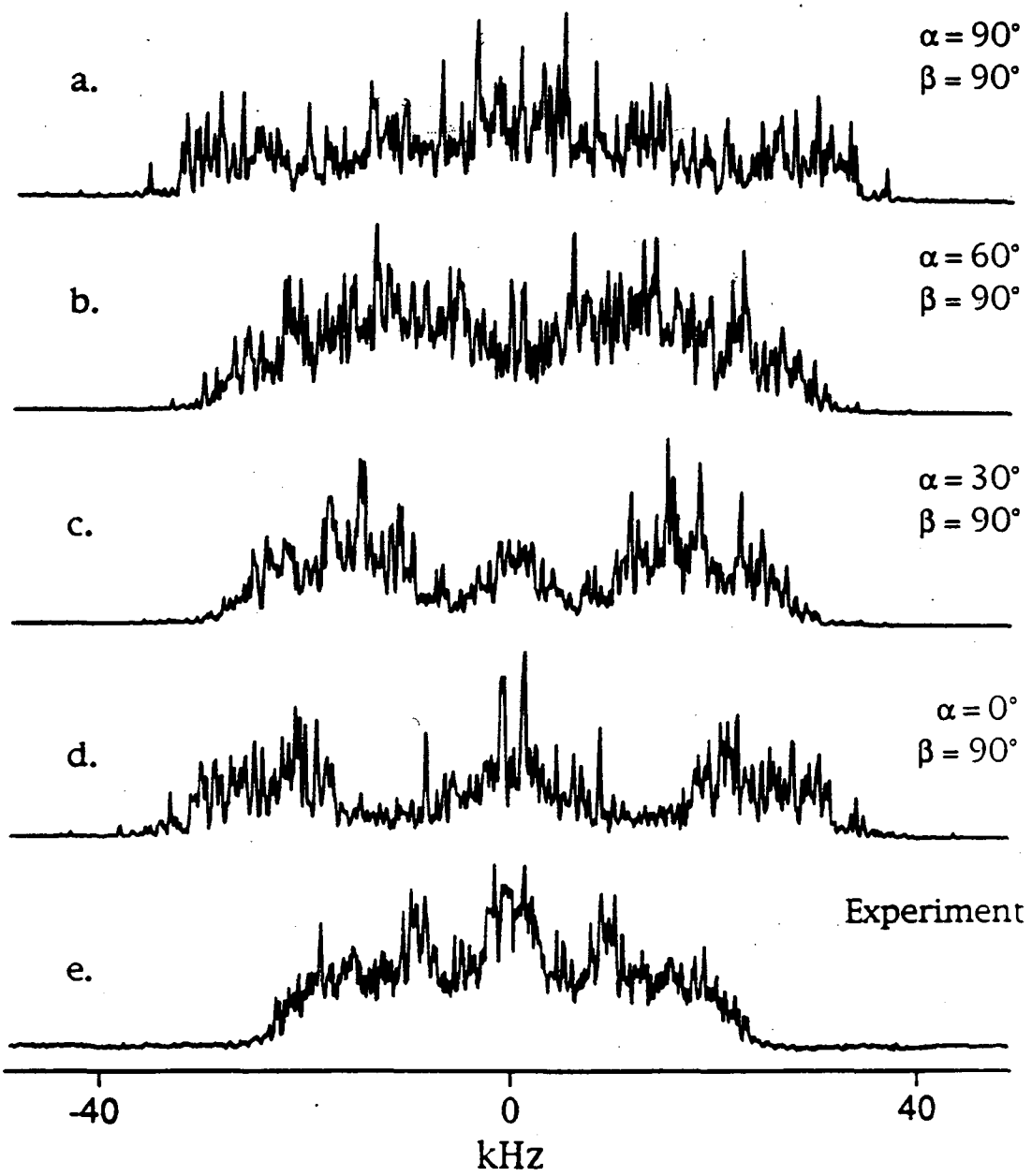

Figure 4.13: Simulated spectra for $K(THF)_{2.5}C_{24}$ with $\beta = 0°$ and several values of α

these alternatives produced a satisfactory fit.

Simulations were then carried out with the mean molecular plane at several different orientations, such as those shown in Fig. 4.14. The best fit was found for $\alpha = 21 \pm 2°$ and $\beta = 56 \pm 2°$, as shown in Fig. 4.15. The simulated spectra are very sensitive to small changes in orientation, and none of the simulations gave perfect agreement with the experimental spectra. The uncertainty in α and β given above represent the range of orientations that show reasonable agreement with the width and features of the experimental spectrum.

An alternative to this orientation was recently found by M. Rosen, using the same pseudorotation potential found for THF in $Cs(THF)_{1.3}C_{24}$ (q = 0.30 Å, V_2 = -15 kJ/mol, V_4 = 3 kJ/mol), with $\beta = 71°$ and α averaged from 40° to 120°. The results for this potential and for a fixed C_s conformation with $\alpha = 56°$ and $\beta = 21°$ are compared to the experimental spectra in Fig. 4.16

While we have been unable to explore all the possible combinations of orientation and conformation, the results so far indicate that the THF molecules are not oriented with their mean planes perpendicular to the graphite layers, and their oxygen atoms are not pointing directly at the layers. This is in agreement with results found for benzene-potassium and furan-potassium TGIC's, which show that the benzene molecules are oriented at about 30° to the layers [50, 51] and the furan molecules at about 15° [52]. Figures 4.17 and 4.18 shows a THF molecule with the two orientations found to give good fits to the experimental data.

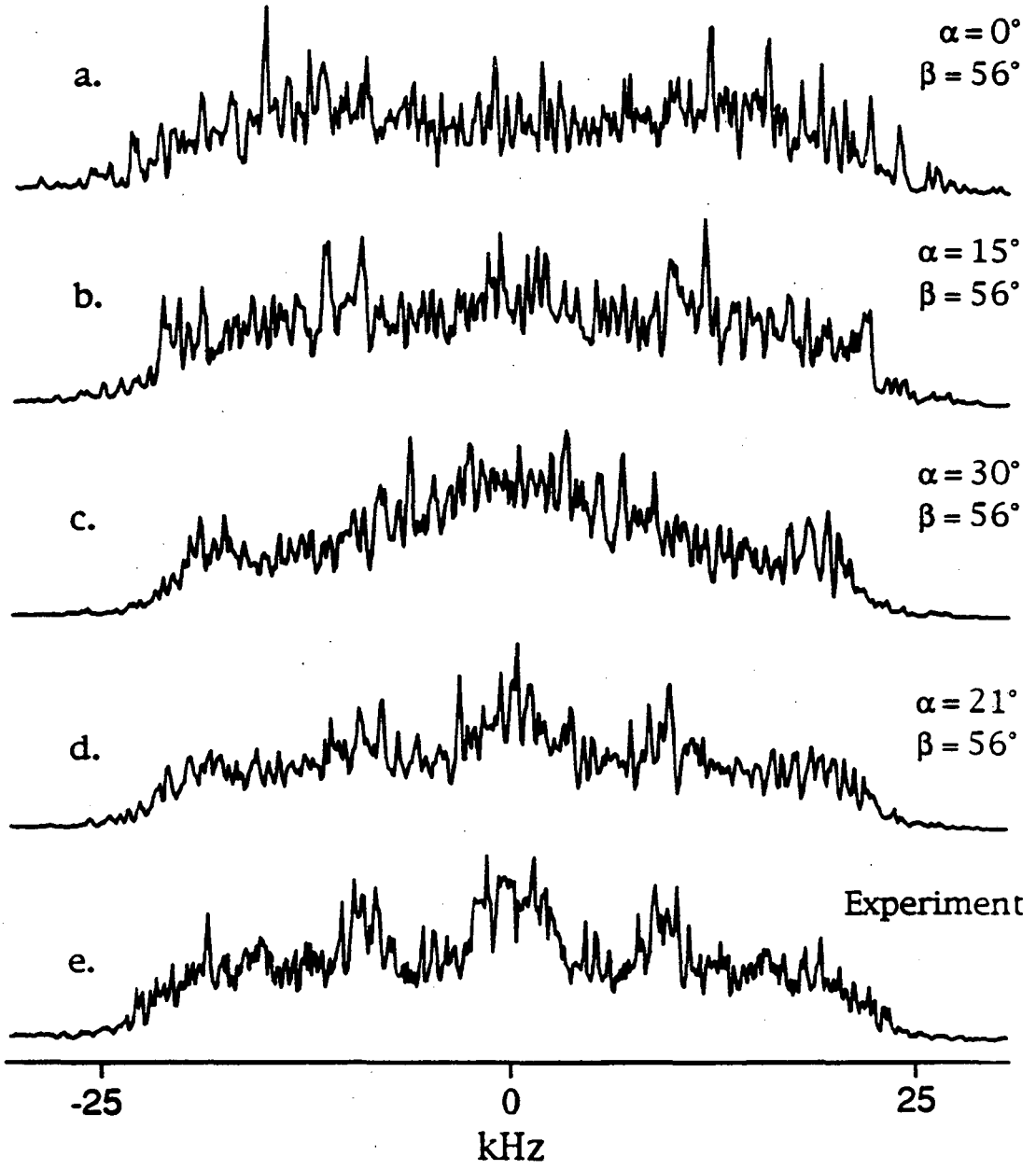

Figure 4.14: Simulated spectra for $K(THF)_{2.5}C_{24}$ with $\alpha = 0°$ and several values of

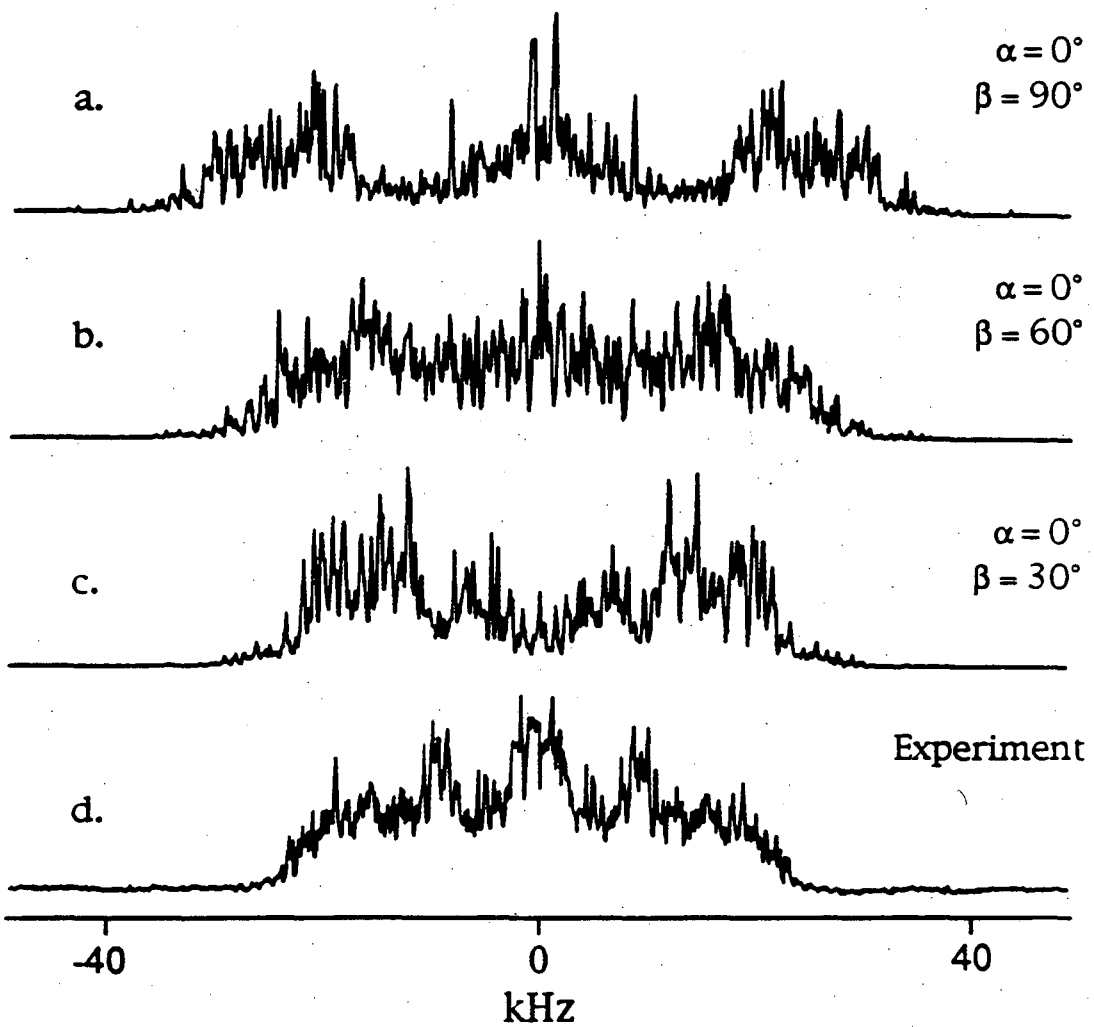

Figure 4.15: Simulated spectra for the K compound with $\beta = 56°$ and several values of α.

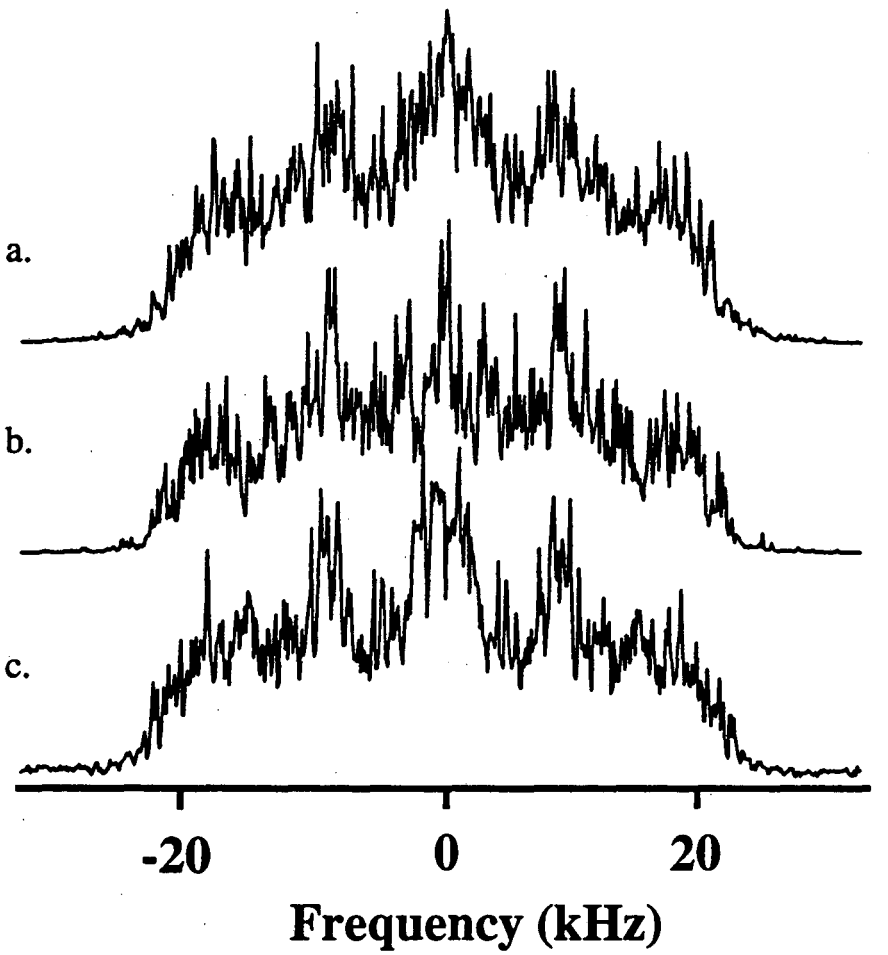

Figure 4.16: The best fits for $K(THF)_{2.5}C_{24}$:
a. $\alpha = 21°$, $\beta = 56°$.
b. α oscillating between 40 and 120°, $\beta = 71°$.
c. Experimental.

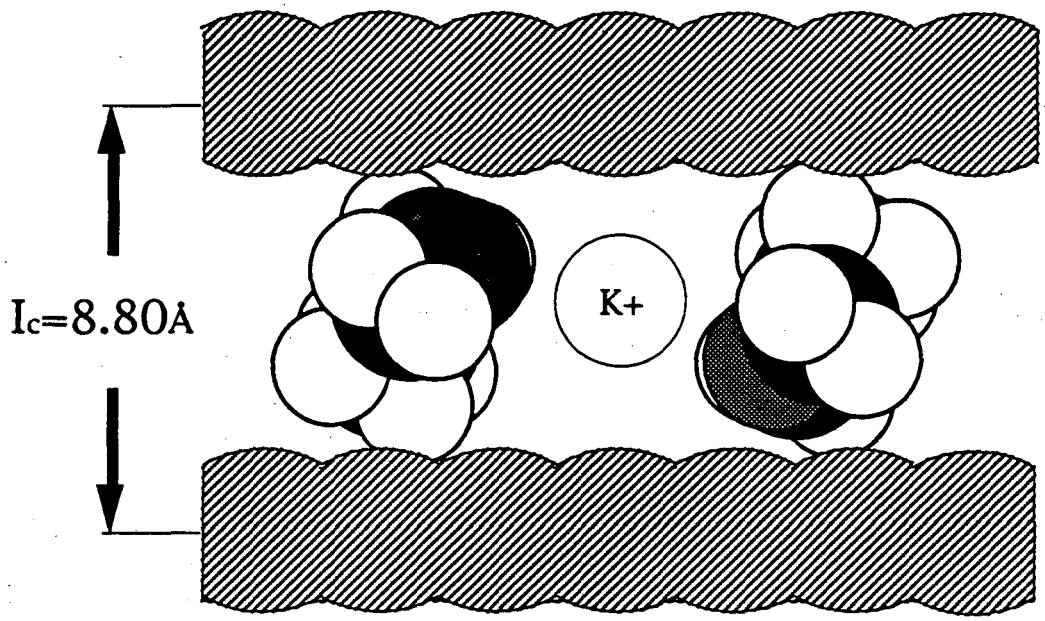

Figure 4.17: THF molecule in $K(THF)_{2.5}C_{24}$ shown at right with α = 21°, β = 56° and at left with α = -21°, β = -56°, which produces an identical NMR spectrum. Both are in the C_s conformation.

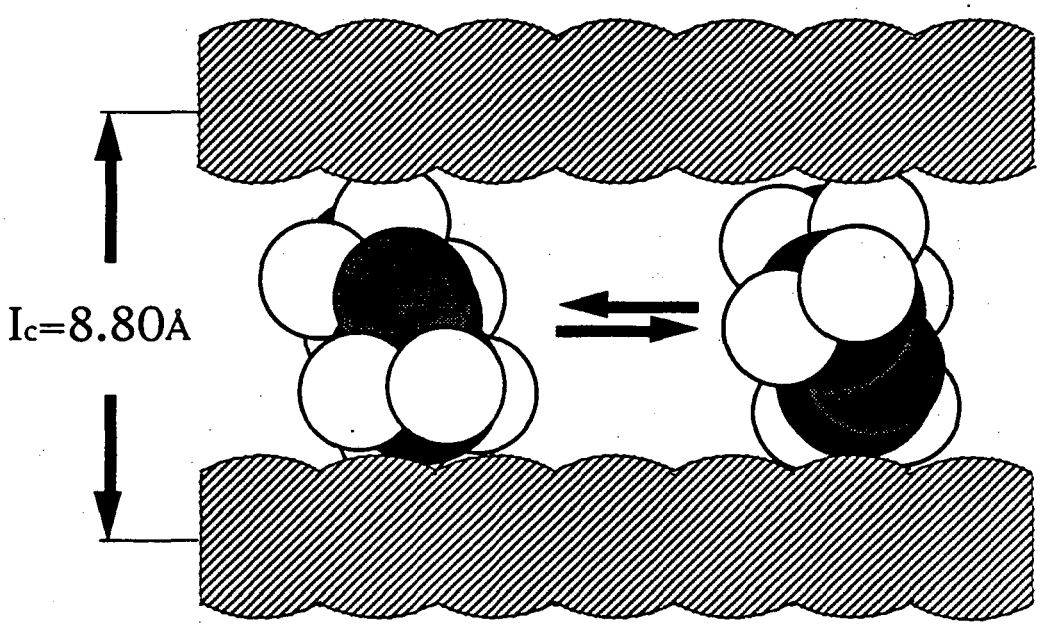

Figure 4.18: THF molecule in $K(THF)_{2.5}C_{24}$ shown in the following orientations:
left: α = 120°, β = 71°.
right: α = 40°, β = 71°.
The conformations are determined by the molecular potential in Eq. (4.1).

Chapter 5

Deuterium and Multiple Quantum Simulations

While single quantum proton spectroscopy has produced interesting information about the behavior of intercalated THF, it is preferable to further refine these results using a complementary technique. One ideally suited to this task would provide spectra that, while simple, are sensitive to small changes in molecular orientation and conformation. For example, it should be able to distinguish between a fixed C_S conformation and interconversion between the two C_S conformations for THF in $Cs(THF)_{1.3}C_{24}$. Simulations were carried out for multiple quantum and deuterated THF spectra in order to determine their suitability to the study of intercalated THF. Since experiments have not yet been carried out with either of these techniques, all the results presented in this chapter are theoretical, and were calculated using q = 0.32 Å and a chemical shift difference of 200 Hz.

5.1 Multiple Quantum Simulations

A well known way of simplifying an NMR spectrum is to examine the coherences of order greater than one. Since many excellent discussions of this technique are

available [42, 50–52], it will not be explained in detail here. The most important point to note here is that, as the number of quanta for a many spin system increases, the number of possible transitions decreases rapidly. The number of ΔM quantum transitions for a system of N spin $\frac{1}{2}$'s is given by

$$\binom{2N}{N-\Delta M} = \frac{(2N)!}{(N-\Delta M)!(N+\Delta M)!} \tag{5.1}$$

which, for THF, where $N = 8$, gives a total of 11440 possible single quantum transitions, but only 120 six quantum, 16 seven quantum and one eight quantum transitions.

The simplest form of multiple quantum experiment consists of three pulses and three corresponding time intervals [42], and can be broken up into three phases. The preparation phase consists of a $90°\bar{y}$ pulse followed by an interval τ, followed by a $90°y$ pulse during which the multiple quantum coherences are generated. The evolution phase consists of an interval t_1 during which the coherences evolve, and the detection phase consists of another $90°\bar{y}$ pulse followed by a delay t_2 during which the multiple quantum coherences are converted to single quantum coherences before they are detected.

In practice, a more complex experiment, such as Time Proportional Phase Incrementation (or TPPI) [56, 57], can be performed in order to separate the transitions corresponding to different values of ΔM. The simulations presented here are for an ultimate tau average TPPI experiment, calculated using the Pines laboratory's "Speque86" program written by J. B. Murdoch.

Figure 5.1 shows six quantum spectra for several conformations of the THF molecule in $Cs(THF)_{1.3}C_{24}$ and Fig. 5.2 shows the corresponding seven quantum spectra. The first three spectra in each figure are included as references, to show the

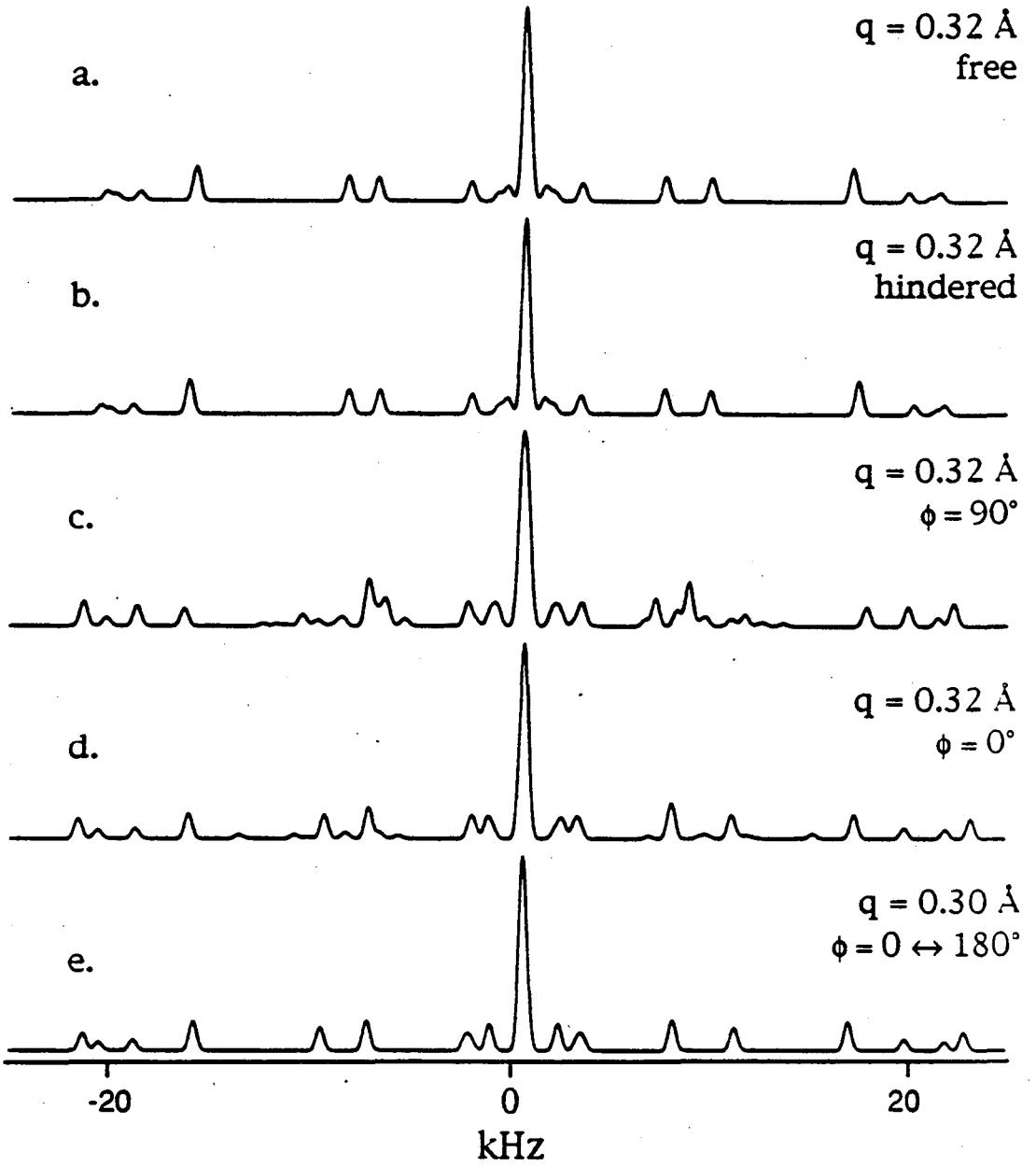

Figure 5.1: Simulated six quantum spectra of $Cs(THF)_{1.3}C_{24}$.

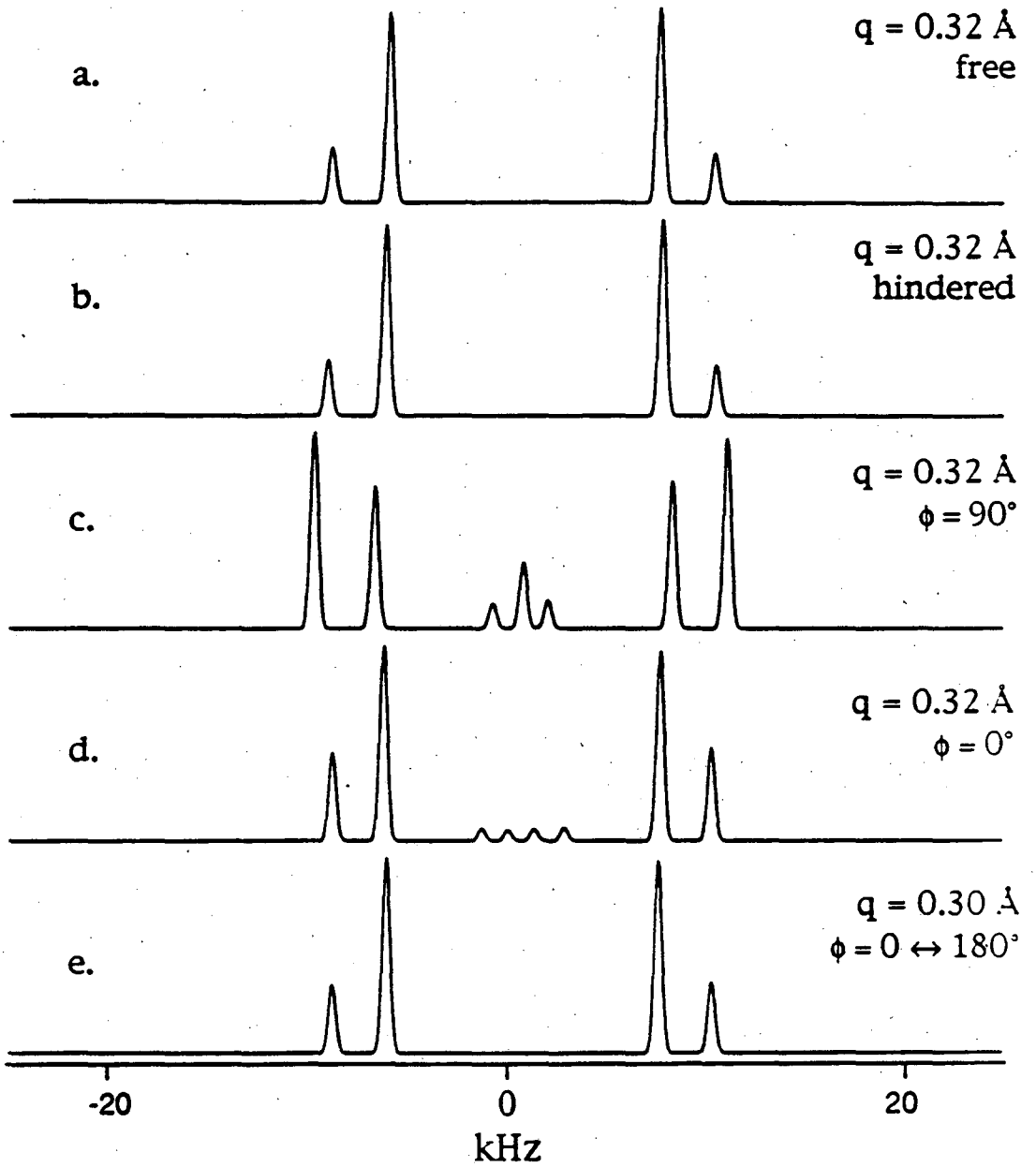

Figure 5.2: Simulated seven quantum spectra of $Cs(THF)_{1.3}C_{24}$.

sensitivity of the multiple quantum spectra to different fixed and fluctuating conformations of the THF molecule. The spectra of greatest interest are "d" and "e" in each of the figures, which use the molecular conformations that produced the best fits to experiment with single quantum spectroscopy. The results indicate that, unless an extremely favorable signal to noise ratio can be obtained for the experimental spectra, six and seven quantum spectra do not appear to be a viable way of determining whether the intercalated THF molecules are in a fixed or interconverting conformation in $Cs(THF)_{1.3}C_{24}$.

Figures 5.3 and 5.4 show six and seven quantum spectra for the THF molecules in several orientations relevant to the study of $K(THF)_{2.5}C_{24}$. The first two spectra in these two figures are included for reference, while spectra "c" and "d" correspond to the two orientations which produced the best single quantum fits. While the six quantum spectrum for the oscillating orientation is noticeably broader than that for the fixed orientation, the difference between these two cases is clearer in the seven quantum spectrum. In summary, it appears that six and seven quantum spectra would not be able to further refine the results already obtained from single quantum spectra for $Cs(THF)_{1.3}C_{24}$, but may be useful in determining whether the THF molecule in $K(THF)_{2.5}C_{24}$has a fixed or oscillating orientation.

5.2 Deuterium Spectra

Deuterium has a quadrupolar nucleus with spin $I = 1$. Its relatively small quadrupolar coupling constant makes it possible to use the high field approximation to the quadrupolar Hamiltonian, which, assuming that the electric field gradient is symmet-

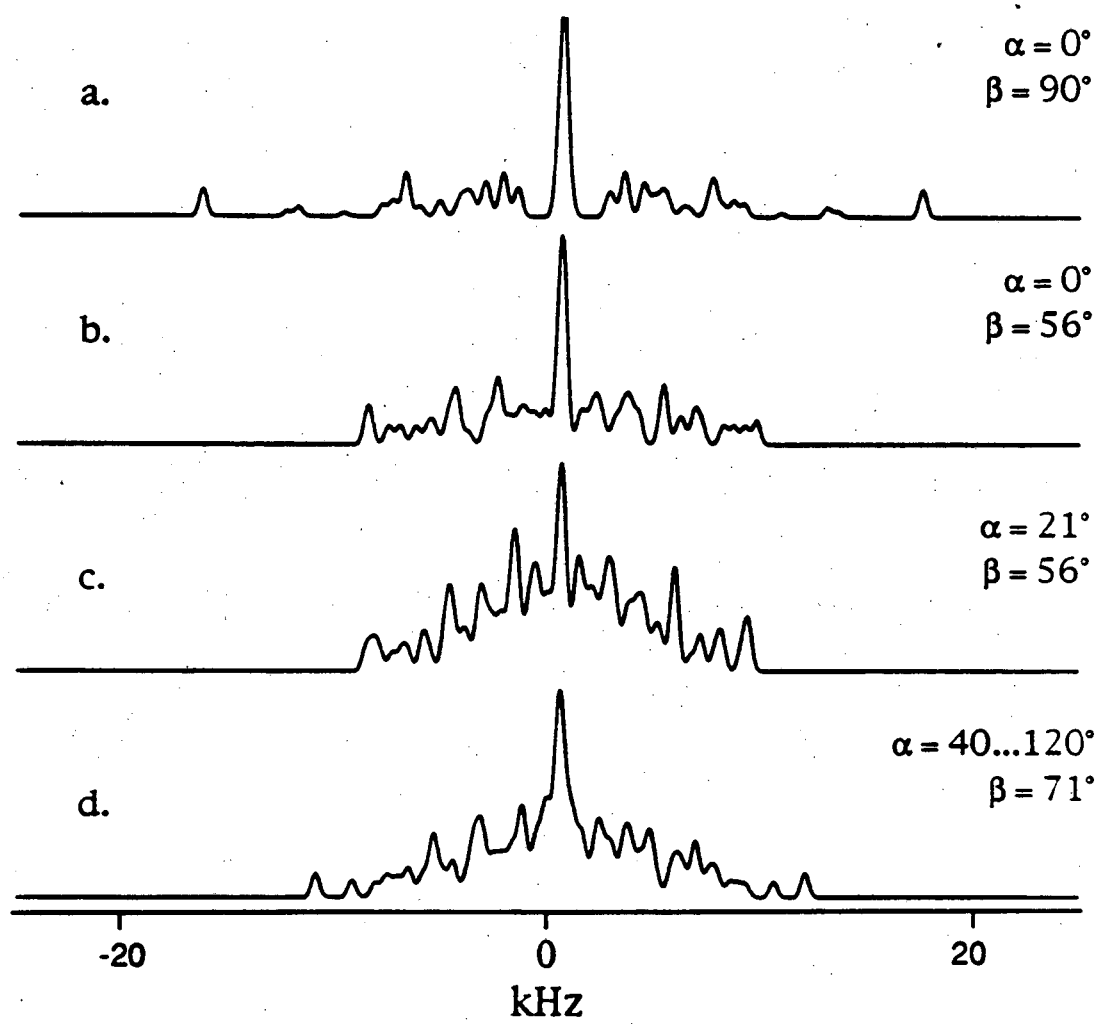

Figure 5.3: Simulated six quantum spectra of $K(THF)_{2.5}C_{24}$.

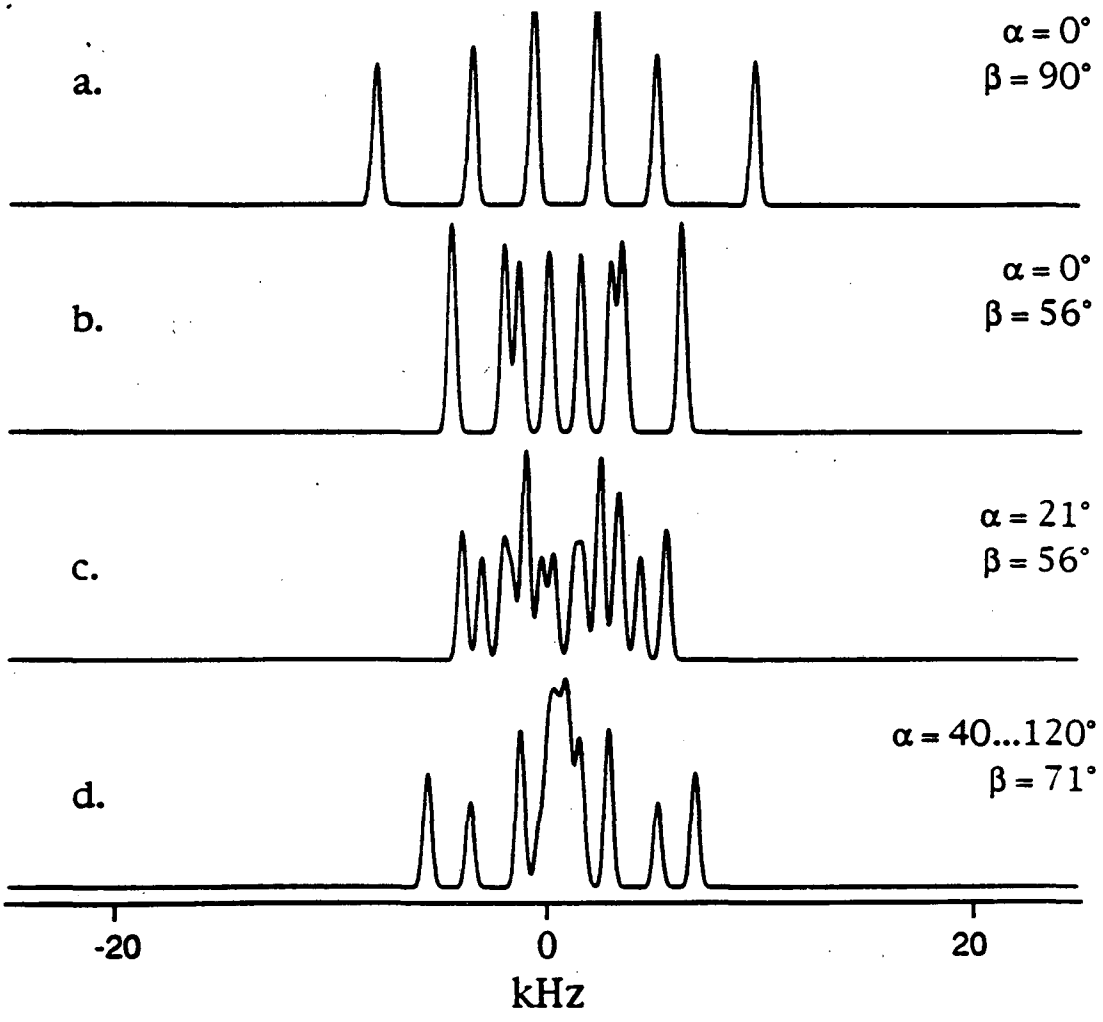

Figure 5.4: Simulated seven quantum spectra of $K(THF)_{2.5}C_{24}$.

ric about the C–H bond, is given in units of Hz by:

$$H_q = \frac{e^2qQ}{4I(2I-1)h}(\frac{3cos^2\theta - 1}{2})(3\mathrm{I}_z^2 - \mathrm{I}^2) \tag{5.2}$$

where eq is the field gradient (along the C–H bond, in this case), and Q the quadrupole moment of the nucleus (see, for example, Ref. 42, p498). Using $I = 1$, and $m = 1, 0,$ or -1, the energy levels are found to be:

$$E_{+1} = \Delta\nu + C_q(\frac{3cos^2\theta - 1}{2}) \tag{5.3}$$

$$E_0 = -2C_q(\frac{3cos^2\theta - 1}{2}) \tag{5.4}$$

$$E_{-1} = \Delta\nu + C_q(\frac{3cos^2\theta - 1}{2}) \tag{5.5}$$

where $\Delta\nu$ is the chemical shift, and $C_q = \frac{e^2qQ}{4I(2I-1)} = \frac{e^2qQ}{4}$. The transition frequencies are found from the energy levels to be:

$$\nu_1 = \Delta\nu + 3C_q(\frac{3cos^2\theta - 1}{2}) \tag{5.6}$$

$$\nu_2 = \Delta\nu - 3C_q(\frac{3cos^2\theta - 1}{2}) \tag{5.7}$$

The value of the constant e^2qQ is best determined experimentally and is usually in the range of 165 kHz to 175 kHz for small deuterated organic molecules [58].

Since experimental spectra were not available to provide additional information, several simplifying assumptions were made: First, that the value of C_q is the same for the α-deuteron nuclei and the β-deuteron nuclei. This is a reasonable assumption since the change would probably be about 5% or less (See Table 6.4 in in ref. 58), and the overall effect of such a change would be to slightly shift some of the lines, in a manner analogous to the chemical shift. Second, dipole-dipole couplings between the

deuterons were ignored since they are small compared to the quadrupolar linewidth. The value of the constants $\frac{1}{2}\frac{\gamma^2\hbar^2}{r_{ij}^3}$ used to calculate the dipole coupling in Eq. (3.37) is 60.06 kHz for protons, but only 1.41 kHz for deuterons, and the quadrupolar coupling constant used for deuterium is 170 kHz. The overall effect of the dipolar couplings would be to broaden the lines in the quadrupolar spectrum, but, since the linewidths are already on the order of 5 kHz, a dipolar broadening on the order of 1.4 kHz would have a negligible effect. Finally, it was assumed that the field gradients due to the Cs^+ and K^+ ions would not have a large effect on the spectrum, either because they are small or averaged out by the motion of the THF molecules. This assumption must be verified experimentally.

The advantages of deuteron spectroscopy are twofold. First, the number of lines in the spectrum is reduced. The reasons for this can be seen in Eq. (5.2). Unlike the dipolar operator H_d, which couples all the spins in the THF molecule or sample together to generate a large density matrix (256 x 256 for the case of an eight spin system such as THF) from which transitions arise, the quadrupole coupling acts on only one spin, so that transitions can occur only among the different states of the same nucleus. Since each deuteron has three possible spin states, only two transitions can occur per deuteron, giving a maximum of 16 transitions for a fully deuterated THF molecule.

The second advantage is that, while the complexity of the spectrum is reduced, spatial information is still present. Equations (5.6) and (5.7) show that the transition frequencies of the lines depend on the factor $(3cos^2\theta - 1)$. It should be noted, however, that the spatial information is not the same as that found in the dipole Hamiltonian,

where the angle θ is measured between the applied magnetic field and the internuclear vector. Here θ is the angle between the applied magnetic field and the quadrupolar axis, which in this case is along the C-H bond.

Figure 5.5 shows simulated spectra for the Cs compound. The first three simulations are again included as references. The simulations show that deuteron spectra are very sensitive to motion that averages the orientation of the C-H bond, as can be seen by the differences between the spectra for fixed conformations, such as "c" or "d", and fluctuating conformations such as "a", "b", and "e". It is interesting to note that deuterium spectroscopy would be unable to distinguish between free pseudorotation, simulated here by sampling conformations from $\phi = 0°$ to $\phi = 357°$ in increments of 3°, and hindered pseudorotation, calculated by sampling only the symmetric conformations. The simulations of greatest interest are for those conformations which fit the single quantum spectra. In Fig. 5.5 these are "d", which represents a fixed conformation with q = 0.32 Å and $\phi = 0°$, and "e", which represents interconversion between the two C_s conformations with q = 0.30 Å.

Figure 5.6 shows simulations for several orientations of the THF in $K(THF)_{2.5}C_{24}$. As the simulations indicate, the deuteron spectra are very sensitive to changes in orientation. The two spectra of greatest interest are "c" ($\alpha = 21°$ and $\beta = 56°$) and "d" (α oscillates from 40° to 120° and $\beta = 71°$) which are the two orientations that produce reasonable fits with single quantum proton spectroscopy. Once again, the deuteron spectra can clearly distinguish between these two possible cases.

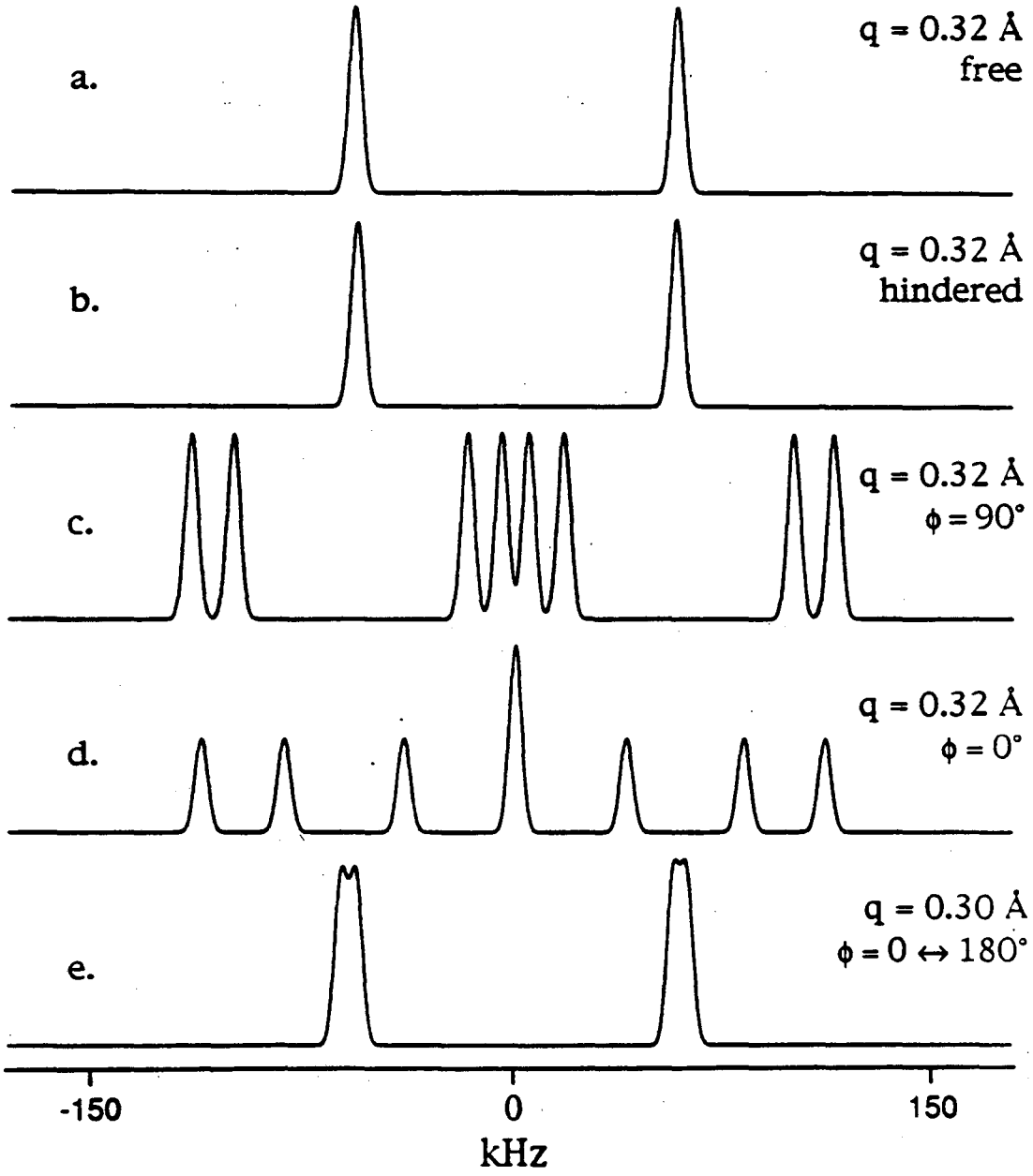

Figure 5.5: Simulated deuterium spectra for $Cs(THF)_{1.3}C_{24}$.

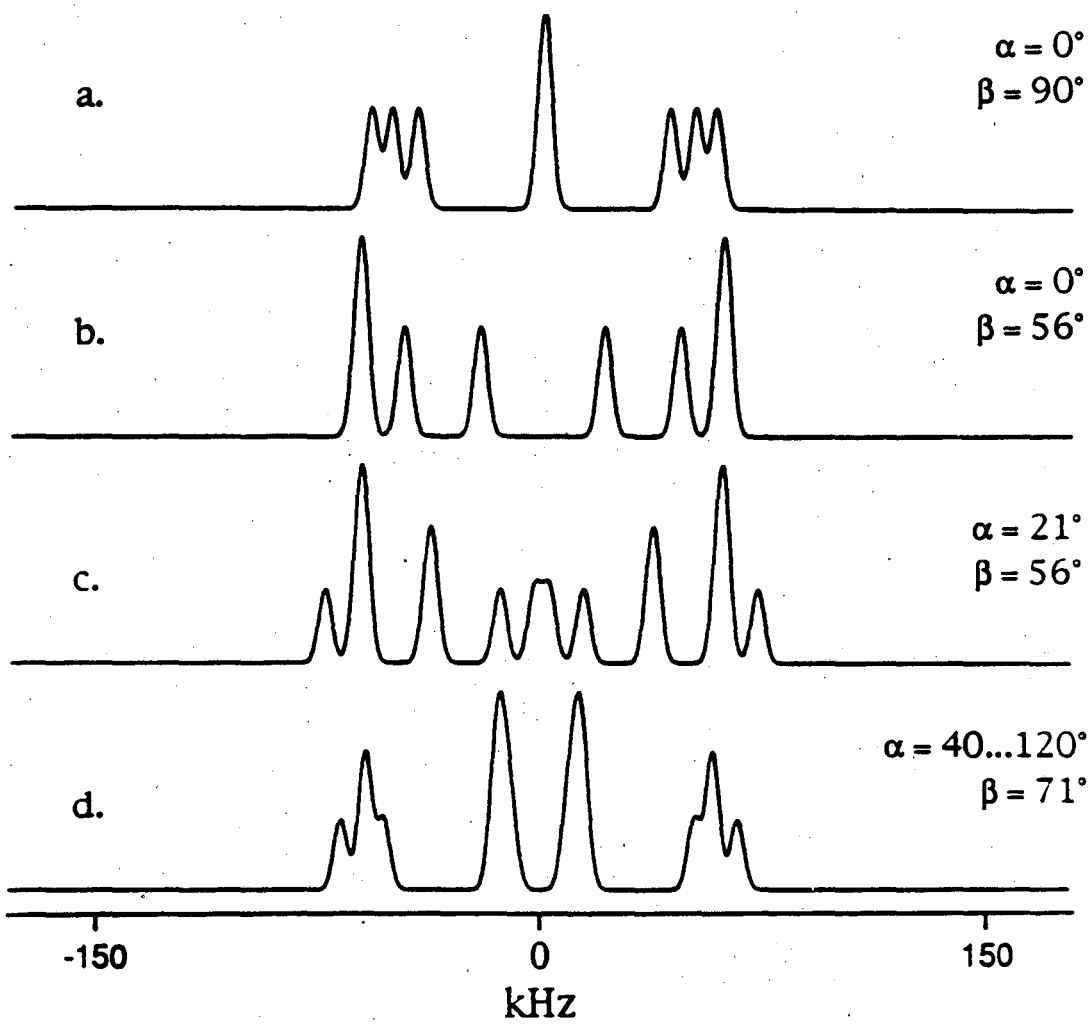

Figure 5.6: Simulated deuterium spectra for $K(THF)_{2.5}C_{24}$.

Chapter 6

Conclusions

Single quantum proton spectroscopy is very sensitive to small changes in the parameters used to model the THF molecule, and to small changes in the molecule's orientation and conformation. The resulting spectrum is complex but analyzable. It is possible to obtain good agreement with the experimental spectra by using Geise's improved version of the model of Pitzer et. al. for the THF molecule.

The results for $Cs(THF)_{1.3}C_{24}$ confirm previous results, that the THF molecules are oriented with their mean molecular planes parallel to the graphite layers, and rotating about the layer's $\vec{c}$ axis, as is demostrated by the scaling of the spectrum when the sample's orientation with respect to the magnetic field is changed. There is a phase change at about 250 K; below that temperature the THF solidifies and the rotation stops, so the spectra no longer scale as $(3\cos^2\Theta - 1)$.

Free pseudorotation does not occur; the THF molecule is in either a fixed C_S conformation or interconverting between the two C_S conformations in such a way that it spends little or no time in other conformations. Good agreement with the experimental spectra is found for a fixed C_S conformation or direct interconversion between the two C_S conformations with q = 0.32 ± 0.01 Å, or for the molecular

potential given in Eq. (4.1) with V_2 = -15 ± 5 kJ/mol, and V_4 = 3 ± 2 kJ/mol, and q = 0.30 ± 0.01 Å, which has minima at the two C_S conformations and a relatively large barrier of about 30 kJ/mol between them, as shown in Fig. 4.7. A phase change at about 120 K may indicate that interconversion takes place at higher temperatures. Interconversion would probably take place by going from one C_S conformation to the other through the planar conformation, rather than by going through the puckered pseudorotation conformations.

The puckering amplitude of intercalated THF is smaller than the gas phase value, indicating that the graphite layers distort the molecule's geometry by making it flatter than it is in the gas phase. However, the GIC environment does not appear to have a large effect on parameters such as the H–C–H angle and C–H bond length.

In $K(THF)_{2.5}C_{24}$ the THF molecule is neither parallel nor perpendicular to the graphite layers and, as in $Cs(THF)_{1.3}C_{24}$, the molecules rotate about the graphite's $\vec{c}$ axis. Two possible orientations found so far, using the same parameters for the molecular geometry found to give best fits in $Cs(THF)_{1.3}C_{24}$, are $\alpha = 21°$, $\beta = 56°$ with a fixed C_S conformation, and $\beta = 71°$ with α oscillating between 40 and 120° using the molecular potential in Eq. (4.1), with an uncertainty of ± 2° in all angles. In either case, the THF molecules are oriented so that the oxygen atom is not pointing at the graphite layers. Since a good fit to the experimental data has not yet been found, it is impossible to reach conclusions about the THF's conformation.

Multiple quantum proton spectra and single quantum deuterium spectra were also simulated to determine if they could refine the single quantum proton spectroscopy results. Multiple quantum proton spectroscopy would probably not be able to dis-

tinguish between fixed and interconverting C_S conformations in $Cs(THF)_{1.3}C_{24}$, but seven quantum proton spectra are sensitive to the THF molecule's orientation, and may be useful in determining the orientation of intercalated THF in $K(THF)_{2.5}C_{24}$.

Deuterium spectra are relatively simple yet very sensitive to orientation and conformation of the THF molecule. If the intercalated alkali metal ions do not have a large effect on the experimental spectra, deuterium spectroscopy could be a valuable tool in the study of the orientation and conformation of $Cs(THF)_{1.3}C_{24}$ and $K(THF)_{2.5}C_{24}$.

Appendix I

```
PROGRAM Avspec (Input, Output, thf, DAv, spectrum, spinbase);
(*  Uses procedures Getcoord and CalcDij from Avproc module.   *)
(*  Link with Avproc, Blockdiag, Eispackn   *)
CONST
 Nsp = 8; Max = 256; pi = 3.141592654;
 basefile = 'eight.spn'; NBLOCK = 9;
TYPE state = (pl,mi);
     ket = ARRAY[1..Nsp] OF state;
     base = ARRAY[1..(Max+1)] OF ket;
     mat = ARRAY[1..Max, 1..Max] OF REAL;
     vect = ARRAY[1..Max] OF REAL;
     SIZE = ARRAY[1..Max] OF INTEGER;
     filename = VARYING[40] OF CHAR;
VAR M, np          :[GLOBAL] INTEGER;
    DipCoup, del   :[GLOBAL] REAL;
    D             :[GLOBAL] ARRAY[1..Nsp, 1..Nsp] OF REAL;
    x,y,z,delom :[GLOBAL] ARRAY[1..Nsp] OF REAL;
    phi           :[GLOBAL] REAL;
    biz           :[GLOBAL] base;
    Hint,rint,Ix,
    Iplus          :[GLOBAL] mat;
    aint           :[GLOBAL] vect;
    rzero          :[GLOBAL] BOOLEAN;
    spectrum       :[GLOBAL] FILE OF REAL;
    thf,
    spinbase       :[GLOBAL] TEXT;
    intham         :[GLOBAL] FILE OF REAL;
    NSIZE               :[GLOBAL] SIZE;
    datafile, spec      :[GLOBAL] filename;
    Cx, Cy, Cz          :[GLOBAL] ARRAY[1..5] OF REAL;
    n, r, p, i, j,
    ra, rb          :  INTEGER;
    alph, bet, firstalph,
    firstbet, firstphi,
    prevalph, prevbet, prevphi     :  REAL;

    k, q, So, initphi, incphi,
    finalphi, CHlength, HCHangle,
    HCHcoupling, initalph, incalph,
    finalalph, initbet, incbet,
    finalbet, alpha, beta           :  [GLOBAL] REAL; (* parameters used
to calculate molecular coordinates *)
    Phase, alphrot,
    betrot              :  ARRAY[1..20000] OF REAL;
    DAv                  :  TEXT;
```

```
    answer, name        :  VARYING[20] OF CHAR;
    shift, DipChange    :  CHAR;
    readphi, readalph,
    readbet             :  BOOLEAN;

(* EXTERNAL PROCEDURES FROM AVPROC MODULE FOLLOW *)

PROCEDURE Getcoords;
  EXTERNAL;
PROCEDURE Getshift;
  EXTERNAL;
PROCEDURE CalcDij;
  EXTERNAL;
PROCEDURE Readbase;
  EXTERNAL;
FUNCTION Find:INTEGER;
  EXTERNAL;
PROCEDURE WriteIxIplus;
  EXTERNAL;
PROCEDURE Blodia;
  EXTERNAL;
PROCEDURE Internalham;
  EXTERNAL;
PROCEDURE CalculatePlus;
  EXTERNAL;
PROCEDURE Readheader;
 EXTERNAL;
PROCEDURE Writeparameters;
 EXTERNAL;

(* LOCAL PROCEDURES FOLLOW *)

PROCEDURE WriteDij;

VAR i, j:  INTEGER;
BEGIN
Open(DAv, 'dav.dat', NEW);
Rewrite(DAv);
For i := 1 to Nsp Do
   BEGIN
   For j := i + 1 to Nsp Do
     BEGIN
     Writeln(DAv, D[i, j]);
     END; (* for j *)
   END; (* for i *)
Close(DAv);
Writeln('Average Dipole coupling data written to Dav.dat ');
Writeln;
Writeln('NOTE:  DIPOLE COUPLINGS NEED TO BE MULTIPLIED BY DIPOLE');
Writeln('COUPLING CONSTANT BEFORE USE!');
Writeln;
END; (* WriteDAv *)

PROCEDURE CalcDAv;
BEGIN
DipCoup := 60.06;
Writeln('Dipole coupling constant is:  ', DipCoup);
Writeln('Enter "y" to change dipole coupling constant.  ');
```

```
Readln(Dipchange);
If (Dipchange = 'y') OR (Dipchange = 'Y') Then
  Begin
  Writeln('Enter new value for coupling constant:  ');
  Readln(DipCoup);
  Writeln('New value for contant is:  ', DipCoup);
  End; (* If dipchange *)
Getshift;
Writeln('Enter name of THF coordinate file to be read.  ');
Readln(datafile);
Writeln('File to be read is:  ', datafile);
Open(thf, datafile, READONLY);
Reset(thf);
r := 0;
ra := 0;
rb := 0;
p := 0;
D := zero;
Readheader;
readalph := TRUE;
readbet := TRUE;
readphi := TRUE;
REPEAT
  Readln(thf, phi, alph, bet);
  r := r + 1; (* Total number of coordinate sets read *)
  If r = 1 Then
   Begin
   firstbet := bet; prevbet := bet;
   firstalph := alph; prevalph := alph;
   firstphi := phi; prevphi := phi;
   End; (* IF r *)
  If readbet Then (* Get values of rotation angle beta *)
     Begin
     If readalph Then (* Get values of alpha *)
        Begin
        If readphi Then
          Begin
          If (phi = firstphi) AND (r > 1) Then
            Begin
            readphi := FALSE  (* Once a full set has been read,stop.*)
            End
          Else
            If (phi <> prevphi) OR (r = 1) Then
             Begin
             p := p + 1;
             Phase[p] := phi;
             prevphi := phi;
             End; (* If phi <> *)
          End; (* If readphi *)
        If (alph = firstalph) AND (readphi = FALSE) Then
          readalph := FALSE
         Else
           If (alph <> prevalph) OR (r = 1) Then
            Begin
            ra := ra + 1;
            alphrot[ra] := alph;
            prevalph := alph;
            End; (* If alph <>  *)
```

```
        End; (* If readalph *)
      If (bet = firstbet) AND (readalph = FALSE) Then
        readbet := FALSE
      Else
        If (bet <> prevbet) OR (r = 1) Then
         Begin
         rb := rb + 1;
         betrot[rb] := bet;
         End; (* If bet <>  *)
      End; (* If readbet *)
  Getcoords;
  CalcDij;
UNTIL EOF(thf);
Close(thf);
For i := 1 to Nsp Do
  BEGIN
  For j := i + 1 to Nsp Do
     BEGIN
     D[i, j] := D[i, j]/SNGL(r) * DipCoup;
     D[j, i] := D[i, j];
     END; (* For j *)
  END; (* For i *)
IF (r = 1) THEN
  Writeln('1 set of coordiantes read.  ')
  ELSE Writeln(r, ' sets of coordinates read.');
Writeln('Phi values for files read are:  ');
For i := 1 to p Do
  Writeln(Phase[i]);
Writeln('Alpha values read are:  ');
For i := 1 to ra Do
   Writeln(alphrot[i]:4);
Writeln('Beta values read are:  ');
For i := 1 to rb Do
   Writeln(betrot[i]:4);
END; (* GetDAv *)

PROCEDURE ReadDAv;
VAR i, j:  INTEGER;
BEGIN
Open(DAv, 'dav.dat', READONLY);
Reset(DAv);
For i := 1 To Nsp Do
   BEGIN
   For j := i + 1 To Nsp Do
     BEGIN
     Readln(DAv,D[i, j]);
     D[j, i] := D[i, j];
     Writeln(D[i, j]);
     END; (* FOR j *)
   END; (* FOR i *)
Close (DAv);
END; (* ReadDAv *)

(* PROGRAM BODY FOLLOWS *)

BEGIN
CalcDAv;
Writeln('Enter "y" if you wish dipole coupling tensor written to file:');
```

```
Readln(answer);
If answer = 'y' Then WriteDij;
(* ReadDav; *)
Readbase;
WriteIxIplus;
Writeln('IxIplus completed.');
Internalham;
Writeln('Internalham completed.');
spec := 'sp' + datafile;
Open(spectrum, spec);
Rewrite(spectrum);
Writeln('Output file opened.');
Writeparameters;
Writeln('Writeparameters completed.');
CalculatePlus;
Writeln('Calculateplus completed.');
Close(spectrum);
Writeln('Program completed.  ');
END.
```

```
MODULE Avproc(input, output);
(* Link compiled code with BLOCKDIAG and  EISPACKN *)
CONST  Nsp = 8; Max = 256; pi = 3.141592654;
        basefile = 'eight.spn'; NBLOCK = 9;
TYPE state = (pl,mi);
     ket = ARRAY[1..Nsp] OF state;
     base = ARRAY[1..(Max+1)] OF ket;
     mat = ARRAY[1..Max, 1..Max] OF REAL;
     vect = ARRAY[1..Max] OF REAL;
     SIZE = ARRAY[1..Max] OF INTEGER;
     filename = VARYING[40] OF CHAR;
VAR M, np        :[EXTERNAL] INTEGER;
    DipCoup      :[EXTERNAL] REAL;
    D            :[EXTERNAL] ARRAY[1..Nsp, 1..Nsp] OF REAL;
    x,y,z,delom :[EXTERNAL] ARRAY[1..Nsp] OF REAL;
    phi          :[EXTERNAL] REAL;
    biz          :[EXTERNAL] base;
    Hint,rint,
    Ix, Iplus     :[EXTERNAL] mat;
    aint          :[EXTERNAL] vect;
    rzero         :[EXTERNAL] BOOLEAN;
    spectrum      :[EXTERNAL] FILE OF REAL;
    thf,
    spinbase      :[EXTERNAL] TEXT;
    intham        :[EXTERNAL] FILE OF REAL;
    NSIZE              :[EXTERNAL] SIZE;
    datafile, spec     :[EXTERNAL] filename;
    Cx, Cy, Cz         :[EXTERNAL] ARRAY[1..5] OF REAL;
    i                  :  INTEGER;
    k, q, So, initphi, incphi, finalphi, CHlength, HCHangle,
    HCHcoupling, initalph, incalph, finalalph, initbet, incbet,
    finalbet, alpha, beta   :  [EXTERNAL] REAL; (* parameters used to
                                        calculate molecular coordinates *)

[GLOBAL] PROCEDURE Getcoords;
(* Gets phase angle "phi" and coordinates of Hydrogen atoms from THF
data file.  *)
BEGIN
(* First read off Oxygen and Carbon atom positions.  Also read blank
spaces in file *)
FOR i := 1 TO 5 DO
   BEGIN
   Read(thf, Cx[i]); Read(thf, Cy[i]); Read(thf, Cz[i]);
      ReadLn(thf);
   END; (* FOR *)
(* Now get Hydrogen coordinates *)
FOR i := 1 TO 8 DO
   BEGIN
   Read(thf, x[i]); Read(thf, y[i]); Readln(thf, z[i]);
   END; (* FOR *)
M := 256;
END; (* Getcoords *)

[GLOBAL] PROCEDURE Getshift;
VAR shift :  CHAR;
    del   :  REAL;
Begin
Writeln('Do you want to include chemical shift?  (If yes enter "y".)');
```

```
Readln(shift);
If (shift = 'y') OR (shift = 'Y') Then
  Begin
  Writeln('Enter shift for hydrogens nearest oxygen:  ');
  Readln(del);
  delom[1] := del;
  delom[2] := del;
  delom[7] := del;
  delom[8] := del;
  Writeln('Enter shift for remaining hydrogens:  ');
  Readln(del);
  delom[3] := del;
  delom[4] := del;
  delom[5] := del;
  delom[6] := del;
  End
  Else delom := zero;
END; (* Getshift *)

[GLOBAL] PROCEDURE CalcDij;
VAR i, j : INTEGER;
    r, cosq : REAL;
BEGIN
FOR i:=1 TO Nsp DO
   BEGIN
   FOR j:=i+1 TO Nsp DO
      BEGIN
      r:=sqrt( (x[i]-x[j])*(x[i]-x[j]) + (y[i]-y[j])*(y[i]-y[j])
             + (z[i]-z[j])*(z[i]-z[j]) );
      IF (r = 0.0) THEN
         BEGIN
         Writeln(' !!! r[', i:1, ',' , j:1, '] = 0 !!!');
         rzero:=TRUE;
         END; (* IF r *)
      cosq := (z[i]-z[j]) * (z[i]-z[j])/(r * r);
      D[i,j]:= D[i, j] + (1.0 - 3.0 * cosq)/(r * r * r);
      D[j,i]:= D[i, j];
   END; (* FOR j *)
END; (* FOR i *)
 END; (* CalcDij; *)

[GLOBAL] PROCEDURE Readbase;
(* Reads basis sets generated by setupbase and stored in files *)
VAR  i, j, spin    :  INTEGER;
BEGIN
Open(spinbase, basefile, READONLY);
Reset(spinbase);
FOR i := 1 TO M DO
   BEGIN
   FOR j := 1 TO Nsp DO
      BEGIN
      Read(spinbase, spin);
      IF spin = 1 THEN biz[i, j] := pl
         ELSE biz[i, j] := mi;
      END; (* FOR j *);
   Readln(spinbase);
    END; (* FOR i *)
Close(spinbase);
```

```
Writeln('Readbase completed.  ');
WriteLn;
END; (* Readbase;*)

FUNCTION Find(Xk : ket) : INTEGER;
VAR i, k, n : INTEGER;
    found,OK : BOOLEAN;
BEGIN
found := FALSE;
(* find total spin of ket *)
n := 0;
For i := 1 to Nsp DO
   IF Xk[i] = pl
   THEN n := n + 1;
(* direct search for conjugate to block of bras with appropriate spin *)
CASE n OF
 8 :  k := 1;
 6 :  k := 2;
 4 :  k := 30;
 2 :  k := 100;
 0 :  k := 128;
 7 :  k := 129;
 5 :  k := 137;
 3 :  k := 193;
 1 :  k := 249;
 END;
WHILE NOT found DO
   BEGIN
   OK :=TRUE;
   i:=1;
   WHILE OK AND (i<Nsp+1) DO
     BEGIN
     IF Xk[i]<>biz[k,i] THEN OK := FALSE
        ELSE i:=i+1;
     END; (* WHILE *)
   IF OK THEN found:=TRUE
      ELSE k:=k+1;
   END; (* WHILE NOT *)
Find := k;
END; (* Find;*)

[GLOBAL] PROCEDURE WriteIx;
VAR i,j,k,l,u,a,b : INTEGER;
    Xk, Yk : ket;
BEGIN
FOR k:=1 TO M  DO
   BEGIN
   FOR l:=1 TO M  DO
      BEGIN
      Ix[k,l] := 0.0;
      END; (* FOR l *)
   END; (* FOR k *)
FOR k:=1 TO M  DO
   BEGIN
   FOR a:=1 TO Nsp  DO
      BEGIN
      FOR i:=1 TO Nsp  DO
         BEGIN
```

```
            Xk[i]:=biz[k,i];
            Yk[i]:=biz[k,i];
            END; (* FOR i *)
         IF Xk[a]=mi THEN
            BEGIN
            Xk[a] := pl;
            b := Find(Xk);
            Ix[b,k] := 0.5;
            END; (* IF *)
         IF Yk[a]=pl THEN
            BEGIN
            Yk[a] := mi;
            b := Find(Yk);
            Ix[b,k] := 0.5;
            END; (* IF *)
         END; (* FOR a *)
      END; (* FOR k*)
   END; (* WriteIx;*)

   [GLOBAL] PROCEDURE WriteIxIplus;
   (* Generates Ix and Iplus matrices used to calculate signal *)
   VAR i,j,k,l,u,a,b : INTEGER;
       Xk, Yk : ket;
   BEGIN
   Ix := zero;
   FOR k:=1 TO M  DO
      BEGIN
      FOR a:=1 TO Nsp  DO
         BEGIN
         FOR i:=1 TO Nsp  DO
            BEGIN
            Xk[i]:=biz[k,i];
            Yk[i]:=biz[k,i];
            END; (* FOR i *)
         CASE Xk[a] OF
           mi: BEGIN
               Xk[a] := pl;
               b := Find(Xk);
               Ix[b,k] := 0.5;
               Iplus[b, k] := 1.0;
               END; (* mi *)
           pl: BEGIN
               Yk[a] := mi;
               b := Find(Yk);
               Ix[b,k] := 0.5;
               END; (* pl *)
           END; (* CASE *)
         END; (* FOR a *)
      END; (* FOR k*)
   END; (* WriteIx;*)

   [GLOBAL] PROCEDURE Readheader;
   Begin
   np := 0;
   Read(thf, k); Readln(thf);
   np := np + 1;
   Read(thf, q); Readln(thf);
   np := np + 1;
```

```
Read(thf, So); Readln(thf);
np := np + 1;
Read(thf, initphi); Readln(thf);
np := np + 1;
Read(thf, incphi); Readln(thf);
np := np + 1;
Read(thf, finalphi); Readln(thf);
np := np + 1;
Read(thf, CHlength); Readln(thf);
np := np + 1;
Read(thf, HCHangle); Readln(thf);
np := np + 1;
Read(thf, HCHcoupling); Readln(thf);
np := np + 1;
Read(thf, initalph); Readln(thf);
np := np + 1;
Read(thf, incalph); Readln(thf);
np := np + 1;
Read(thf, finalalph); Readln(thf);
np := np + 1;
Read(thf, initbet); Readln(thf);
np := np + 1;
Read(thf, incbet); Readln(thf);
np := np + 1;
Read(thf, finalbet); Readln(thf);
np := np + 1;
Read(thf, alpha); Readln(thf);
np := np + 1;
Read(thf, beta); Readln(thf);
np := np + 1;
For i := np + 1 To 100 Do
Readln(thf);
END; (* Readheader *)

[GLOBAL] PROCEDURE Writeparameters;
BEGIN
np := 0;
Write(spectrum, k);
np := np + 1;
Write(spectrum, q);
np := np + 1;
Write(spectrum, So);
np := np + 1;
Write(spectrum, initphi);
np := np + 1;
Write(spectrum, incphi);
np := np + 1;
Write(spectrum, finalphi);
np := np + 1;
Write(spectrum, CHlength);
np := np + 1;
Write(spectrum, HCHangle);
np := np + 1;
Write(spectrum, HCHcoupling);
np := np + 1;
Write(spectrum, initalph);
np := np + 1;
Write(spectrum, incalph);
```

```
np := np + 1;
Write(spectrum, finalalph);
np := np + 1;
Write(spectrum, initbet);
np := np + 1;
Write(spectrum, incbet);
np := np + 1;
Write(spectrum, finalbet);
np := np + 1;
Write(spectrum, alpha);
np := np + 1;
Write(spectrum, beta);
np := np + 1;
Write(spectrum, DipCoup);
np := np + 1;
Write(spectrum, delom[1]);
np := np + 1;
Write(spectrum, delom[3]);
np := np + 1;
For i := np+1 to 100 Do
  Write(spectrum, 0.0);
End; (* Writeparameters *)

PROCEDURE Blodia(M :  INTEGER; NSIZE : SIZE; NBLOCK :  INTEGER;
         VAR Hint, Hi, rint, iint: Mat; VAR aint :  vect);  External;

[GLOBAL] PROCEDURE Internalham;
VAR i, j, k, a,
    b, fac, ierr : INTEGER;
    Xk, Yk : ket;
    Hi, iint : mat;
BEGIN
NSIZE[1] := 1;
NSIZE[2] := 28;
NSIZE[3] := 70;
NSIZE[4] := 28;
NSIZE[5] := 1;
NSIZE[6] := 8;
NSIZE[7] := 56;
NSIZE[8] := 56;
NSIZE[9] := 8;
FOR i:=1 TO M  DO
   BEGIN
   FOR j:=1 TO M  DO
      BEGIN
      Hint[i,j]:=0.0;
      END; (* FOR j *)
   END; (* FOR i *)
FOR k:=1 TO M  DO
   BEGIN
   FOR i:=1 TO Nsp  DO
      BEGIN
      IF biz[k,i] = pl THEN fac:=1
        ELSE fac:=-1;
      Hint[k,k] := Hint[k,k] + SNGL(fac) * delom[i]/2.0;
      END; (* FOR i *)
   END;
FOR i:=1 TO Nsp  DO
```

```
   BEGIN
   FOR j:=i+1 TO Nsp  DO
      BEGIN
      FOR k:=1 TO M  DO
         BEGIN
         IF biz[k,i] = pl THEN fac:=+1
            ELSE fac:=-1;
         IF biz[k,j] = mi THEN fac:=-fac;
         Hint[k,k] := Hint[k,k] + SNGL(fac) * D[i,j]/2.0;
         FOR a:=1 TO Nsp  DO
            BEGIN
            Xk[a] := biz[k,a];
            Yk[a] := biz[k,a];
            END; (* FOR a *)
         IF (Xk[i]=pl) AND (Xk[j]=mi) THEN
            BEGIN
            Xk[i] := mi;
            Xk[j] := pl;
            b := Find(Xk);
            Hint[b,k] := Hint[b,k] - D[i,j]/2.0;
            END;  (* IF *)
         IF (Yk[i]=mi) AND (Yk[j]=pl) THEN
            BEGIN
            Yk[i] := pl;
            Yk[j] := mi;
            b := Find(Yk);
            Hint[b,k] := Hint[b,k] - D[i,j]/2.0;
            END; (* IF *)
         END; (* FOR k *)
      END; (* FOR j *)
   END; (* FOR i *)
FOR i:=1 TO M  DO
   BEGIN
   FOR j:=1 TO M  DO
      BEGIN
      Hi[i,j]:=0.0;
      END; (* FOR j *)
   END; (* FOR i *)

Blodia(Max, NSIZE, NBLOCK, Hint, Hi, rint, iint, aint);
END; (* Internalham;*)

[GLOBAL] PROCEDURE CalculatePlus;
VAR i, j, k, l : INTEGER;
    u, w, om, tot : REAL;
    RIx, RIplus,
    RIxRtrans, RIplusRtrans : mat;
BEGIN
Writeln('1D signal: intensity and frequency');
WriteLn;
tot:=0.0;
(*** Matrix multiplication: prov = rint * Ix  ***)
(* Calculate RIx *)
For i := 1 To M Do
  Begin
  For j := 1 to M do
    Begin
    RIx[i, j] := 0.0;
```

```
      For k := 1 to M do
        RIx[i, j] := RIx[i, j] + rint[i, k] * Ix[k, j];
      End; (* for j *)
    End; (* for i *)
  (* Calculate RIxRtrans *)
  For i := 1 to M do
    Begin
    For j := 1 to M do
      Begin
      RIxRtrans[i, j] := 0.0;
      For k := 1 to M do
        RIxRtrans[i, j] := RIxRtrans[i, j] + RIx[i, k] * rint[j, k]
      End; (* for j *)
    End; (* for i *)
  (* Calculate RIplus *)
  For i := 1 To M Do
    Begin
    For j := 1 to M do
      Begin
      RIplus[i, j] := 0.0;
      For k := 1 to M do
        RIplus[i, j] := RIplus[i, j] + rint[i, k] * Iplus[k, j];
      End; (* for j *)
    End; (* for i *)
  (* Calculate RIplusRtrans *)
  For i := 1 to M do
    Begin
    For j := 1 to M do
      Begin
      RIplusRtrans[i, j] := 0.0;
      For k := 1 to M do
        RIplusRtrans[i, j] := RIplusRtrans[i, j] + RIplus[i, k] *
        rint[j,k]
      End; (* for j *)
    End; (* for i *)
  FOR i:=1 TO M  DO
     BEGIN
     FOR j:= 1 TO M  DO
        BEGIN
        w:=0.0;
        w := RIplusRtrans[i, j] * RIxRtrans[j, i];
        tot := tot + w;
        om := aint[j] - aint[i];
         IF w > 0.00001 THEN
           BEGIN
           Write(spectrum, w, om);
         END; (* IF *)
        END; (* FOR j *)
     END; (* FOR i *)
     tot := tot * 4.0/SNGL(M);
     Writeln('total intensity = ', tot:8);
     Writeln('Data written to file ', spec);
   END; (* CalculatePlus *)

  END.
```

Appendix II

```
MODULE Coord;

(* This program is a modification of thfrotcoord which can be used by a
   batch job and which writes the parameters used in calculating
   coordinates to a file.  This program is to replace Thfcoord, Thfcoordset
   and Thfrotcoord.   Working version finished by on 5/7/89 by D. C.  *)

(* Working version THFCOORD.MOD;129 finished 10/25/88 by D. Caplan *)

FROM InOut IMPORT WriteInt, ReadString, ReadReal;
FROM TextIO IMPORT EOL, Write, WriteString, WriteReal, Close, OpenOutput, tty,
WriteLn, File, ReadLn, Read;
FROM MathLib0 IMPORT cos, sin, sqrt, arcsin, arctan;
FROM Conversions IMPORT IntToReal, StringToReal;
FROM rotate IMPORT rotate,vect;

TYPE coord = RECORD
        x, y, z : REAL;
        END;
String = ARRAY[1..40] OF CHAR;

VAR  C, Hplus, Hminus     :  ARRAY [0..4] OF coord; (* positions of H and C
atoms in molecular frame *)
     O, C1, C2, C3, C4,
     OP, C1P, C2P, C3P, C4P   :  vect;

     Hlocplus, Hlocminus,  (* coordinates of Hydrogen in local frame *)
     Xloc, Yloc, Zloc,     (* local unit vectors expressed in molecular
                              coordinates *)
     Hmolplus, Hmolminus,  (* vector from carbon atom to hydrogen atom
                              expressed in molecular coordinates *)
     Vprev, Vnext          (* vector from previous or next carbon
                              to current carbon *)
                          : coord;

     i, next, prev, np, blanks                : INTEGER;

     n, ratio, phi, nalpha, angle,
     xyangle, HCHangle, Origangle, HCHcoupling,
     avx, avz, initphi, finalphi,
     increment, initalph, initbet, finalbet,
     incbet, dipnum, alph, bet, gamma,
     finalalph, incalph
     ,q, k, So            : REAL;

     S                    : ARRAY [0..4] OF REAL;

     Variable, outputname : String;
```

```
     outputfile, out       : File;

     rotation, dipframe    : CHAR;

CONST
      pi = 3.14159265;
      beta = 68.22000;
      alpha = 74.52000;
      CHlength = 1.11500;

(* ---- Procedures CrossProd, Normalize and GetReal follow ----*)

PROCEDURE CrossProd(vec1, vec2 : coord; VAR prod : coord);
   (* Calculates the cross product of vec1 and vec2; result is prod *)
BEGIN
prod.x := (vec1.y * vec2.z) - (vec1.z * vec2.y);
prod.y := (vec1.z * vec2.x) - (vec1.x * vec2.z);
prod.z := (vec1.x * vec2.y) - (vec1.y * vec2.x);
END CrossProd;

PROCEDURE Normalize (VAR vec : coord);
    (* Normalizes a vector *)
VAR length : REAL;
BEGIN
length := sqrt((vec.x * vec.x) + (vec.y * vec.y) + (vec.z * vec.z));
vec.x := vec.x/length;
vec.y := vec.y/length;
vec.z := vec.z/length;
END Normalize;

PROCEDURE GetReal (Default: REAL; VAR Input : REAL; Variable : ARRAY OF CHAR);
VAR number : ARRAY[1..40] OF CHAR;
BEGIN
WriteString(tty, "Enter "); WriteString(tty,  Variable);
 WriteString(tty,  ".  (Default is:");
WriteReal(tty, Default, 3); WriteString(tty, ")   ");
WriteLn(tty);
ReadString(number);
IF number[1] = CHR(0)
   THEN Input := Default;
   ELSE Input := StringToReal(number);
   END; (* IF *)
END GetReal;

PROCEDURE wrtnum(out:  File (* outputfile *); initcomment:  ARRAY OF CHAR;
num:  REAL; field:  CARDINAL; finalcomment:  ARRAY OF CHAR);

(* Writes number accompanying text to screen or file *)
BEGIN
WriteString(tty,  initcomment); WriteReal(out, num, field);
  WriteString(out, finalcomment); WriteLn(out);
END wrtnum;

(* ------------ Program Body Follows ------------- *)

BEGIN
```

```
(* Get parameters for calculations *)

GetReal(0.38, q, "q");
GetReal(0.65, k, "k");
GetReal(1.277, So, "So");
GetReal(110.0, HCHangle, "H-C-H Angle");
GetReal(0.0, HCHcoupling, "HCH-pseudorotation coupling");

GetReal(0.0, initphi, "initial pseudorotation angle");
GetReal(180.0, finalphi, "final pseudorotation angle");
GetReal(5.0, increment, "increment");

WriteString(tty, "Do you want molecule in dipole frame?  "); WriteLn(tty);
Read(tty, dipframe); ReadLn(tty);
IF ((dipframe <> "y") AND (dipframe <> "Y")) THEN
  WriteString(tty, "Do you want to rotate molecule?  ");  WriteLn(tty);
  Read(tty, rotation);
  IF ((rotation= "y") OR (rotation = "Y")) THEN
    ReadLn(tty);
    GetReal(0.0, initalph, "inital rotation about 'z' axis");
    GetReal(180.0, finalalph, "final rotation about 'z' axis");
    GetReal(5.0, incalph, "increment");
    GetReal(90.0, initbet, "initial rotation about 'y' axis");
    GetReal(90.0, finalbet, "final rotation about 'y' axis");
    GetReal(5.0, incbet, "increment");
    (* GetReal(0.0, gamma, "angle of second rotation about 'z' axis");*)
    gamma := 0.0;
    END; (* IF rotation *)
  END; (* IF dipframe *)

(* If there is no rotation and dipole frame is used, set rotation angles
   to zero *)
IF ((rotation <> "Y") AND (rotation <> "y")) OR ((dipframe = "Y") OR
    (dipframe = "y")) THEN
    WriteString(tty, "No Rotation");
    WriteLn(tty);
    initalph := 0.0;
    finalalph := 0.0;
    incalph := 5.0;
    initbet := 0.0;
    finalbet := 0.0;
    incbet := 5.0;
    gamma := 0.0;
  END; (* IF *)

wrtnum(tty, "k = ", k, 3, "");
wrtnum(tty, "q = ", q, 3, "");
wrtnum(tty, "So =", So, 3, "");
wrtnum(tty, "phi = ", phi, 3, "");
wrtnum(tty, "CH = ", CHlength, 3, "");
wrtnum(tty, "HCH =", HCHangle, 3, "");
wrtnum(tty, "HCHcoupling = ", HCHcoupling, 3, "");
wrtnum(tty, "alpha = ", initalph, 3, "");
wrtnum(tty, "incalpha = ", incalph, 3, "");
wrtnum(tty, "finalalpha = ", finalalph, 3, "");
wrtnum(tty, "beta = ", initbet, 3, "");
wrtnum(tty, "incbet = ", incbet, 3, "");
wrtnum(tty, "finalbet = ", finalbet, 3, "");
```

```
WriteString(tty, "Enter name for data file:  ");
OpenOutput(outputfile, ".dat");

(* Write parameters to file.  Block containing parameters should be
   100 lines long.  *)
np := 0;
wrtnum(outputfile, "", k, 10, "  :  k");
 np := np + 1;
wrtnum(outputfile, "", q, 10, "  :  q");
 np := np + 1;
wrtnum(outputfile, "", So, 10, "  :  So");
 np := np + 1;
wrtnum(outputfile, "", initphi, 10, "  :  initphi");
 np := np + 1;
wrtnum(outputfile, "", increment, 10, "  :  incphi");
 np := np + 1;
wrtnum(outputfile, "", finalphi, 10, "  :  finalphi");
 np := np + 1;
wrtnum(outputfile, "", CHlength, 10, "  :  CHlength");
 np := np + 1;
wrtnum(outputfile, "", HCHangle, 10, "  :  HCHangle");
 np := np + 1;
wrtnum(outputfile, "", HCHcoupling, 10, "  :  HCHcoupling");
 np := np + 1;
wrtnum(outputfile, "", initalph, 10, "  :  initalph, rot. about z axis");
 np := np + 1;
wrtnum(outputfile, "", incalph, 10, "  :  incalph");
 np := np + 1;
wrtnum(outputfile, "", finalalph, 10, "  :  finalalph");
 np := np + 1;
wrtnum(outputfile, "", initbet, 10, "  :  initbet");
 np := np + 1;
wrtnum(outputfile, "", incbet, 10, "  :  incbet");
 np := np + 1;
wrtnum(outputfile, "", finalbet, 10, "  :  finalbet");
 np := np + 1;
wrtnum(outputfile, "", alpha, 10, "  :  alpha, Ox-Origin-Carbon angle");
 np := np + 1;
wrtnum(outputfile, "", beta, 10, "  :  beta, Carbon-Origin-Carbon angle");
 np := np + 1;
IF (dipframe = "y") OR (dipframe = "Y") THEN
  dipnum := 1.0;
ELSE
  dipnum := 0.0;
  END; (* IF *)
wrtnum(outputfile, "", dipnum, 10, "  :  dipole frame (1.0 = yes)");
 np := np + 1;
wrtnum(outputfile, "", 1.0, 10,"  :  actual phi");
 np := np + 1;
(* fill in rest of 100 lines with blanks *)
FOR blanks := (np + 1) TO 100 DO
  WriteLn(outputfile);
  END; (* FOR *)

bet := initbet;

WHILE bet <= finalbet DO
```

```
WriteString(tty, "Beta = "); WriteReal(tty, bet, 4); WriteLn(tty);
alph := initalph;

WHILE alph <= finalalph DO
WriteString(tty, "Alpha = "); WriteReal(tty, alph, 4); WriteLn(tty);
phi := initphi;

WHILE phi <= finalphi DO
WriteString(tty, "Phi = "); WriteReal(tty, phi, 4); WriteLn(tty);

(* Calculate carbon atom coordinates *)

FOR i := 0 TO 4 BY 1 DO
   C[i].z := sqrt(2.0/5.0) * q * cos((4.0 * pi/5.0 * IntToReal(i))
         + (pi/180.0) * phi);
   S[i] := So * (1.0 - (k * (C[i].z * C[i].z)) );
   ratio := C[i].z/S[i];
   angle := arcsin(ratio);
   nalpha := IntToReal(i) - 1.0;
   xyangle:= (beta + (nalpha * alpha)) * pi/180.0;
   IF i >= 1 THEN
     C[i].x := S[i] * cos(angle) * cos(xyangle);
     C[i].y := S[i] * cos(angle) * sin(xyangle);
   ELSE
     C[i].x := S[i] * cos(angle);
     C[i].y := 0.0;
   END; (* IF *)
   END;  (* FOR *)

IF ((dipframe = "y") OR (dipframe = "Y")) THEN
  (* Find angle between dipole vector and horizontal axis *)
  (* First find average coordinates of C[2] and C[3] *)
  avx := (C[2].x + C[3].x)/2.0;
  avz := (C[2].z + C[3].z)/2.0;
  bet := arctan((C[0].z - avz)/(C[0].x - avx)) * 180.0/pi;
  alph := 0.0;
  gamma := 0.0;
END; (* IF dipframe *)

(* Rotation of O and C coordinates *)
   O[1] := C[0].x;
   O[2] := C[0].y;
   O[3] := C[0].z;
   C1[1] := C[1].x;
   C1[2] := C[1].y;
   C1[3] := C[1].z;
   C2[1] := C[2].x;
   C2[2] := C[2].y;
   C2[3] := C[2].z;
   C3[1] := C[3].x;
   C3[2] := C[3].y;
   C3[3] := C[3].z;
   C4[1] := C[4].x;
   C4[2] := C[4].y;
   C4[3] := C[4].z;

rotate(O,alph,bet,gamma,OP);
rotate(C1,alph,bet,gamma,C1P);
```

```
rotate(C2,alph,bet,gamma,C2P);
rotate(C3,alph,bet,gamma,C3P);
rotate(C4,alph,bet,gamma,C4P);

   C[0].x := OP[1];
   C[0].y := OP[2];
   C[0].z := OP[3];
   C[1].x := C1P[1];
   C[1].y := C1P[2];
   C[1].z := C1P[3];
   C[2].x := C2P[1];
   C[2].y := C2P[2];
   C[2].z := C2P[3];
   C[3].x := C3P[1];
   C[3].y := C3P[2];
   C[3].z := C3P[3];
   C[4].x := C4P[1];
   C[4].y := C4P[2];
   C[4].z := C4P[3];

(* Calculate Hydrogen coordinates *)
FOR i := 1 TO 4 BY 1 DO
    (* Hydrogen positions in local coordinates follow:  *)
Hlocplus.x := 0.0;
Hlocplus.y := CHlength * cos((HCHangle/2.0) * pi/180.0);
Hlocplus.z := CHlength * sin((HCHangle/2.0) * pi/180.0);
Hlocminus.x := Hlocplus.x;
Hlocminus.y := Hlocplus.y;
Hlocminus.z := -Hlocplus.z;

(* Convert local Hydrogen coordinates to molecular coordinates *)
     (* First express local unit vectors in terms of molecular frame
        x, y and z vectors *)
   prev := i - 1;
   IF i = 4
     THEN next := 0;
     ELSE next := i + 1;
     END; (* IF *)

   Vnext.x := C[i].x - C[next].x;
   Vnext.y := C[i].y - C[next].y;
   Vnext.z := C[i].z - C[next].z;
   Vprev.x := C[i].x - C[prev].x;
   Vprev.y := C[i].y - C[prev].y;
   Vprev.z := C[i].z - C[prev].z;

   Normalize(Vnext);
   Normalize(Vprev);

   Xloc.x := Vnext.x - Vprev.x; (* Xloc = Vprev - Vnext *)
   Xloc.y := Vnext.y - Vprev.y;
   Xloc.z := Vnext.z - Vprev.z;
   Yloc.x := Vprev.x + Vnext.x; (* Yloc = Vprev + Vnext *)
   Yloc.y := Vprev.y + Vnext.y;
   Yloc.z := Vprev.z + Vnext.z;

   CrossProd(Xloc, Yloc, Zloc); (* Zloc is cross product of Xloc and Yloc *)
```

```
   Normalize(Xloc);
   Normalize(Yloc);
   Normalize(Zloc);
(* Convert the local frame Hydrogen vectors to molecular frame Hydrogen
   vectors using the unit vectors we have just found. *)
(* Note:  Hloc*.x := 0 *)
   Hmolplus.x := ((Hlocplus.y * Yloc.x) + (Hlocplus.z * Zloc.x));
   Hmolplus.y := ((Hlocplus.y * Yloc.y) + (Hlocplus.z * Zloc.y));
   Hmolplus.z := ((Hlocplus.y * Yloc.z) + (Hlocplus.z * Zloc.z));
   Hmolminus.x := ((Hlocminus.y * Yloc.x) + (Hlocminus.z * Zloc.x));
   Hmolminus.y := ((Hlocminus.y * Yloc.y) + (Hlocminus.z * Zloc.y));
   Hmolminus.z := ((Hlocminus.y * Yloc.z) + (Hlocminus.z * Zloc.z));
(* Get the molecular frame Hydrogen coordinates by adding the molecular frame
   hydrogen vectors to the molecular frame Carbon vectors *)
   Hplus[i].x := Hmolplus.x + C[i].x;
   Hplus[i].y := Hmolplus.y + C[i].y;
   Hplus[i].z := Hmolplus.z + C[i].z;
   Hminus[i].x := Hmolminus.x + C[i].x;
   Hminus[i].y := Hmolminus.y + C[i].y;
   Hminus[i].z := Hmolminus.z + C[i].z;
END; (* FOR *)
  (* Write data to file *)
 WriteReal(outputfile, phi, 10); WriteReal(outputfile, alph, 20);
      WriteReal(outputfile, bet, 20); WriteLn(outputfile);
FOR i := 0 TO 4 BY 1 DO
   WriteReal(outputfile, C[i].x, 18); (*WriteString("     ");*)
   WriteReal(outputfile, C[i].y, 18); (*WriteString("     ");*)
   WriteReal(outputfile, C[i].z, 18); (*WriteString("     ");*)
   Write(outputfile, EOL);
   END; (* FOR *)
FOR i := 1 TO 4 BY 1 DO
   WriteReal(outputfile, Hplus[i].x, 18); (*WriteString("     ");*)
   WriteReal(outputfile, Hplus[i].y, 18); (*WriteString("     ");*)
   WriteReal(outputfile, Hplus[i].z, 18); (*WriteString("     ");*)
   Write(outputfile, EOL);
   WriteReal(outputfile, Hminus[i].x, 18); (*WriteString("     ");*)
   WriteReal(outputfile, Hminus[i].y, 18); (*WriteString("     ");*)
   WriteReal(outputfile, Hminus[i].z, 18); (*WriteString("     ");*)
   Write(outputfile, EOL);
   END; (* FOR *)
phi := phi + increment;
END; (* phi WHILE loop which starts near beginning of program *)
 alph := alph + incalph;
END; (* alph WHILE loop *)
bet := bet + incbet;
END; (* bet WHILE loop *)

Close(outputfile);
WriteString(tty, "Data Written to File.");
WriteLn(tty);
WriteString(tty, "Program completed");
WriteLn(tty);
END Coord.
```

References

[1] R. Setton, *Synt. Met.* **23**, 467 (1988).

[2] A. P. Legrand and S. Flandrois (eds.), *Chemical Physics of Intercalation*, Nato ASI Series B Physics, 172, Plenum, New York, 1987.

[3] S. A. Solin and H. Zabel, *The Physics of Ternary Graphite Intercalation Compounds*, Adv. Phys. **37**, 87 (1988).

[4] H. L. Strauss, *Ann. Rev. Phys. Chem.* **34**, 301 (1983).

[5] W. J. Lafferty, D. W. Robinson, R. V. St. Louis, J. W. Russell and H. L. Strauss, *J. Chem. Phys.* **42**, 2915 (1965).

[6] H. J. Geise, W. J. Adams, and L. S. Bartell, *Tetrahedron* **25**, 3045 (1969).

[7] G. G. Engerholm, A. C. Luntz, W. D. Gwinn and D. O. Harris, *J. Chem. Phys.* **50**, 2446 (1969).

[8] H. M. Seip, *Acta Chem. Scand.* **23**, 2741 (1969).

[9] A. Almenningen, H. M. Seip and T. Willadsen, *Acta Chem. Scand.* **23**, 2748 (1969).

[10] J. E. Kilpatrick, K. S. Pitzer, and R. Spitzer, *J. Am. Chem. Soc.* **69**, 2483 (1947).

[11] *Ibid.* **80**, 6697, (1958).

[12] K. S. Pitzer and W. E. Donath, *J. Am. Chem. Soc.* **81**, 3213 (1959).

[13] B. Fuchs, In: *Topics in Stereochemistry 10*, Wiley, New York, 1977.

[14] A. C. Legon, *Chem. Rev.* **80**, 231 (1980).

[15] D. Cremer and J. A. Pople, *J. Am. Chem. Soc.* **97**, 1358 (1975).

[16] D. Cremer, *Israel J. Chem.* **23**, 72 (1983).

[17] J. A. Greenhouse and H. L. Strauss, *J. Chem. Phys.* **50**, 124 (1969).

[18] R. Davidson and P. A. Warsop, *J. Chem. Soc. Faraday Trans. II* **68**, 1875 (1972).

[19] E. Diez, A. L. Esteban, and M. Rico, *J. Magn. Reson.* **16**, 136 (1974).

[20] A. L. Esteban, M. P. Galache, E. Diez, J. S. Fabian, J. Guilleme, *J. Mol. Struct.* **142**, 375 (1986).

[21] A. L. Esteban, M. P. Galache, E. Diez, J. S. Fabian, F. J. Bermejo, *Mol. Phys.* **69**, 429, (1990).

[22] M. Nomine and L. Bonnetain *J. Chim. Phys.* **66**, 173 (1969).

[23] M. F. Quinton, C. Fretigny, and A. P. Legrand, *Synth. Met.* **34**, 569 (1989).

[24] F. Béguin, H. Estrade-Szwarckopf, J. Conard, P. Lauginie, P. Marceau, D. Guerard, and L. Facchini, *Synth. Met.* **7**, 77 (1983).

[25] L. Facchini, M. F. Quinton, A. P. Legrand, F. Béguin, and R. Setton, *Physica* **99B**, 525 (1980).

[26] F. Béguin, C. Laroche, B. Gonzalez, M. Goldmann, and M. F. Quinton, *Synth. Met.* **23**, 155 (1988).

[27] M. F. Quinton, personal communication.

[28] F. Béguin, R. Setton, A. Hamwi and P. Touzain, *Mat. Sci. Eng.* **40**, 167 (1979).

[29] R. Setton, F. Béguin, J. Jegoudez and C. Mazieres, *Rev. Chim. Min.* **19**, 360 (1982).

[30] M. F. Quinton, A. P. Legrand, and F. Béguin, *Synth. Met.* 14, 179 (1986).

[31] N. Daumas and A. Herold, *C. R. Acad. Sc. C* **268**, 373 (1969) and *Bull. Soc. Chim. Fr.*, 1598 (1971).

[32] M. F. Quinton, A. P. Legrand, L. Facchini, and F. Béguin, *Synth. Met.* **23**, 271 (1988).

[33] M. Goldmann, J. Pannetier, F. Béguin, and B. Gonzalez, *Synth. Met.* **23**, 133 (1988).

[34] A. P. Legrand, L. Facchini, D. Bonnin, J. Bouat, M. F. Quinton, and F. Béguin, *Synth. Met.* **12**, 175 (1985).

[35] F. Béguin, D. Guerard, and M. Goldmann, *Synth. Met.* **34**, 33 (1989).

[36] M. Goldmann, A. J. Dianoux, B. Gonzalez, F. Béguin, H. Estrade-Szwarckopf, and J. Conard, *Synth. Met.* **23**, 55 (1988).

[37] M. Goldman, H. Pilliere, F. Béguin, *Synth. Met.* **34**, 59 (1989).

[38] F. Béguin, P. Vast, *Synth. Met.* **23**, 427 (1988).

[39] R. Liboff, *Introductory Quantum Mechanics*, Holden-Day, Oakland, 1980.

[40] J. J. Sakurai, *Modern Quantum Mechanics*, Benjamin/Cummings, Menlo Park, 1985.

[41] M. Munowitz, *Coherence and NMR*, John Wiley and Sons, New York, 1988.

[42] C. P. Slichter, *Principles of Magnetic Resonance*, Springer Verlag, Berlin, 1990.

[43] H. S. Gutowsky and G. E. Pake, *J. Chem. Phys.* **16**, 1164 (1948).

[44] H. S. Gutowsky and G. E. Pake, *J. Chem. Phys.* **18**, 162 (1950).

[45] M. F. Quinton, L. Facchini, F. Beguin, A. Legrand, *Rev. Chim. Min.* **19**, 407 (1982).

[46] R. Lozach, B. Lemarie, and B. Braillon, *J. Chim. Phys.* **72**, 873 (1975).

[47] J. M. Zhang and P. C. Eklund, *Synth. Met.* **26**, 357 (1988).

[48] D. O. Harris, G. C. Engerholm, C. A. Tolman, A. C. Luntz, R. A. Keller, H. Kim, W. D. Gwinn, *J. Chem. Phys.* **50**, 2438 (1969).

[49] M. F. Quinton, *Groupe d'Etude de Resonance Magnetique*, 1988.

[50] A. L. Blumenfeld, E. I. Fedin, Yu. V. Isaev, Yu. N Novikov, *Synth. Met.* **6**, 15 (1983).

[51] F. Béguin, R. Setton, L. Facchini, *Synth. Met.* **7**, 263 (1983).

[52] J. Jegoudez, C. Mazieres, R. Setton, *Carbon* **24**, 747 (1986).

[53] J. B. Murdoch, *Computer Studies of Multiple Quantum Spin Dynamics*, Ph. D. Thesis (University of California at Berkeley, 1982).

[54] R. Ernst, G. Bodenhausen and A. Wokaun, *Principles of Nuclear Magnetic Resonance in One and Two Dimensions*, Oxford University Press, Oxford, 1990.

[55] D. P. Weitekamp, *Adv. Magn. Reson.* 11, 111 (1983).

[56] G. Drobny, A. Pines, S. Sinton, W. S. Warren and D. P. Weitekamp, *Phil. Trans. R. Soc. Lond.* A**299**, 585 (1981).

[57] G. Bodenhausen, R. L. Vold and R. R. Vold, *J. Magn. Reson.*, **37**, 93 (1980).

[58] J. W. Emsley and J. C. Lindon, *NMR Spectroscopy Using Liquid Crystals as Solvents*, Compton Printing Limited, Aylesbury, 1975.

LAWRENCE BERKELEY LABORATORY
UNIVERSITY OF CALIFORNIA
TECHNICAL INFORMATION DEPARTMENT
BERKELEY, CALIFORNIA 94720